DOCKET: EPA-HQ-OAR-2024-0309-0059
EPA 402-R-25-003

EPA Review of DOE Replacement Panels
Planned Change Request

Part 1: Review of DOE 12-Panel Sensitivity Study

U.S. Environmental Protection Agency
Office of Radiation and Indoor Air
Center for Waste Management and Regulations
1200 Pennsylvania Ave, NW

Washington, DC 20460
July 2025

CONTENTS

TABLES

FIGURES

ABBREVIATIONS AND ACRONYMS

Am	americium
APPA	Additional Panels Performance Assessment
BFL	baseline FEP list
CCA	compliance certification application
CCDF	complementary cumulative distribution function
CDF	cumulative distribution function
CH	contact-handled
CRA	compliance recertification application
CRP	Culebra release point
DBDSP	Delaware Basin Drilling Surveillance Program
DBMAR	Delaware Basin Monitoring Annual Report
DBR	direct brine release
DOE	U.S. Department of Energy
DRZ	disturbed rock zone
EPA	U.S. Environmental Protection Agency
ft	feet
GWB	generic weep brine
FEP	features, events, and processes
LWA	Land Withdrawal Act
m	meter
N	natural
Nd	neodymium
Np	neptunium
PA	performance assessment
PAIR	Performance Assessment Inventory Report
PCR	planned change request
Pu	plutonium
QAPP	Quality Assurance Project Plan
RoR	rest-of-repository

RPPCR	Replacement Panels Planned Change Request
Th	thorium
TRU	transuranic
U	uranium
WIPP	Waste Isolation Pilot Plant

1.0 INTRODUCTION

On March 12, 2024, the U.S. Department of Energy (DOE or the Department) submitted a Planned Change Request (PCR) to the U.S. Environmental Protection Agency (EPA or the Agency) for approval to use replacement Panels 11 and 12 at the Waste Isolation Pilot Plant (WIPP) repository for disposal of transuranic (TRU) radioactive waste (DOE 2024a). This request was accompanied by a performance assessment (PA) of a repository that included the original waste Panels 1 through 10, two replacement Panels 11 and 12, and seven conceptual Panels 13 through 19. DOE called this 19-panel analysis the Replacement Panels Planned Change Request (RPPCR) PA.

Replacement Panels 11 and 12 were identified by DOE as needed to replace underutilized and lost waste disposal capacity in the original ten panels. DOE had approved these two panels for excavation and waste disposal, and their operational use was approved by the New Mexico Environment Department prior to submittal of the PCR (Falta et al., 2021, pp. 5, 6). The RPPCR PA also addressed seven additional panels, numbered 13 through 19, that had been proposed but not approved by DOE. These additional panels were identified by DOE as conceptual because they were based on internal strategic planning as needed to provide sufficient capacity to hold the 6.2 million cubic feet of TRU waste authorized by the WIPP Land Withdrawal Act (LWA).

The Agency reviewed DOE's 19-Panel RPPCR PA and prepared comments and questions for further clarification. During the review, EPA determined that the RPPCR PA submitted by DOE, even when supplemented by efforts to translate the results to a 12-panel repository, did not provide the information needed to support a decision regarding the Department's RPPCR and that a 12-panel analysis would be required (EPA 2024). Although DOE identified the subsequent 12-panel analysis as a sensitivity study, EPA found it to meet all the requirements of a PA and suitable for supporting the decision on the two proposed panels. Although EPA did not find DOE's 19-Panel RPPCR PA to sufficiently support its RPPCR, it was found to document the potential for the WIPP repository to accommodate the full LWA waste volume.

EPA subsequently performed a detailed review of DOE's supporting documentation pertaining to its 12-panel sensitivity study. EPA is in general agreement with DOE's approach and DOE's interpretation of the PA results. Although EPA had concerns pertaining to several of DOE's input parameters, these concerns were alleviated based on the results of EPA's independent sensitivity analysis, demonstrating that the total mean normalized releases still fall below EPA's regulatory limits. As a result, the Agency has determined that there is a reasonable expectation that the 12-panel configuration of the repository will comply with the standards and requirements in 40 CFR parts 191 and 194. EPA therefore approves DOE's Planned Change Request to use replacement Panels 11 and 12 at the WIPP repository for disposal of TRU radioactive waste.

EPA is documenting its review of the Department's RPPCR in two reports. This report (Part 1) reviews DOE's 12-panel sensitivity study and evaluates the effects on WIPP performance of increasing the number of waste panels from ten to twelve. This report forms the basis of EPA's decision regarding DOE's RPPCR. The second report (Part 2), to come at a later date, will address issues specific to DOE's 19-panel RPPCR PA and will provide feedback to DOE on changes to models and parameters that could be made in future PAs to address additional expansions of the geographic extent of the WIPP repository. These reports, as well as other supporting information for DOE's request and EPA's review, may be found at regulations.gov in Docket No. EPA-HQ-OAR-2024-0309.

DOE has formally identified its 12-panel sensitivity study as the CRA19_12P PA (Zeitler et al. 2025, Section 1). The study is variously referred to in DOE documents and in this report as the 12-panel sensitivity study, the 12-panel analysis, the CRA19_12P analysis, and the CRA19_12P PA. It was modeled after the Department's 2019 Compliance Recertification Application (CRA-2019) PA and includes many of the assumptions and parameter values used in that PA.

Section 2 of this report summarizes EPA's review of the Additional Panels Performance Assessment (APPA) Peer Review of the 19-panel APPA model. That model introduced an approach for simulating an off-axis repository design that was approved by the Peer Panel and by the Agency and was used by DOE in both the 12-panel analysis and the 19-panel RPPCR PA.

Section 3 of this report provides the Agency's evaluation of DOE's updates to the CRA-2019 PA in developing the 12-panel analysis. Section 4 summarizes the results of DOE's 12-panel analysis. Section 5 provides EPA's evaluation of those results and summarizes EPA's legacy concerns about the Department's development of the CRA-2019 PA that also affect the 12-panel analysis. Section 6 describes EPA's evaluations of the sensitivity of the performance of a 12-panel repository to the Agency's concerns. Section 7 provides the Agency's conclusions and guidance for future DOE submittals.

2.0 EPA EVALUATION OF APPA PEER REVIEW

EPA regulations at 40 CFR 194.23(a)(3)(v) require conceptual models developed by DOE for assessing WIPP performance to be independently peer reviewed, consistent with 40 CFR 194.27. In accordance with these requirements, in 2021, DOE conducted a peer review of conceptual WIPP performance model changes for the addition of nine new off-axis waste panels to the existing WIPP repository footprint. DOE incorporated these conceptual changes into the APPA model to illustrate their effects on WIPP performance. The conduct and results of the APPA peer review are documented by Falta et al. (2021).

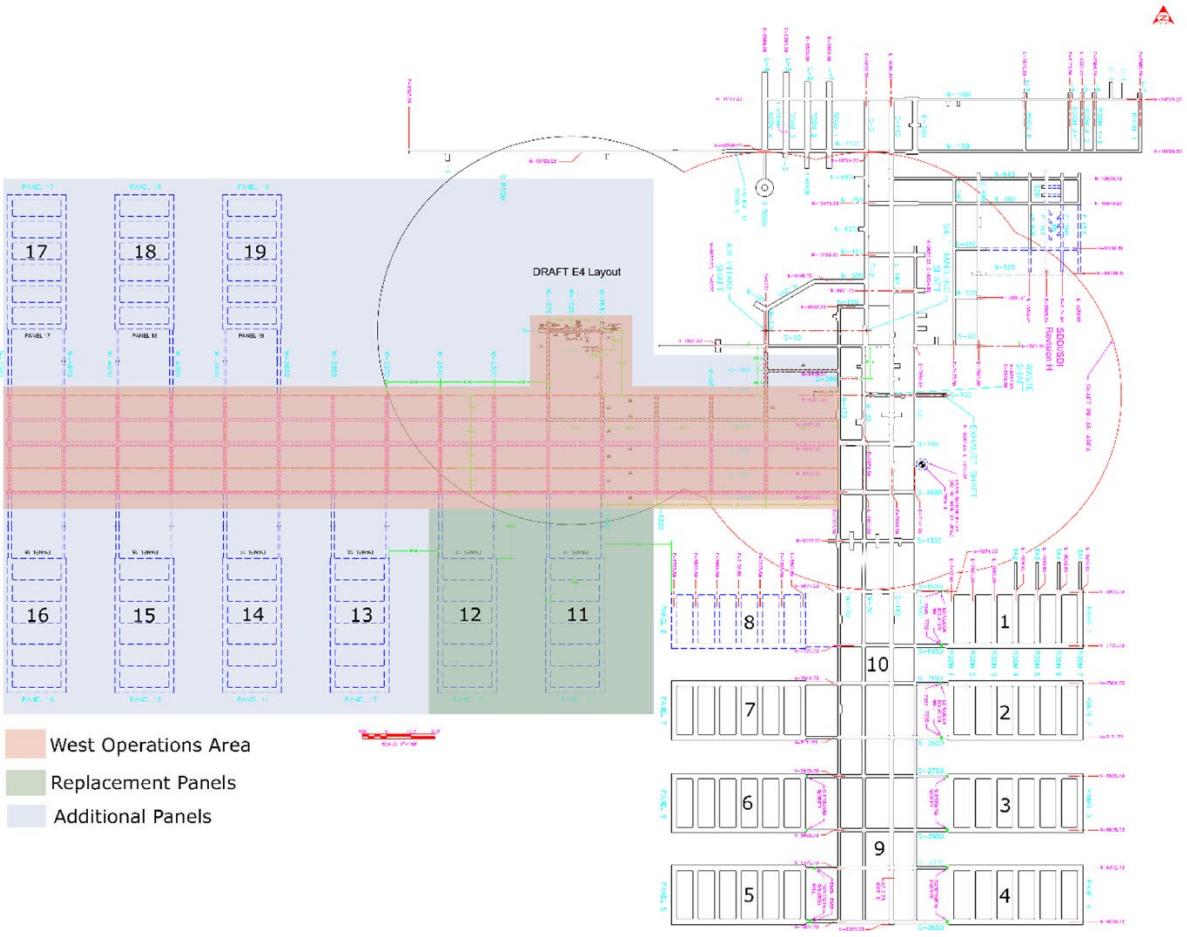

Source: Hansen et al. 2023, Figure 1

Figure 1. WIPP repository layout showing original Panels 1–10 on a north-south axis, replacement Panels 11–12 on an east-west axis, and conceptual additional Panels 13–19 also on an east-west axis

The excavation and use of the two replacement Panels, 11 and 12, were approved by DOE prior to the peer review. The APPA model reviewed by the peer panel also addressed seven additional panels, identified as Panels 13 through 19, that had not been approved by DOE but

were identified by DOE as conceptual, based on internal strategic planning, and were not to be included for approval in the future PCR for Panels 11 and 12 (Falta et al. 2021, pp. 5, 6).

As shown in Figure 1, the original Panels 1 through 10 are located along a north-south axis that facilitated a simplified, two-dimensional approach to numerical modeling. Panels 11 and 12 were to be located along an adjoining east-west axis that complicated the original modeling approach, and Panels 13 through 19 were conceptually located on an extension of that axis. The Department presented the peer panel with a simplified, two-dimensional approach for simultaneously modeling both axes and illustrated its use by applying it to a 19-panel repository that included the original ten panels, the two replacement panels, and the seven conceptual panels.

The peer panel concluded that the new APPA model was reasonable and consistent with past PA approaches, subject to the assumption that there would be no significant differences in the waste inventory or in the material properties of the halite in the off-axis panels (Falta et al. 2021, p. 37).

The Agency's review of the APPA peer review is documented in EPA (2023). EPA found the peer panel's conclusion to be reasonable and appropriate for addressing an off-axis repository extension and found the methodology's application to a nine-panel off-axis repository design to be illustrative of its use. The Agency, therefore, considers the methodology for addressing off-axis waste panels that was accepted by the peer panel to be acceptable for use in a 12-panel PA, where two of those panels are in an off-axis repository extension.

The Department observed that the results of the CRA19_12P analysis can be compared with the results of the APPA. Although the APPA was based on a 19-panel repository, it also used the same inventory and many of the same input parameters as the CRA-2019 PA. DOE noted that this consistency in inventory and input parameters allowed for a direct evaluation of how variations in the number of waste panels – 10 in the CRA-2019 PA, 12 in the CRA19_12P analysis, and 19 in the APPA – impact performance outcomes. DOE stated that the results of these three scenarios can provide valuable insights into the relationship between the number of waste panels and overall system performance. These results are further described in Section 4 of this report.

3.0 EPA EVALUATION OF UPDATES TO CRA-2019 PA IN DOE 12-PANEL SENSITIVITY STUDY

This section explains and evaluates updates made by DOE to the CRA-2019 PA database for the CRA19_12P sensitivity study. Most of DOE's updates were associated with the new configuration that increased the repository footprint and capacity, but updates were also made in the computer codes used to perform the study.

3.1 FEP Review

A Features, Events, Processes (FEP) review is conducted by DOE and its contractors as a required, early step in preparing PAs. A FEP review is a formalized way to document what is and what is not considered in PA. The review starts with a baseline FEP list (BFL) derived from the most recent certification (Kirkes 2021a and 2021b). For the CRA19_12P PA, the Department used many of the assumptions and parameter values from the CRA-2019 PA (Zeitler et al. 2025), but the FEP analysis for the CRA19_12P PA was instead carried over from the more recent APPA peer review (Falta et al. 2021). The APPA FEP analysis (Kirkes 2021c) was updated from the CRA-2019 FEP analysis to account for the addition of new off-axis waste panels. No changes were made to the APPA screening decisions when applying the APPA FEP review to the CRA19_12P PA. The APPA peer review and EPA's review of it are discussed in Section 2.0.

Based on the comparability between the APPA and the CRA19_12P PA, EPA finds the reuse of the APPA FEP analysis for the CRA19_12P PA reasonable and adequately documented for the purpose of this review. EPA's review of the CRA-2019 PA noted a few residual concerns that needed to be addressed for the next CRA (EPA 2022b). For example, several of the N (natural) FEPs had failed to incorporate and/or document new information, such as subsurface data obtained by industry since the original 1996 WIPP Compliance Certification Application (CCA). EPA anticipates few, if any, changes to screening decisions will be made due to incorporation of this new information for the next PA, but DOE needs to keep up to date on new information relevant to WIPP.

3.2 Conceptual Models

When developing the APPA model, DOE determined that changing from a 10-panel repository design in the CRA-2019 PA to a 19-panel design in the APPA required modifying three conceptual submodels: Disposal System Geometry; Repository Fluid Flow; and Direct Brine Release. The Agency observes that changing from a 10-panel repository design in the CRA-2019 PA to a 12-panel design in the CRA19_12P analysis involved the same types of conceptual model changes.

Disposal System Geometry. The repository area, volume, and panel neighboring assignments in the CRA-2019 PA were updated to account for the two replacement panels.

Repository Fluid Flow. The BRAGFLO Salado flow model grid in the CRA-2019 PA was modified to accommodate the two replacement panels.

Direct Brine Release. The BRAGFLO DBR grid for computing a direct brine release (DBR) in the CRA-2019 PA was modified to account for the two replacement panels.

In compliance with 40 CFR 194.27, these conceptual model changes were selected and developed by DOE and evaluated by an independent peer review panel as described in Section 2.0 of this report. The Agency accepted DOE's conceptual model assignments.

3.3 Repository Volume and Area

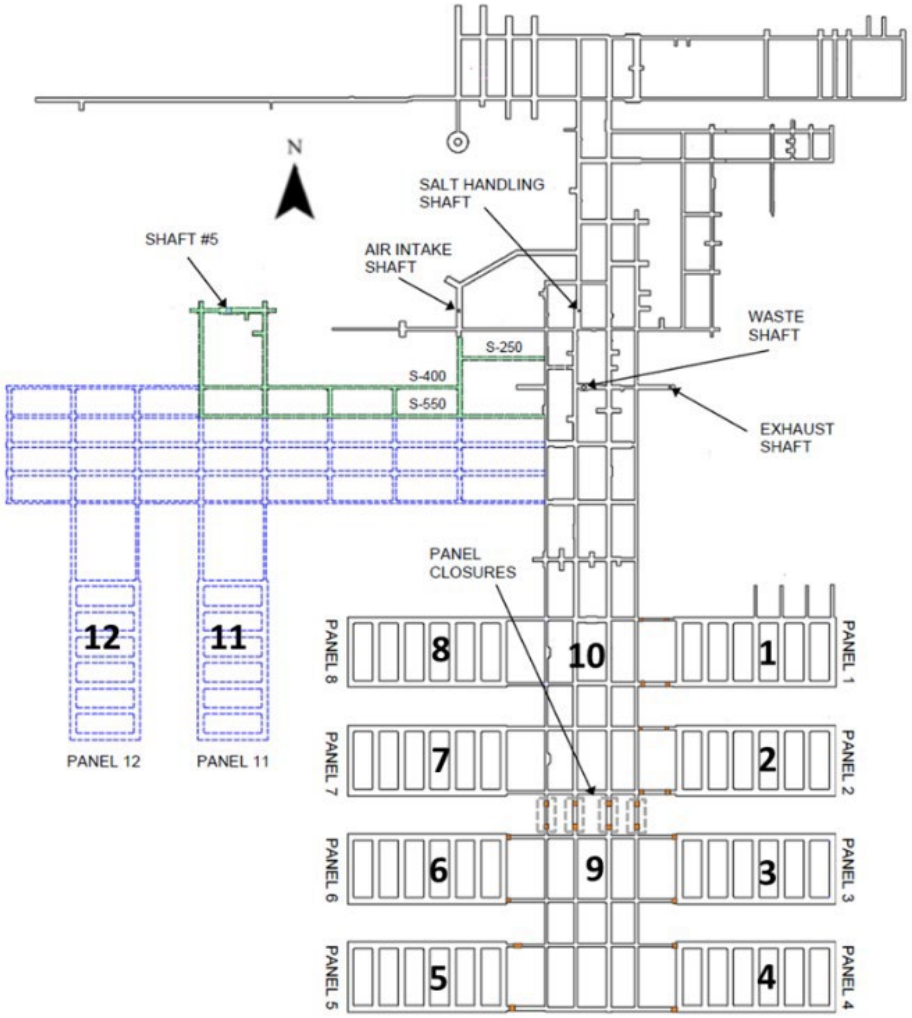

Source: Zeitler et al. 2025, Figure 2-2

Figure 2. Repository footprint for the CRA19_12P analysis

Conversion from a 10-panel to a 12-panel repository design requires two replacement waste panels, new access drifts, and a new operations area. The expanded layout is essentially the same as the layout reviewed by the APPA peer panel and shown in Figure 1 The replacement waste Panels 11 and 12 are similar in design to the original Panels 1 through 8, except that the

abutment pillar width (between the waste rooms and the access drifts) was increased from 61.0 m (200 ft) to 122.0 m (400 ft) and the isolation pillar width (separating two adjacent panels) was increased from 61.0 m (200 ft) to 91.5 m (300 ft). Five access drifts running east-west connect the two new West Area panels with the rest of the underground facility, as compared with four access drifts used to access the existing Panels 1 through 8. The repository footprint for the 12-Panel Analysis is shown in Figure 2.

The model parameters for waste storage volume, the area of the berm to be placed on the ground surface above the waste panels, the area of contact-handled (CH) waste disposal, and the fraction of the repository volume occupied by CH waste have been updated and are shown in Table 1.

Unlike the access drifts that comprise Panel 10 which, for modeling purposes, are assumed to contain waste, DOE stated that there is no plan to place waste in the new west access drifts for Panels 11 and 12, and there are also no plans for panel closures between the West Drifts and the operations and experimental areas (DOE 2024a, p. 17). EPA considers these numerical model changes to be consistent with the revised conceptual models.

Table 1. Repository model parameters updated in the CRA19_12P analysis

Parameter Description	CRA-2019 Value	12-Panel Analysis Value
Total excavated waste storage volume (m^3)	438,406.08	530,600.50
Area of the berm placed over the waste panels (m^2)	628,500	750,000
Disposal area for contact-handled (CH) waste disposal (m^2)	111,500	135,456.84
Fraction of waste storage volume occupied by waste (FVW)	0.385	0.318

Source: Zeitler et al. 2025, Table 2-2.

3.4 Salado Flow and DBR Grids

The BRAGFLO Salado flow and DBR computational grids were updated to account for the new repository layout. The BRAGFLO Salado flow grid is used in WIPP PA to simulate long-term brine and gas flow within the excavated repository drifts and in the surrounding geologic media. The grid provides a stylized, two-dimensional vertical section of the repository geometry, the locations and volumes of the waste panels within the repository, and the stratigraphy of the surrounding geologic media. The 12-panel BRAGFLO Salado flow grid used in the 12-Panel analysis is presented in Figure 3. This grid is similar in concept to the 19-panel grid prepared by DOE for the APPA Peer Review (Falta et al. 2021, Figure 4-1). Both the 12-panel and APPA grids are modifications of the BRAGFLO grid used in the CRA-2019 PA (DOE 2019, Appendix PA-2019, Figure PA-12). The modifications were made to account for the increased volumes and footprints of the off-axis West Operations Area, the West Rest-of-Repository (RoR) and Panel Closures, and the West Drifts (waste panel access drifts). In addition, the composite shaft representing the five vertical shafts in the CRA-2019 PA was relocated between the Experimental Area and the West Operations Area.

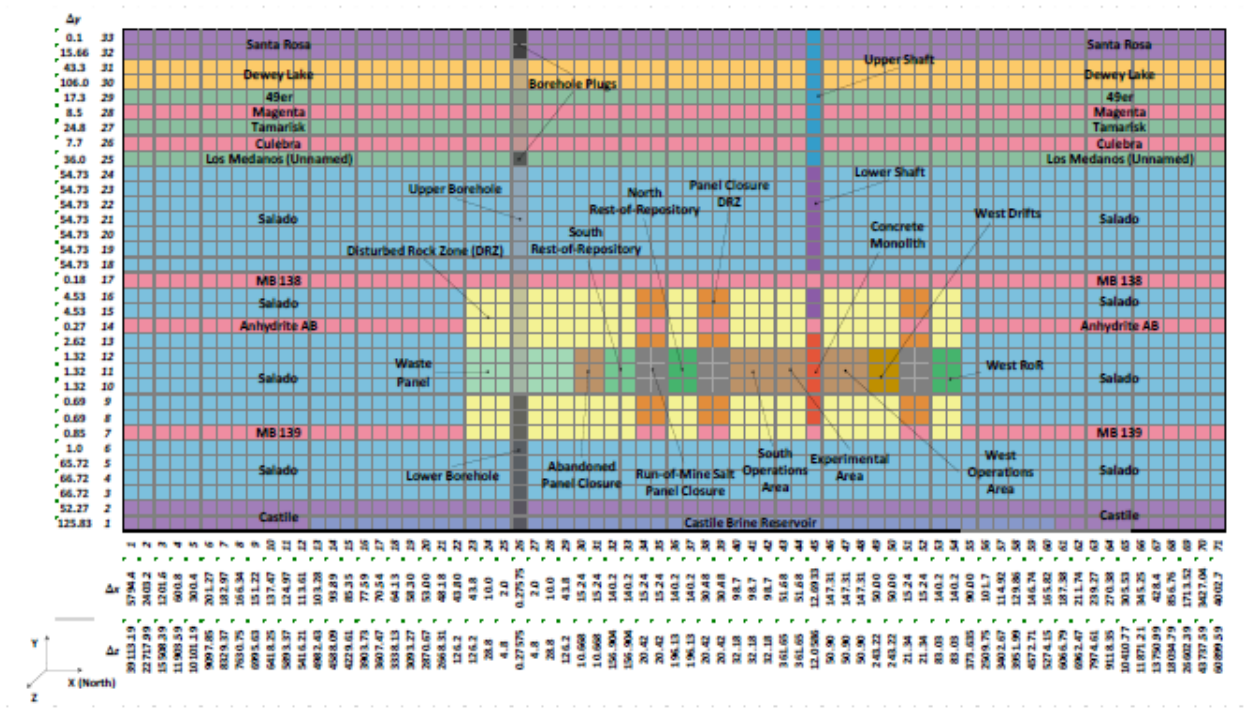

Source: Zeitler et al. 2025, Figure 2-3

Figure 3. BRAGFLO grid used in the CRA19_12P analysis with modeled area descriptions (dimensions in meters)

The BRAGFLO DBR grid is used in WIPP PA to simulate short-term brine and gas flow within the excavated repository drifts during a DBR. It provides a stylized, two-dimensional plan view of the locations and volumes of the waste panels within the repository. An illustration of the BRAGFLO DBR grid used in the CRA19-12P analysis is presented in Figure 4. The 12-panel DBR grid is physically similar to but conceptually different from the CRA-2019 DBR grid (DOE 2019, Appendix PA-2019, Figure PA-25). The CRA-2019 DBR grid represented a plan view of the ten original waste panels that was accurate in both layout and volume. The grid was conceptually modified for the CRA19-12P analysis by splitting the CRA-2019 grid representing Panels 1, 2, 7, 8 and 10 in the North RoR in half and inserting panel closures between the two halves. The upper half of the old North RoR grid (see Panels 1, 8 and the north (10N) half of Panel 10) now conceptually represents the West RoR, and the lower half (see Panels 2, 7, and the south (10S) half of Panel 10) of the old North RoR grid now conceptually represents the North RoR. The representations of the South RoR and Waste Panel (Panel 5) in the CRA-2019 DBR grid were unchanged in the CRA19_12P analysis. This grid is similar to the 19-panel DBR grid prepared by DOE for the APPA Peer Review (Falta et al. 2021, Figure 4-2), but the upper half of the old North RoR grid now represents only the two replacement panels 11 and 12.

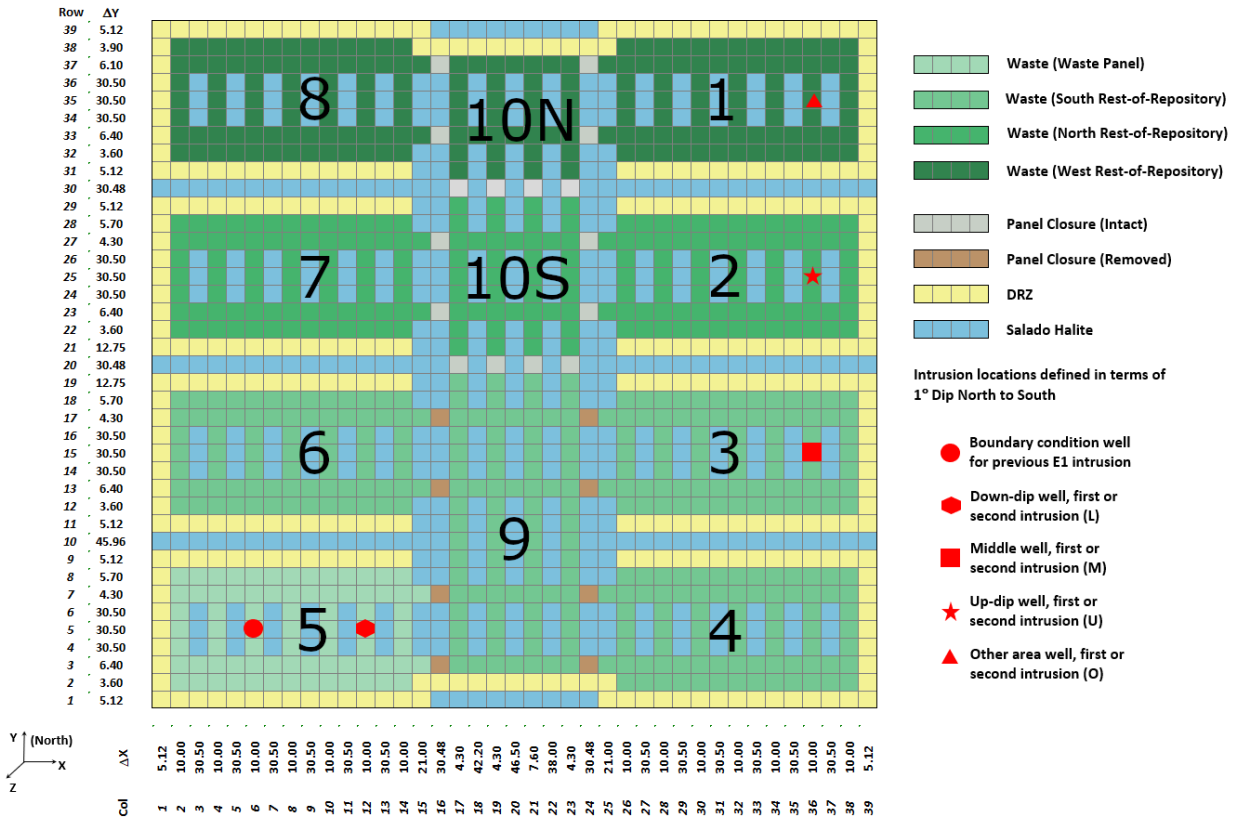

Source: Zeitler et al. 2025, Figure 2-4

Figure 4. BRAGFLO grid used in 12-panel analysis DBR calculations with modeled area descriptions (dimensions in meters)

In this modified conceptualization of the DBR grid, the actual volumes of the 5-panel North and 2-panel West RoRs are each represented by the volumes of two and one-half waste panels. The actual volume of the North RoR is therefore under-represented, and the actual volume of the West RoR is over-represented. DOE justified these changes because DBRs occur over a relatively short time, and the North and West RoRs are isolated from the Waste Panel by one or more sets of low permeability panel closures. These considerations make conditions in the North and West RoRs relatively unaffected by pressure surges in the Waste Panel and therefore relatively insensitive to the actual panel volumes.

The conceptual modifications of the BRAGFLO Salado flow and DBR models proposed by DOE to accommodate off-axis, western waste panels were considered adequate for a 19-panel repository by the APPA Peer Panel (Falta et al. 2021, p. 28) and are also considered adequate for accommodating off-axis waste panels by the Agency. EPA, therefore, concludes that similar conceptual approaches are appropriate for developing Salado flow and DBR grids for a 12-panel analysis where two of those panels are located in an off-axis, West RoR.

The BRAGFLO Salado flow grid used in the 12-panel analysis also has an expanded representation of a Castile brine reservoir below the repository. This representation was proposed by Docherty (2023) for the RPPCR 19-panel PA to allow more realistic values of reservoir porosity to be incorporated into WIPP PA so a reasonable value of Castile pore compressibility could be directly calculated instead of being taken as a constant from the parameter database. According to Zeitler et al. (2025, p. 14), Docherty's expanded representation of a Castile brine reservoir was retained in the 12-Panel Analysis Salado flow grid, but the properties of the Castile brine reservoir were modified to yield the same reservoir brine volumes as in the CRA-2019 PA. The Agency concurs with this approach and agrees with DOE that the increase in the volume of grid cells representing the reservoir in the CRA19_12P BRAGFLO Salado flow grid is expected to have an inconsequential effect.

3.5 Panel Neighboring Assignments

The Department developed the concept of waste panel neighbors to enable the BRAGFLO Salado flow grid, which has only one borehole intrusion location, to simulate the effects of multiple intrusions into multiple, randomly selected waste panels. The panel neighboring assignments are based on the premise that a single, selected borehole intrusion, conservatively located in the BRAGFLO grid where conditions are generally more favorable to repository releases, can act as a surrogate for an intrusion into any waste panel. The neighboring assignments also assume that the effects of earlier intrusions on later intrusions will be related to the number of low permeability panel closures between the two intruded panels. This is especially important when an earlier intrusion results in a release of pressurized brine from the Castile Formation into the repository because contaminated brine releases to the ground surface can occur through a subsequent borehole that intersects a part of the repository that was previously pressurized by Castile brine. A description of panel neighboring assignments in the 12-panel analysis is provided in Zeitler et al. (2025, Section 2.1.2.5). The following is a summary of that description.

The CRA19_12P BRAGFLO Salado flow grid is shown in Figure 3. The single intruding, surrogate borehole is shown intersecting a waste-bearing area on the left side of the grid, identified on the figure as the *Waste Panel*. Panel 5 always serves as the surrogate location for the first intruding borehole. This borehole location is conservative because the Waste Panel has the down-dip location and other physical characteristics of Panel 5 in Figure 2 that tend to result in higher brine saturations and greater repository releases. The remaining waste panels are up-dip from the Waste Panel and tend to be drier. The second and subsequent intruding boreholes can intersect the repository in any of the four waste-bearing areas, and the surrogate locations for these boreholes are shown in Figure 4.

With reference to the repository layout in Figure 2, the CRA19_12P BRAGFLO Salado flow grid in Figure 3, and the CRA19_12P DBR grid in Figure 4, the South Rest-of-Repository (South RoR) in the grid is a waste area with the physical characteristics of Panels 3, 4, 6, and 9, and represents an area with no closures between panels within it or between it and the Waste

Panel. The North Rest-of-Repository (North RoR) is a waste area with the physical characteristics of Panels 1, 2, 7, 8, and 10. It represents an area with one or more sets of closures between any two panels within it and one or more sets of closures between any panel within it and the Waste Panel. The West Rest-of-Repository (West RoR) is a waste area with the physical characteristics of Panels 11 and 12. It represents an area with two sets of closures between any two panels within it and two or more sets of closures between any panel within it and any panel in the repository south area.

In the CRA19_12P PA, neighboring assignments for two intruded panels were made as follows.

Same: Two intruded panels are the "Same" if both earlier and later intrusions occur in the same panel. In WIPP PA, the earlier borehole is always modeled at the surrogate borehole location in the Waste Panel, thus in this case both boreholes are treated as intruding the Waste Panel, which conceptually represents the physical characteristics of Panel 5. Under the Same neighboring assignment, repository conditions such as pressure and brine saturation encountered in the later intrusion are those simulated by BRAGFLO for the Waste Panel at the time of the later intrusion.

Connected: Two panels are "Connected" if the two intrusions occur in panels with no closures between them. Boreholes intruding Panel 5 and a panel in the South RoR, or any two panels within the South RoR, are treated as *Connected* because there are no intervening panel closures within the South RoR or between the South RoR and Panel 5. The earlier intrusion is modeled as encountering conditions in the Waste Panel and the later intrusion is treated as encountering conditions in the South RoR, both at the time of the later intrusion. For example, Panels 6 and 3 are "Connected" and, at the time of the later intrusion, the earlier intruded panel (Panel 6) is assigned the conditions occurring in the Waste Panel, and the later intruded panel (Panel 3) is assigned the conditions occurring in the South RoR.

Adjacent: Two panels are "Adjacent" if the two intrusions occur in panels on the same repository axis (either the north-south axis or the east-west axis) and in panels that are separated by one or more intervening sets of panel closures. Both panels on the east-west axis meet these criteria, and all panels on the north-south axis also meet them if at least one intruded panel is in the North RoR. For example, Panels 11 and 12 are adjacent because they are both on the east-west repository axis, and they are separated by two sets of panel closures. If Panel 11 is the earlier intruded panel, conditions in the Waste Panel at the time of the later intrusion would be assigned to Panel 11, and conditions in the North RoR would be assigned to Panel 12 because the North RoR panels are separated from the Waste Panel by one or more sets of panel closures.

Non-Adjacent: Two panels are "Non-Adjacent" if the two intruded panels are on different repository axes. These panels would be separated by at least two intervening sets of panel closures. Conditions in the Waste Panel at the time of the later intrusion would be assigned to the earlier intruded panel, and conditions in the West RoR would be assigned to the later

intruded panel. For example, Panels 8 and 12 are non-adjacent because they are on different repository axes. If Panel 12 is intruded earlier, it would be assigned conditions in the Waste Panel, and Panel 8 would be assigned conditions in the West RoR.

The panel neighboring scheme used by DOE in the 12-Panel Analysis is summarized in Table 2. Inspection of the BRAGFLO Salado flow grid in Figure 3 suggests that the greater the physical separation of the two intruded panels in the model, the less effect the earlier intrusion will have on conditions in the panel that was intruded at a later time. EPA notes that, in the extreme case of non-adjacent panels, the pressure and brine saturation in the Waste Panel would likely have little effect on conditions in the West RoR because they are separated by a greater distance and at least two sets of intervening panel closures.

The adequacy of the neighboring approach depends on the degree to which conditions in the surrogate Waste Panel (Panel 5) conservatively approximate conditions in the first intruded panel. The most significant conditions are those identified by the APPA Peer Review Panel: there should be no significant differences between Panel 5 and the first intruded panel in 1) the waste inventory, and 2) the material properties of the surrounding Salado halite. To this, the Agency adds a third consideration, that there should be no significant differences in panel design.

Table 2. Panel neighboring scheme for the CRA19_12P analysis

Intruded Panel	Same Panel	Connected Panels	Adjacent Panels	Non-Adjacent Panels
1	1	-	2-10	11-12
2	2	-	1,3-10	11-12
3	3	4,5,6,9	1,2,7,8,10	11-12
4	4	3,5,6,9	1,2,7,8,10	11-12
5	5	3,4,6,9	1,2,7,8,10	11-12
6	6	3,4,5,9	1,2,7,8,10	11-12
7	7	-	1-6,8,9,10	11-12
8	8	-	1-7,9,10	11-12
9	9	3,4,5,6	1,2,7,8,10	11-12
10	10	-	1-9	11-12
11	11	-	12	1-10
12	12	-	11	1-10

Modified from Table 2-1 in Zeitler et al. (2025)

The design of Panel 5 differs from most other panels because it has no closures. As a result, there is little constraint to gas and brine flow between Panel 5 and the four South RoR panels, effectively giving Panel 5 a much bigger volume for gas and brine than a panel with low permeability closures. For example, in the event of a Castile brine inflow, the larger effective volume could impact gas pressure and brine saturation in Panel 5, which could overstate the significance of DBR releases. Although the effect of this difference may be minor because Castile brine inflows are controlled by pressure rather than volume, the difference may become increasingly significant because the proportion of panels with closures is increasing with the

addition of the West waste area. Since the design of Panel 5 differs from most other panels because it has no closures, it provides a conservative approximation of the potential conditions. EPA, therefore, considers the neighboring approach adopted by DOE to be reasonable for a 12-panel analysis.

3.6 Culebra Release Points

An additional discharge point from the repository into the Culebra, identified as Culebra Release Point 2 (CRP-2), was included in the CRA19_12P analyses. This release point was located above the centroid of the two replacement panels and was added to better simulate flow from borehole intrusions in the western area of the repository. The original release point (CRP-1), located at a point above the centroid of the ten original waste panels, was retained unchanged from the CRA-2019 PA. The locations of the two release points are shown in Figure 5. EPA considers the addition of a second release point to be appropriate.

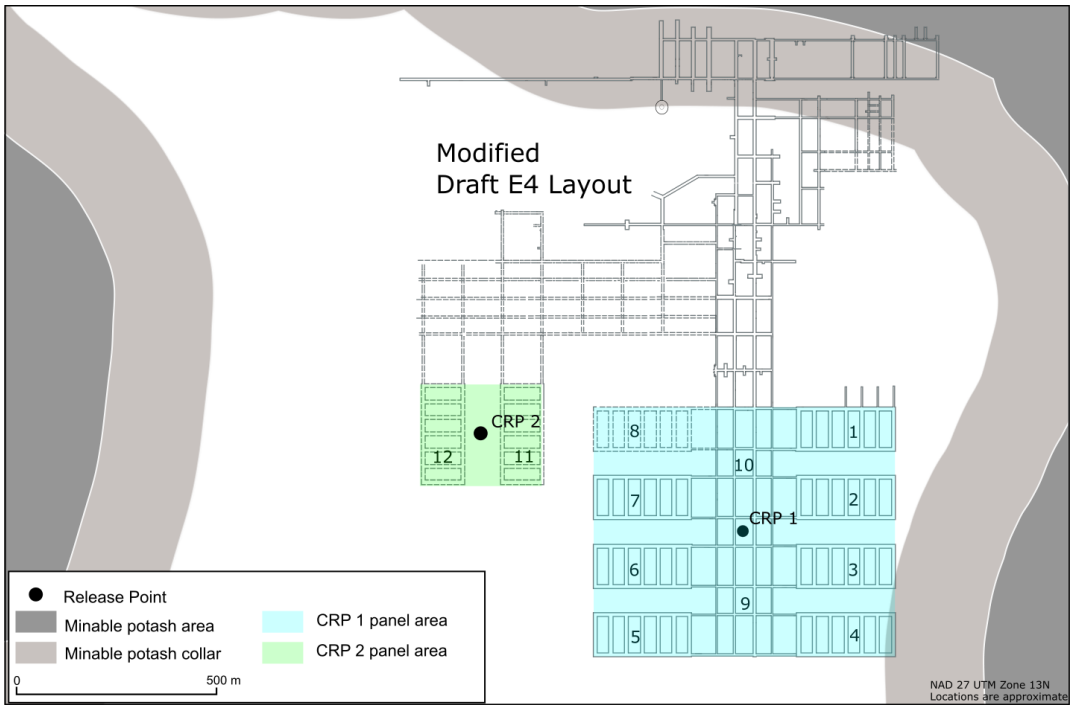

Source: Zeitler et al. 2025, Figure 2-5

Figure 5. Culebra release point locations

3.7 Codes and Code Migration

The Department operates the WIPP repository under the regulatory oversight of EPA. The ability of the WIPP facility to continue to meet the certification requirements of the Agency is demonstrated in part by applying PA computer codes. DOE must demonstrate on an ongoing basis that PA computer software complies with regulations outlined in 40 CFR 194.22 *Quality Assurance,* and 194.23 *Models and Computer Codes*. To demonstrate that computer software

complies with disposal regulations, DOE established a life-cycle management process for software used to support the PA. The qualification approach for the software follows the life-cycle phases outlined in ASME NQA-2a-1990 addenda, part 2.7.

Table 3. Computer code versions approved by the Agency

Computer Code	CCA	2004 CRA 2004 PABC	2009 CRA 2009 PABC	2014 CRA	2019 CRA	CRA19_12P 2024 PCR
ALGEBRACDB	2.35	2.35	2.35	2.36	2.36	**2.37**
BLOTCDB	--	--	1.37	1.38	1.38	**1.39**
BRAGFLO	4.0	5.0	6.0	6.02	7.0	**7.01**
CCDFGF	1.01	5.0A	5.02	6.02	7.03	**8.01**
CCDFGFVECTOR_STATS	---	---	---	---	1.01	**1.02**
CCDFSUM	1.01	2.00	2.00	2.0	2.0	2.0
CUTTINGS_S	5.03	5.04A	6.02	6.03	6.03	**6.04**
DRSPALL	NA	1.0	1.10	1.22	1.22	**1.24**
DTRKMF	NA	1.0	1.0	1.01	1.01	**1.02**
EPAUNI	1.14	1.15A	1.15A	1.16	1.19	**1.2**
GENMESH	6.08	6.08	6.08	6.09	6.10	**6.11**
GROPECDB	2.12	2.12	2.12	2.13	2.13	**2.14**
ICSET	2.21	2.22	2.22	2.23	2.23	**2.24**
LHS	2.32Z0	2.41	2.42	2.43	2.44	**3.0**
MATSET	9.0	9.10	9.10	9.21	9.24	**9.25**
MODFLOW6	---	---	---	---	---	**6.22**
MODFLOW2000	NA	1.60	1.60	1.70	1.70	1.70
MWT3D	---	---	2.51	2.51	2.51	2.51
NONLIN	---	---	2.01	2.02	2.02	**2.03**
NUTS	2.02	2.05A	2.05C	2.06	2.06	**2.08**
PANEL	3.6	4.02	4.03	4.04	5.0	**5.02**
PEST	NA	5.51	9.11	9.12	9.12	**9.13**
PEST++	---	---	---	---	---	**5.16**
POSTBRAG	4.00	4.00	4.00	4.02	4.02	**4.03**
POSTLHS	4.07	4.07	4.07A	4.08	4.08	**4.12**
POSTSECOTP2D	1.02	1.04	1.04	1.05	1.05	**1.06**
PREBRAG	6.0	7.00	8.00	8.03	9.0	**9.01**
PRECCDFGF	1.0	1.00B	1.01	2.0	2.0	**3.01**
PRELHS	2.10	2.10	2.30	2.40	2.44	**2.46**
PRESECOTP2D	1.20	1.22	1.22	1.23	1.23	**1.25**
RELATE	1.43	1.43	1.43	1.45	1.45	**1.46**
SCREEN_NUTS	---	---	---	---	1.02	**1.03**
SECOTP2D	1.30	1.41	1.41A	1.43	1.43	**1.44**
STEPWISE	2.20	2.21	2.21	2.22	2.22	**2.23**
SUMMARIZE	2.10	2.20	3.01	3.02	3.02	**3.03**

Since the time of the CCA, DOE has implemented upgrades to the software operating systems and computer hardware. To demonstrate continued compliance, the Department performs regression and functionality testing on the upgraded operating systems and hardware. Regression testing, as a discipline, consists of running a set of one or more tests for a computer

program and verifying that the output produced in the tests is within previously specified acceptable limits. Functionality testing involves comparing the results to other models and analytical solutions.

The WIPP PA codes have been migrated to the WIPP PA HPC/Linux Cluster, which consists of the login node FWM and 24 Dell PowerEdge C6420 compute nodes running CentOS 7. A full description of the run control for the RPPCR analysis, including names and locations of input and output files, can be found in Long (2023).

Input files were prepared by individual analysts, and the run control coordinator prepared the run scripts. The CRA19_12P study and the RPPCR PA were performed using qualified code versions on the WIPP PA HPC/Linux Cluster (Table 3). As described in AP-204 (Hansen et al. 2023), the DRSPALL and MERGESPALL codes were not run for these analyses; instead, results from a previous analysis were used as input (Kirchner et al. 2014; Kirchner et al. 2015).

EPA has reviewed the documentation that DOE developed during its migration of the WIPP PA codes to the HPC/Linux Cluster to assess whether the computer codes still meet the requirements of 40 CFR 194.23. EPA reviewed user manuals, validation documents, implementation documents, requirement documents/verification validation plans, and regression test results. The review results indicate that the versions of the computer codes specified in Table 3 are approved for use in regulatory compliance calculations on the WIPP HPC/Linux Cluster, which consists of the login node FWM and 24 Dell PowerEdge C6420 compute nodes running CentOS 7.

In conclusion, the Agency finds that the versions of the computer codes specified in Table 3 are approved for use in PA compliance calculations on the WIPP PA HPC/Linux Cluster, which consists of the login node FWM and 24 Dell PowerEdge C6420 compute nodes running CentOS 7.

3.8 Waste Concentration

The 12-panel analysis used the same waste inventory as the CRA-2019 PA submitted by DOE to EPA in 2019 (DOE 2019). The CRA-2019 PA assumed a 10-panel repository design, and the inventory was based on the 2018 Performance Assessment Inventory Report (PAIR-2018). That report used inventory data collected through December 2017 (Van Soest 2018) and estimated future waste generation through the calendar year 2033. As described in Zeitler et al. (2025, Section 2.1.1), the CRA-2019 PA assumed that the total waste volume, including waste containers and packaging materials, was equal to the WIPP disposal limit of 6.2 million cubic feet of TRU waste. The inventory volume did not include a later change to the way in which the maximum allowed repository waste volume (called the Volume of Record) is calculated. The 19-panel RPPCR PA did use the Volume of Record approach, applied to an inventory estimate developed after CRA-2019.

As used in the CRA19_12P analysis, the waste concentration is the fraction (parameter REFCON:FVW) of waste panel volume occupied by waste, calculated as the total waste volume divided by the total waste panel volume. An assumption was made in the CRA-2019 PA that the entire waste volume would fit into a 10-panel repository footprint. For the 10-panel repository, this fraction was 0.385. Increasing the number of waste panels from 10 to 12 increased the total waste panel volume and decreased the fraction occupied by waste to 0.318 (Zeitler et al. 2025, p. 12).

The Agency observes that although decreasing the waste fraction would tend to decrease calculated repository releases compared with the CRA-2019 PA, a waste fraction of 0.318 is still relatively high. This fraction is equivalent to a waste room porosity of 0.682 (= 1 - 0.318), which is essentially the same as the initial waste room porosity of 0.681 used in the WIPP PA's legacy waste material model (refer to Vignes et al. 2023, p. 24). WIPP PA's new waste material model, as developed by Vignes et al. (2023, Table 2.3), increases the initial waste room porosity to 0.825, which is equivalent to an even lower waste fraction of 0.175. The Agency, therefore, considers a waste fraction of 0.318 used in the 12-Panel Analysis to be appropriately conservative.

4.0 CRA19_12P ANALYSIS RESULTS

Calculated WIPP repository releases are modeled to occur along four pathways, all resulting from the effects of a hypothetical, future exploratory borehole penetrating repository waste. The first of these is the transport of waste solids up an intruding borehole during drilling (called *cuttings and cavings*). This pathway results from the mechanical effects of drilling and does not depend on conditions in the intruded waste panel. The other three pathways depend on the presence of brine and pressurized fluid (gas and brine) within an intruded waste panel. The *spallings* pathway results from waste solids spalling into an intruding borehole and migrating up the borehole to the ground surface due to high fluid pressure in the intruded waste panel. The *direct brine release,* or *DBR,* pathway occurs when high fluid pressures and brine saturations in a waste panel drive brine contaminated by dissolved and colloidal radionuclides up an intruding borehole to the ground surface. In the *Culebra* pathway, subsurface releases of contaminated brine to the accessible environment occur from the overlying Culebra dolomite horizon due to the flow of pressure-driven, contaminated brine up an intruding borehole into the Culebra and subsequent lateral transport within the Culebra to the LWA boundary.

Although DOE performs three replicate calculations consisting of 100 release vectors each when assessing WIPP performance, only results for the first replicate are discussed because results for the other two replicates show the same trends. As previously noted, the 12-panel CRA19_12P calculations were based on the 10-panel CRA-2019 PA calculations as modified to consider the effects of a larger repository waste disposal volume and footprint. The following subsections summarize the results of the 12-panel sensitivity study as presented in Zeitler et al. (2025).

4.1 Cuttings and Cavings Release Volumes

Cuttings and cavings release volumes are described in Zeitler et al. (2025, Section 6). Zeitler et al. (2025, p. 51) report that there were no changes to parameters associated with the cuttings and cavings processes in the CRA19_12P analysis and no changes to the cuttings and cavings input files. They further state that because the volumes of cuttings and cavings released from an individual penetrating borehole are independent of repository conditions, there were no changes to individual borehole release volumes between the CRA-2019 and the CRA19_12P analyses.

4.2 Spalling Release Volumes

Spalling release volumes are described in Zeitler et al. (2025, Section 6). Zeitler et al. (2025, Section 4.2.1) found little change in mean pressure in the Waste Panel between the CRA-2019 and CRA19_12P calculations. However, for scenarios that do not involve a Castile brine intrusion, maximum pressures were higher over the first 4,000 years after repository closure in the CRA19_12P analysis, while after 4,000 years the pressures showed a small decrease. As discussed in Zeitler et al. (2025, Section 4.2.4), gas generation is dominated by iron corrosion. They believe that an increased rate of iron corrosion in scenarios that do not involve a Castile

brine intrusion is the likely driver for increased gas generation and for the increase in early time pressures because iron surface area concentration in the 10-panel CRA-2019 analysis was held unchanged at 11.2 m^2 per m^3 of repository volume in the 12-panel CRA19_12P analysis and the larger volume of the 12-panel repository resulted in an increase in iron surface area. This decision is further discussed in Section 5 of this report. Zeitler et al. (2025, Section 4.2.4) consider the expanded volume of the repository and the depletion of iron in down-dip waste panels with higher brine saturations to be the driver for the decrease in late time pressures. Little change was seen in scenarios that involve a Castile brine intrusion because of the dominant influence of the intruded brine on corrosion rates.

The CRA19_12P analysis showed a continuing trend toward an increasing number of spalling events but a similar release volume per event. Zeitler et al. (2025, Section 6.2.1) observed that most spalling events had low spalling volumes in the 0–1 m^3 range, and the increases in the number of events were attributed to the increased repository footprint in the CRA19_12P analysis. The maximum volumes of about 10 m^3 were about the same for the two analyses, and the mean volumes of about 1 m^3 were nearly the same (Zeitler et al. 2025, Table 6-2).

For a single intrusion, spallings releases are calculated by multiplying spallings volumes, the fraction of excavated repository volume that is occupied by waste, and the volume-average activity concentration of radionuclides in CH waste. Zeitler et al. (2025, Section 6.1 and 6.2) observed that since the waste volume and inventory for the CRA19_12P analysis are unchanged from the CRA-2019 analysis, the radionuclide activity per unit of solid waste volume (waste-volume-based) in spalling releases did not change in the CRA19_12P analysis. The increase in repository volume, with the addition of panels 11 and 12, decreased the repository-volume-based activity concentration in the CRA19_12P analysis and resulted in lower releases for a given spalling volume.

4.3 Direct Brine Release Volumes

As discussed in Section 4.2, mean fluid pressures in the 12-panel analysis were little changed from those in the CRA-2019 PA. Zeitler et al. (2025, Section 4.2.2) found that, beginning at about 1,000 years after repository closure, the mean brine saturations in the Waste Panel were lower in scenarios without a Castile brine intrusion and largely the same in scenarios with a Castile brine intrusion. Although the increased repository volume should result in more brine draining into the repository from the Salado Formation, Zeitler et al. (2025, p. 33) observe that the extra panel closure between the up-dip west waste area and the Waste Panel tends to inhibit brine flow down-dip into the Waste Panel leading to a decrease in brine saturation in scenarios without a Castile brine intrusion. In addition, EPA observes that higher maximum gas pressures in the first 4,000 years after repository closure would reduce brine inflows and contribute to a long-term decrease in saturation. Zeitler et al. (2025, p. 33) also observe that in scenarios with a Castile brine intrusion, brine saturation in the waste panel is controlled by pressurized brine from the Castile and is largely unchanged by the increased up-dip repository volume.

DBR results are described by Zeitler et al. (2025, Section 5). They found that overall, DBR brine volumes were similar or perhaps slightly smaller in the CRA19_12P analysis than in the CRA-2019 analysis (refer to, for example, Zeitler et al. 2025, Figure 5-5). They also found a trend toward an increase in the number of brine releases but a decrease in the volumes of those releases in the CRA19_12P analysis. For both the CRA-2019 and the CRA19_12P analyses, the largest number of releases and the largest mean release volumes occurred in scenarios with a Castile brine intrusion and at down-dip intrusion locations. EPA observes that these trends are consistent with an increasing proportion of waste panels that are modeled as isolated by run-of-mine (ROM) salt panel closures in the CRA19_12P analysis.

The mobile actinide concentrations in repository brine released in DBR events are described in Zeitler et al. (2025, Section 7). The code PANEL is used in WIPP PA to simulate the radionuclide inventory in the waste panels as it decays and mixes with brine. This code calculates the radioactive decay and ingrowth of the radionuclide inventory in the waste panels, calculates the aqueous mobility of each actinide of interest either as dissolved constituents or associated with colloids, and calculates, as a function of time, the aqueous concentration of each radionuclide in brine that is in contact with the waste inventory in the waste panels. In the CRA19_12P analysis, PANEL uses an updated value for the repository volume, while the DBR minimum brine volume, waste inventory data, actinide baseline solubilities, solubility uncertainty factors, and colloid enhancement factors are the same as in the CRA-2019 PA. Therefore, as a function of the brine volume in the repository, the mobile concentrations of radionuclides in the CRA19_12P analysis are also the same as in the CRA-2019 PA.

As previously discussed, the waste inventory in the WIPP repository and the relative inventories among the individual radionuclides at closure are the same in the CRA-2019 and the CRA19_12P analyses. However, Zeitler et al. (2025, Section 7.2.1) calculate that the increase in repository volume due to the 12-panel repository layout in the CRA19_12P analysis decreases the fractional volume of a waste panel in the repository from 0.105 in the CRA-2019 to 0.087 in the CRA19_12P, leading to a corresponding decrease in the inventory in the ten original waste panels as that inventory is spread over more panels in the analysis.

As a result, the increase in waste panel volume in the CRA19_12P analysis affects the calculated mobile concentrations of radionuclides in every waste panel. Although the concentrations are the same when considering the total brine volume in the repository, Zeitler et al. (2025, p. 62) point out that when calculating mobile concentrations in brine for DBRs, the PA considers the brine volume in the intruded panel, not the volume in the entire repository. Because the volume of the repository is larger in the 12-panel model, the scaling from repository brine volume to panel brine volume has changed from the aforementioned 0.105 in the CRA-2019 to 0.087 in the CRA19_12P. This difference results in a decrease in the mean total mobilized radionuclide concentrations in DBR release volumes.

4.4 Culebra Release Volumes

The Culebra release pathway is calculated in two stages: the flow of contaminated brine up an intruding borehole to the Culebra dolomite horizon, and the lateral flow of that brine within the Culebra to the LWA boundary. Zeitler et al. (2025, Section 4.2.3) note that there is a slight increase in brine flow up the borehole in the CRA19_12P analysis compared to the CRA-2019 PA in scenarios with a Castile brine intrusion. They observe that scenarios with such an intrusion resulted in slight increases in pressure with little change in the brine saturation, leading to a slight increase in brine flow up the borehole. Their results show practically no difference in flow up the borehole for scenarios without a Castile brine intrusion.

The lateral flow of brine within the Culebra to the LWA boundary is simulated in WIPP PA using the MODFLOW code. The Culebra flow model scenarios and inputs are the same in both the CRA-2019 and CRA19_12P analyses; however, the flow simulations were rerun using the updated groundwater flow software MODFLOW6. Radionuclide transport through the Culebra to the LWA boundary is simulated with the SECOTP2D code, which assumes fluid flow restricted to parallel plate fractures (the advective continuum) and the transfer of mass between the fractures and the porous matrix by molecular diffusion (the diffusive continuum). Particle tracks are computed using the new DTRKMF code to characterize the advective pathways and travel times taken by simulated water particles from the two release points to the WIPP LWA boundary.

As previously noted, an additional discharge point from the repository into the Culebra, identified as Culebra Release Point 2 (CRP-2), was included in the CRA19_12P analyses. This release point was located above the centroid of the two replacement panels and was added to better simulate flow from borehole intrusions in the western area of the repository. The original release point (CRP-1), located at a point above the centroid of the ten original waste panels, was retained unchanged from the CRA-2019 PA.

Subsidence from potential future potash mining below the Culebra in and near the WIPP site could increase the transmissivity of the Culebra and affect Culebra flow and transport characteristics. The impact of mining is simulated in WIPP PA by multiplying the transmissivity in the Culebra directly over the mined area by a constant. Culebra flow calculations are performed for a “partial mining” scenario in which all potash outside of the LWA is mined, and a “full mining” scenario in which all potash in the model domain is mined. Although an additional release point for flow to the Culebra has been added to the Culebra transport modeling, the flow and transport characteristics and the treatment of potential potash mining are the same in the CRA-2019 and CRA19_12P analyses.

Particle tracks for the CRP-1 and CRP-2 release points are shown in Figure 6 and Figure 7. In the full mining scenario, particles released at both points generally move toward the mining impacted area to the southeast and then deflect to the south following the interface with the mining affected region to the southern extent of the LWA boundary. Zeitler et al. (2025, Section

9.2) note that radionuclide releases at CRP-2 must travel farther to reach the LWA boundary than those released at CRP-1. The partial mining particle tracks are not focused by the transmissivity contrast between mined and unmined areas and are more broadly distributed across the east-west direction but are also generally directed toward the south.

The cumulative distribution function (CDF) of the time taken for a particle to reach the LWA boundary along each particle track is plotted for each replicate, mining scenario, and release point in Figure 8. These plots describe the likelihood of a particle crossing the LWA boundary by the indicated travel time. In the full mining scenario, median travel time for the CRP-1 release point is about 5,200 years and for the CRP-2 release point is about 16,000 years. In the partial mining scenario, median travel time is about 22,000 years for CRP-1 and 36,000 years for CRP-2 (refer to Zeitler et al. 2025, Table 9-1). These results indicate that relatively few releases from CRP-2 are likely to reach the LWA boundary within the 10,000-year regulatory time frame. Zeitler et al. (2025, p. 72) note that cumulative mass discharge results in CRP-1 simulations are generally consistent with the CRA-2019 results, with minor differences likely resulting from the change from the MODFLOW-2000 to MODFLOW6 flow simulation software.

4.5 Normalized Total Releases

Normalized total releases for the CRA19_12P analysis are described in Zeitler et al. (2025, Section 10). These releases are calculated using the CCDFGF code, which uses the outputs of the other WIPP PA codes to produce complementary cumulative distribution functions (CCDFs) of releases in EPA units. Full descriptions of the normalization process and the use of CCDFGF in preparing the CRA-2019 PA are presented in Brunell (2019). For the CRA19_12P analysis, the CCDFGF code was updated to account for the addition of Panels 11 and 12 and to incorporate extended panel neighboring relationships. Zeitler et al. (2025) compare the results for the CRA19_12P analysis with those of the CRA-2019 PA (Brunell 2019) and the APPA (Brunell et al. 2021).

Cuttings and Cavings Releases: Overall mean CCDFs for cuttings and cavings releases are shown in Figure 9. As previously noted, the cuttings and cavings parameters and volumes for individual boreholes are identical between the three analyses. Although the larger repository footprints in the CRA19_12P and APPA analyses result in a greater number of borehole penetrations than in the CRA-2019, the waste concentration and releases decrease proportionally. As Brunell et al. (2021) point out, as the sample size increases, the cumulative releases from individual futures will converge toward a mean value. As a result, mean cuttings and cavings releases are essentially the same for the three analyses. Zeitler et al. (2025, p. 80) conclude that these results demonstrate that the additional repository volume has a minor effect on the cuttings and cavings releases.

Spalling Releases: Overall mean CCDFs for spalling releases are shown in Figure 10. Spalling releases are discussed in Zeitler et al. (2025, Section 10.2.2). Mean spalling releases in the CRA19_12P analysis were slightly smaller than in the CRA-2019 PA but larger than in the APPA.

Spalling releases depend on spalling volumes, which are a function of waste area pressure at the time of intrusion, and spalling concentrations, which are calculated as the average CH waste concentration at the time of intrusion. Zeitler et al. (2025, p. 81) note that although mean spalling volumes are similar in the three analyses, the changes in releases result from the decreasing trend in waste concentration in the larger repository volumes.

Direct Brine Releases: Overall mean CCDFs for DBRs are shown in Figure 11. Direct brine releases for the CRA19_12P analysis are discussed in Zeitler et al. (2025, Section 10.2.3). Mean DBRs were lower in the CRA19_12P analysis than in the CRA-2019 PA at all probabilities but when compared with the APPA, they were lower at high probabilities and higher at low probabilities. Zeitler et al. (2025, p. 84) attribute the higher releases at high probabilities in the APPA to the larger repository footprint modeled in the 19-panel APPA. The larger footprint resulted in a greater excavated area in contact with the disturbed rock zone (DRZ), more brine inflow from the Salado, a higher mean brine saturation, and a resulting increase in smaller volume brine releases. The reduced radionuclide concentrations in the brine due to a larger repository volume primarily affected the higher volume but lower probability DBRs, resulting in lower releases at low probabilities in the 19-panel APPA than in the 12-panel CRA19_12P analysis (Zeitler et al. 2025, p. 84).

Releases from the Culebra: Overall mean CCDFs for releases from the Culebra to the WIPP LWA boundary are shown in Figure 12. These releases for the CRA19_12P analysis are discussed in Zeitler et al. (2025, Section 10.2.4). Although mean releases from the Culebra are small and comparable to those from cuttings and cavings at low probabilities, the highest releases from the Culebra were from the APPA, followed by lower releases in the CRA19_12P analysis and only slightly lower still in the CRA-2019 PA. Transport to the Culebra followed this same pattern, with the APPA being the highest, followed by the closely-matched CRA19_12P and CRA-2019 PA results (Zeitler et al. 2025, Figure 10-6).

The increase seen in the APPA is consistent with the increase in the number of borehole penetrations in a 19-panel footprint and the continued use of a single release point. The effect of a greater footprint is reduced in the 12-panel PA and further reduced by the introduction of a second release point with greater travel times to the LWA boundary. The CRA-2019 PA has the smallest footprint and hence the lowest releases from the Culebra. Zeitler et al. (2025, p. 85) point out that, on a per-radionuclide basis, transport to and releases from the Culebra are very similar across the three analyses.

Total Releases: Total cumulative releases for the CRA19_12P analysis are described in Zeitler et al. (2025, Section 10.2.5). For each future in a realization, total releases are calculated by summing the releases from each of the primary release pathways: cuttings and cavings releases, spallings releases, DBRs, and releases from the Culebra. Individual CCDFs representing total cumulative releases obtained in the 100 realizations (vectors) in Replicate 1 are shown in Figure 13. The results for Replicates 2 and 3 are shown in Figures 10-12 and 10-13 of Zeitler et al. (2025) and are similar to those of Replicate 1. Each CCDF vector on Figure 13 represents the

distribution of total releases calculated from a single set of sampled, uncertain parameter values and 10,000 individual futures. The red dashed line on the figure represents the mean total release. No individual vector in any of the three replicates exceeded EPA release limits.

Overall mean CCDFs for the individual release pathways in the CRA19_12P analysis are shown in Figure 14. As seen in the figure, total normalized releases are dominated in each analysis by cuttings and cavings at high probabilities and by direct brine releases at low probabilities, while spalling releases and releases from the Culebra provide minor contributions.

Total mean releases from the CRA-2019 PA, the APPA, and the CRA19_12P analysis are shown in Figure 15. As seen in the figure, total mean releases from the CRA19_12P analysis are slightly lower than in the CRA-2019 PA but slightly higher than in the APPA. Mean total releases at the 0.1 and 0.001 EPA release probability limits are compared for the three analyses in Table 4.

4.6 DOE Summary

The results of the CRA19_12P analysis are summarized in Zeitler et al. (2025, Section 12). They observe that the CRA19_12P analysis was performed to supplement DOE's RPPCR analysis, and that both analyses were performed to support DOE's PCR to EPA for approval to add two replacement waste disposal panels to the 10-panel WIPP repository. The CRA19_12P calculations differ from the CRA-2019 calculations by considering the effects of a larger repository waste disposal volume and footprint. The CRA19_12P PA was performed in accordance with Sandia National Laboratories WIPP QA Procedure NP 9-1.

WIPP PA calculations estimate the probability and consequence of potential radionuclide releases from the repository to the accessible environment for a regulatory period of 10,000 years after facility closure. Zeitler et al. (2025, p. 99) conclude that total mean normalized releases are similar between the CRA-2019 and CRA19_12P analyses at the highest probabilities. At lower probabilities, releases are slightly lower in the CRA19_12P than in the CRA-2019. The total mean normalized releases were less than EPA release limits for all vectors. In general, Zeitler et al. conclude that the differences between the results for the CRA-2019 PA and the CRA19_12P analysis are minor.

Table 4. Comparison of releases for the CRA-2019, APPA, and CRA19_12P analyses at EPA release limits

Probability	Analysis	Mean Total Release	Lower 95% CL	Upper 95% CL	Release Limit
0.1	CRA-2019	0.0685	0.0636	0.0753	1
0.1	APPA	0.0564	0.0515	0.0665	1
0.1	CRA19_12P	0.0610	0.0564	0.0680	1
0.001	CRA-2019	0.7505	0.4487	0.9595	10
0.001	APPA	0.4540	0.1475	0.5970	10
0.001	CRA19_12P	0.5436	0.3687	0.6691	10

Source: Zeitler et al. 2025, Table 10-5

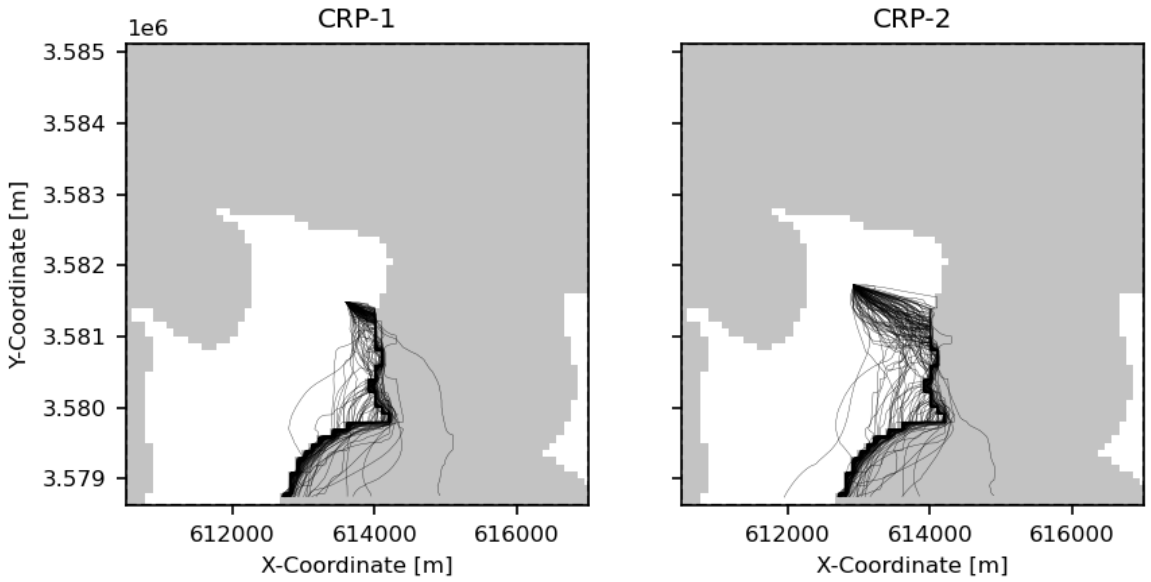

Source: Zeitler et al. 2025, Figure 9-2

Figure 6. Particle tracks for individual releases from release points CRP-1 and CRP-2 for the full mining scenario

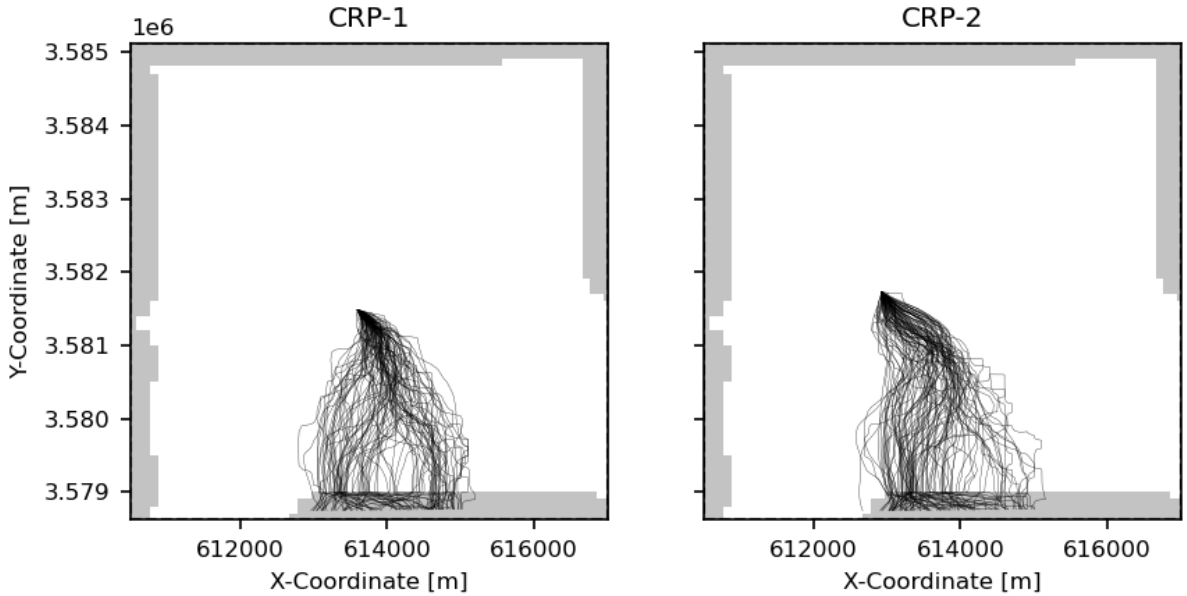

Source: Zeitler et al. 2025, Figure 9-3

Figure 7. Particle tracks for individual releases from release points CRP-1 and CRP-2 for the partial mining scenario

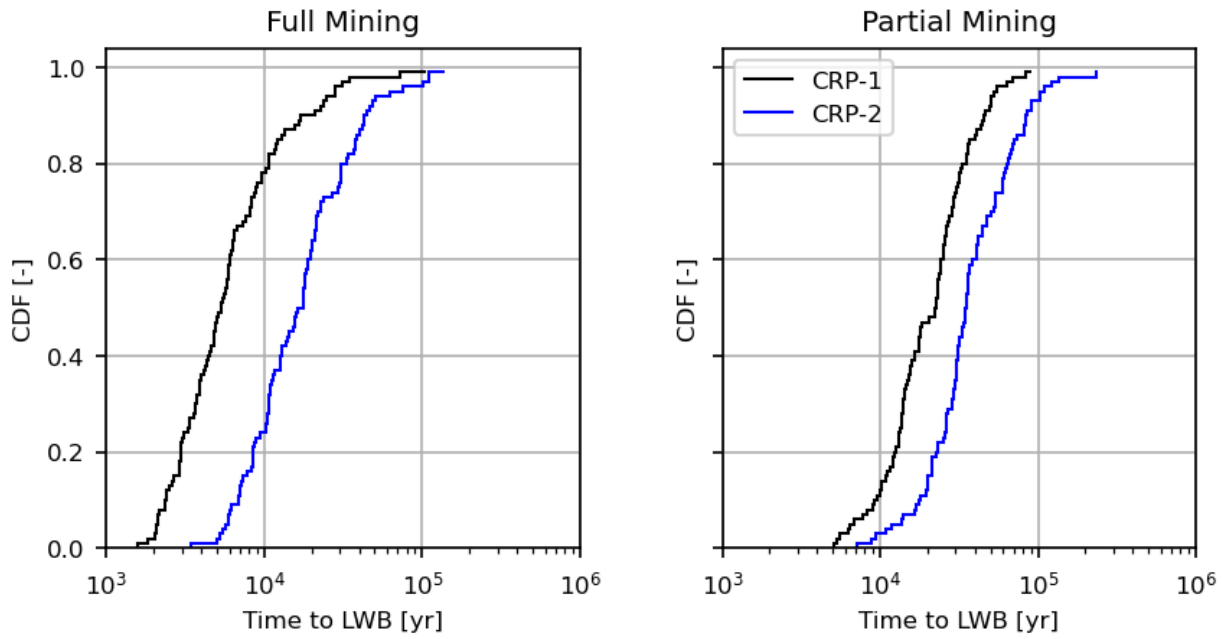

Source: Zeitler et al. 2025, Figure 9-4

Figure 8. Cumulative distributions of radionuclide travel times to the LWA boundary for the full mining and partial mining scenarios

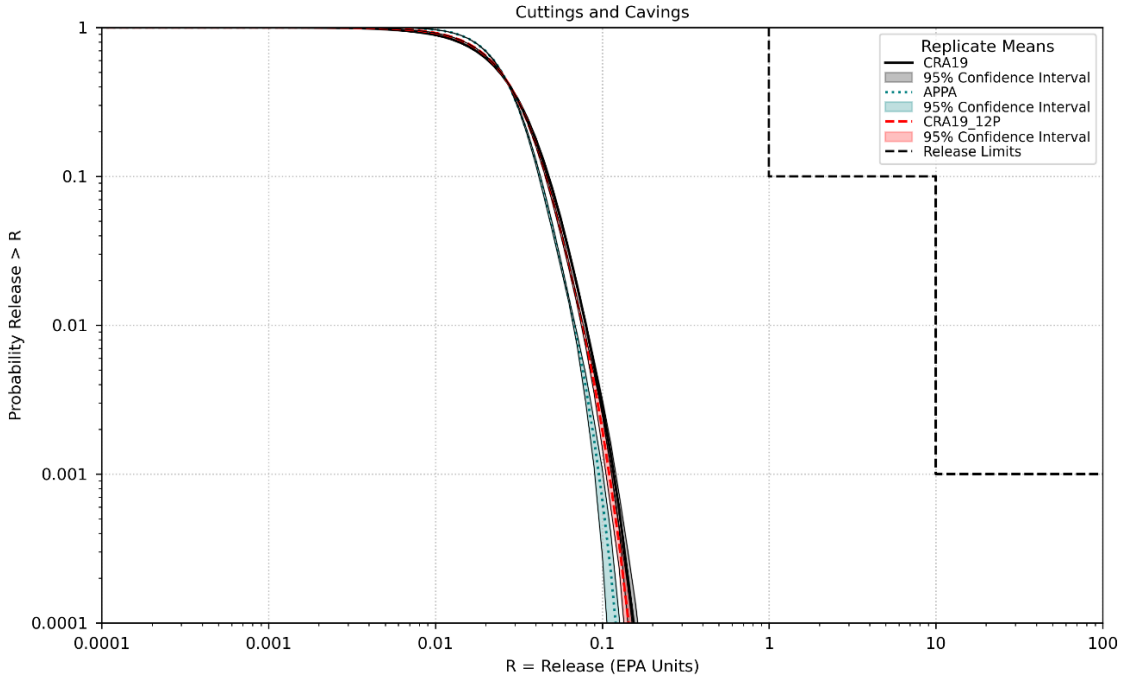

Source: Zeitler et al. 2025, Figure 10-1

Figure 9. Overall mean CCDFs for cuttings and cavings releases from CRA-2019 (CRA19) and CRA19_12P analyses

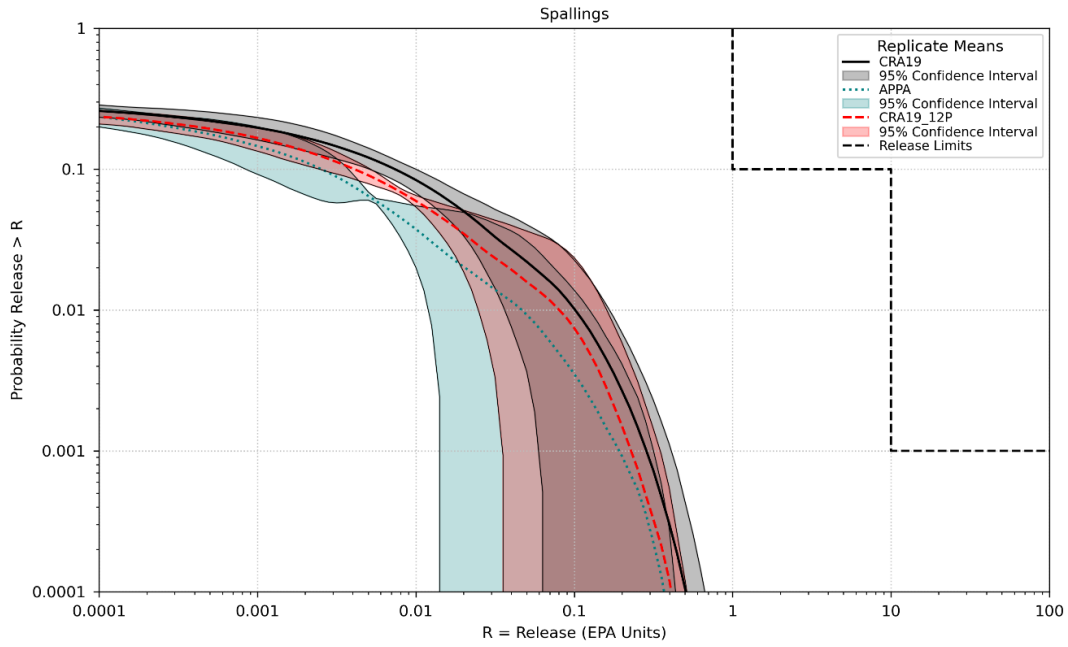

Source: Zeitler et al. 2025, Figure 10-3

Figure 10. Overall mean CCDFs for spalling releases from CRA-2019 (CRA19) and CRA19_12P analyses

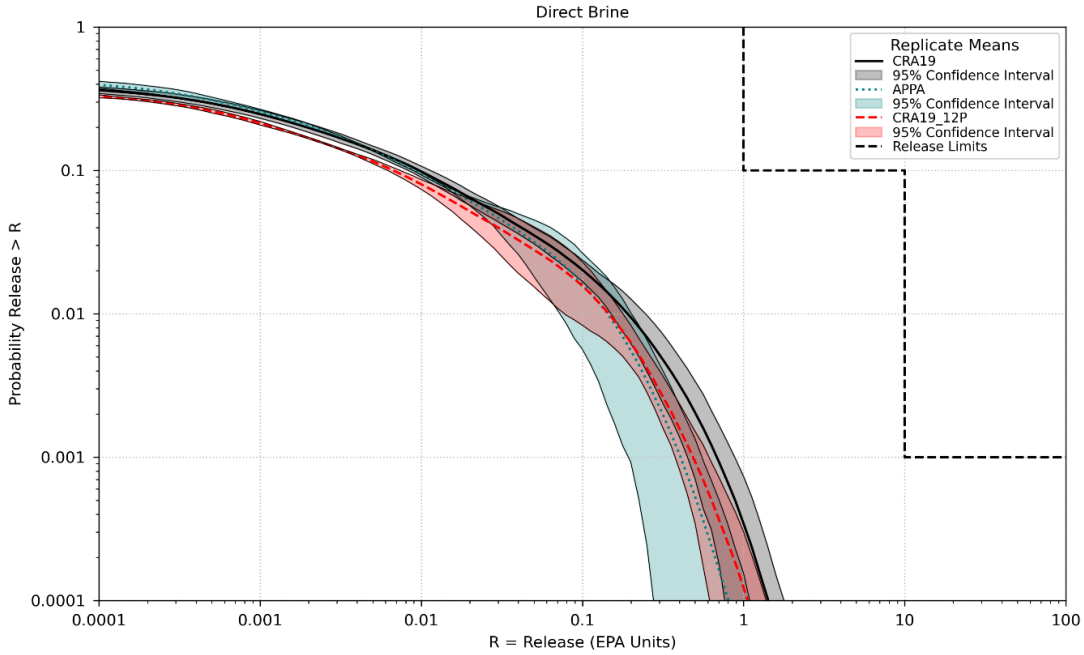

Source: Zeitler et al. 2025, Figure 10-4

Figure 11. Overall mean CCDFs for direct brine releases from CRA-2019 (CRA19) and CRA19_12P analyses

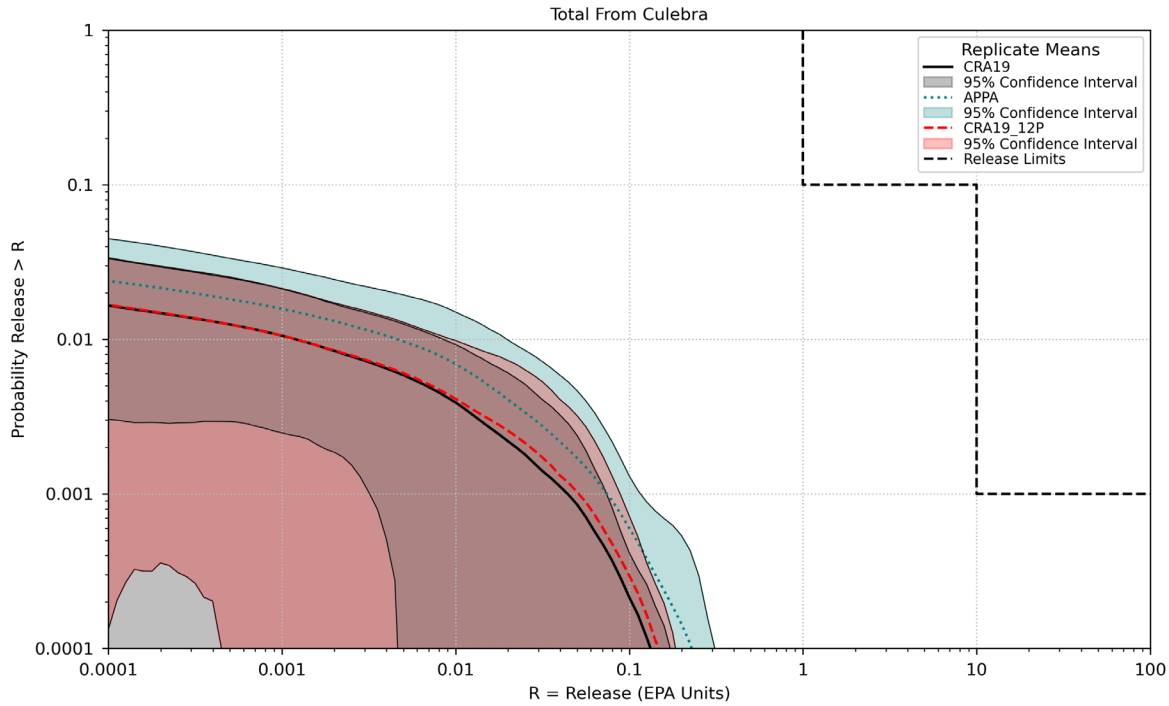

Source: Zeitler et al. 2025, Figure 10-7

Figure 12. Overall mean CCDFs for releases from the Culebra from CRA-2019 (CRA19) and CRA19_12P analyses

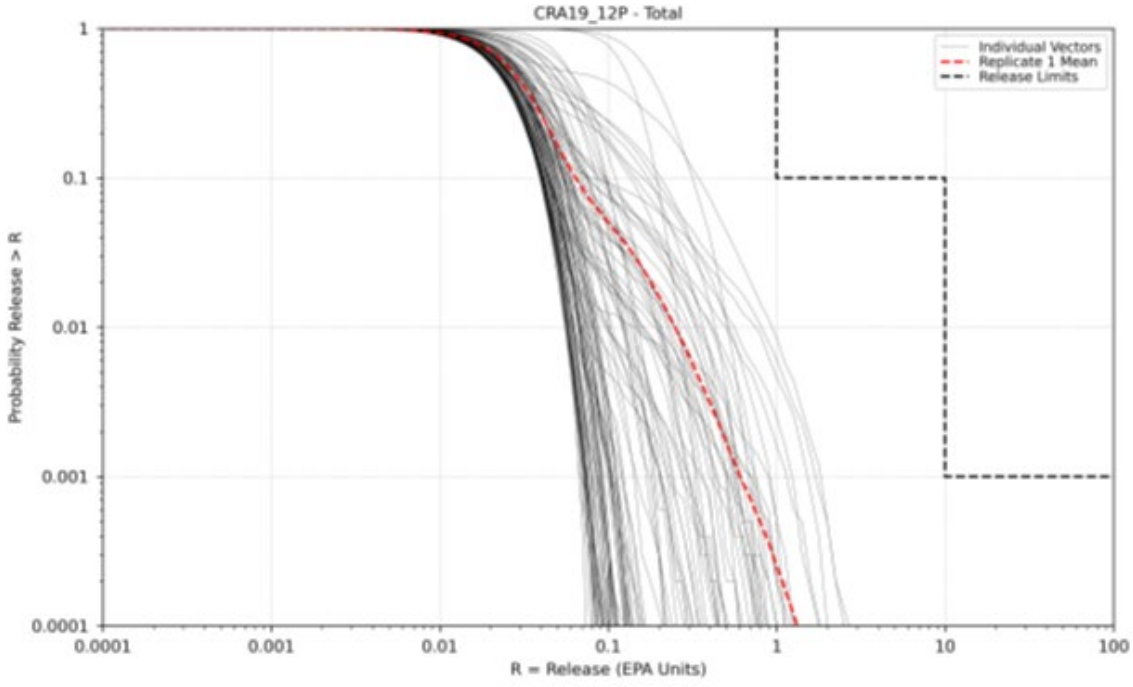

Source: Zeitler et al. 2025, Figure 10-11

Figure 13. Total normalized releases, CRA19_12P Replicate 1

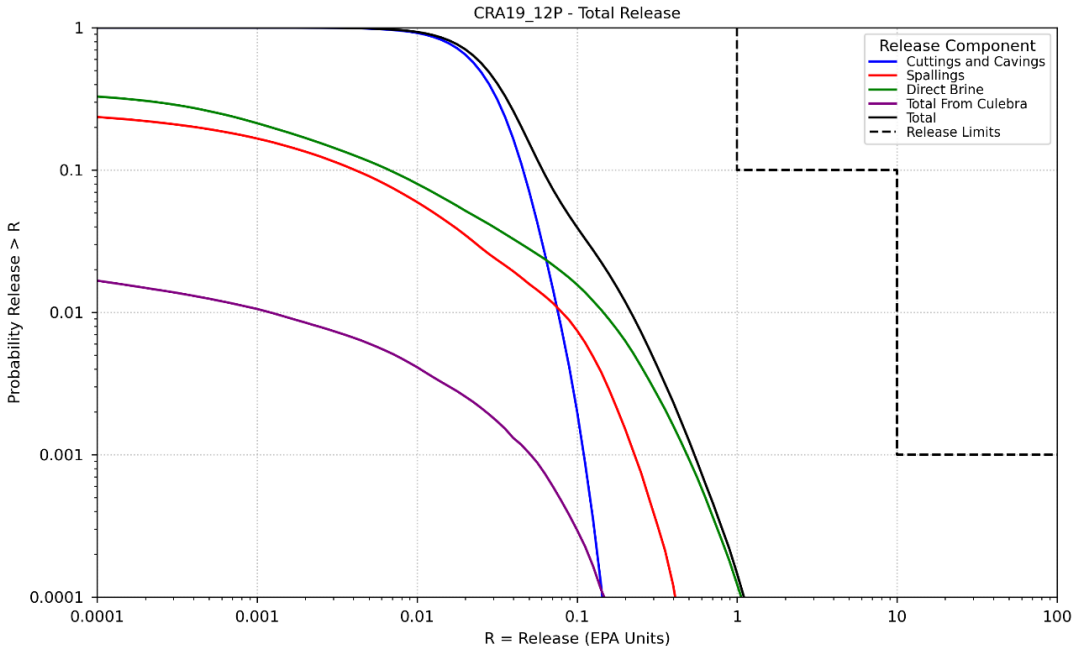

Source: Zeitler et al. 2025, Figure 10-16

Figure 14. Comparison of overall means for major release pathways in the CRA19_12P analysis

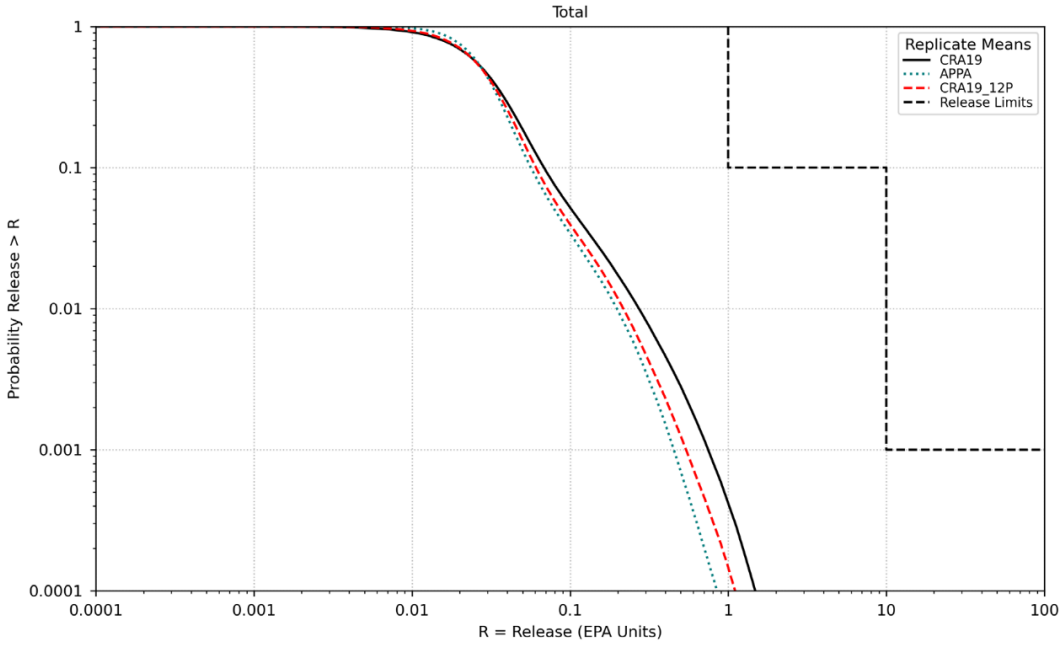

Source: Zeitler et al. 2025, Figure 10-17

Figure 15. Comparison of overall mean total normalized releases for the CRA-2019, APPA, and CRA19_12P analyses

5.0 EPA EVALUATION OF DOE 12-PANEL SENSITIVITY STUDY RESULTS

EPA concurs with the Department's conclusion that the differences between the results for the CRA-2019 PA and the CRA19_12P sensitivity study are minor. EPA notes that the lack of a significant difference could have been expected because the two calculations used similar input parameters and increases in drilling penetrations due to a larger repository footprint were offset by decreases in waste concentration due to a larger repository volume.

As part of its review, EPA identified several concerns that are further discussed in the following subsections and were resolved in the Agency's sensitivity analysis described in Section 6. Section 5.1 describes an inconsistency in the CRA19_12P analysis, where the decrease in waste concentration due to a larger repository volume was addressed but the decrease in iron surface area per unit volume, which is also a function of repository volume in WIPP PA, was not included. Section 5.2 provides a similar discussion where the effect of a larger repository volume on the minimum brine volume needed for a DBR was not included in the analysis. Section 5.3 describes updates in the calculation of borehole drilling rates and plugging frequencies that had been approved by EPA but were not included in the CRA19_12P study. Sections 5.4, 5.5 and 5.6 describe EPA's legacy geochemical concerns with DOE's CRA-2019 PA that were carried over into the CRA19_12P study because the two calculations used the same actinide solubilities, colloid properties, and oxidation state assumptions. The updated parameter values described in Section 5 were used in the Agency's sensitivity analysis described in Section 6.

5.1 Steel Surface Area

For each WIPP PA realization, DOE calculates the anoxic corrosion gas generation rate per cubic meter of repository volume using effective brine saturation and sampled inundated and humid anoxic steel corrosion rates (DOE 2019, Appendix GEOCHEM-2.2). This approach is applied to the surface area of all iron-based metals in the repository. The anoxic steel corrosion gas generation rate in WIPP PA calculations is directly proportional to the steel surface area per unit disposal volume (D_s):

$$q_{rgc} = (R_{ci}\, S_{b,eff} + R_{ch}\, S_g^*)\, D_s\, \rho_{Fe}\, X_C\, (H_2/Fe)\, M_{H2} \qquad \textbf{Equation 1}$$

Where:

q_{rgc} is the rate of gas production per unit volume of waste due to anoxic corrosion of iron-based metals (kg/m^3/sec);

R_{ci} is the corrosion rate under inundated conditions (parameter STEEL:CORRMCO2, m/s);

$S_{b,eff}$ is the effective brine saturation due to capillary action in the waste materials;

R_{ch} is the corrosion rate under humid conditions (parameter STEEL:HUMCORR, m/s);

S_g* equals 1- $S_{b,eff}$ if $S_{b,eff} > 0$, or equals 0 if $S_{b,eff} = 0$;

D_s is the steel surface area per unit disposal volume in the repository (11.2 m^2/m^3), calculated for the CRA-2019 PA from the parameters REFCON:ASDRUM (6 m^2/drum), REFCON:DRROOM (6,800 drums/room), and REFCON:VROOM (3,640 m^3/room);

ρ_{Fe} is the molar density of steel calculated from the density of iron (parameter REFCON:DN_FE) and the molecular weight of iron (parameter REFCON:MW_FE);

X_C (H_2|Fe) is the stoichiometric coefficient for gas generation due to the corrosion of steel (1 mole H_2 per mole Fe, parameter STEEL:STOIFX, Kim and Feng 2019)]; and

M_{H2} is the molecular weight of H_2 (parameter REFCON:MW_H2, kg H_2 per mole H_2).

The CRA-2019 PA repository volume (REFCON:VREPOS) of 4.38×10^5 m^3 increased to 5.31×10^5 m^3 for the CRA19_12P PA (Zeitler et al. 2025). The increased repository volume decreases D_s because the same inventory is distributed into two replacement panels. This will cause lower predicted anoxic corrosion gas generation and brine consumption rates. As noted in Section 4.2, Zeitler et al. (2025) did not revise D_s for the CRA19_12P PA to account for the increased repository volume. EPA recalculated D_s for the Agency's 12-panel repository sensitivity study to assess the possible effects of decreased D_s on predicted repository performance.

The CRA19_12P PA used the same waste inventory as the CRA-2019 PA. The WIPP waste inventory provides the total masses of iron-based metals in the waste and in the packaging materials (Table 5) but does not provide the surface areas. EPA separately calculated the steel surface area for waste packaging in the 12-panel repository using the numbers of each waste container type in the CRA-2019 PA inventory and the surface areas reported for each waste container type (Table 6).

Table 5. Mass of iron-based metals in the CRA-2019 PA inventory

Parameter	(kg)	(%)
CH Waste Iron-Based Metal and Alloys	14,100,000	22
CH Steel Packaging Materials	31,200,000	50
RH Waste Iron-Based Metal and Alloys	1,330,000	2
RH Steel Packaging Materials	16,500,000	26
Repository Total	63,130,000	100

Source: Van Soest 2018, Table 5-5

EPA approximated the iron-based metal surface area for the repository waste using two bounding assumptions about the configuration of the iron-based metal waste. One bounding assumption is that all iron-based metal waste has the same surface area to mass ratio as 1-cm diameter spheres, which provides a lower limit for the waste surface area to mass ratio (Day 2015). Because a large percentage of iron-based metal waste in the repository is compressed drums in waste from the Advanced Mixed Waste Treatment Facility, EPA (2017) developed the second bounding assumption that all iron-based metal waste has the surface area to tare weight ratio of a 55-gallon drum. This 55-gallon drum assumption provides an upper bound for

the iron-based metal waste surface area to mass ratio. These ratios can then be used with the WIPP inventory mass data (Table 5) to estimate reasonably bounding values for the total iron-based waste surface area (Table 7).

Table 6. Container surface areas in the CRA-2019 PA inventory

Container Type	Number of containers	Container surface area (m^2) - outer and overpacked containers	Repository total container surface area (m^2)
55GD	335,409	4.58	1,536,173
POP 12-in	25,626	6.34	162,469
POP S100	814	6.34	5,161
POP S300	45	6.34	285
85GD OP	5	10.92	55
100GD	42,414	6.62	280,781
SWB DL	13,689	21.93	300,200
SWB OP	6,662	40.23	268,012
SLB2	682	52.58	35,860
TDOP DL	32	31.42	1,005
TDOP OP	8,553	77.19	660,206
SCA	31,942	8.98	286,839
FLC DL	18	14.06	253
FRLC DL	1	14.06	14
RLC OP	700	27.79	19,453
Shield Plug	179	10.18	1,822
Repository total packaging steel surface area			3,558,588

Source: LANL 2018, Appendix A

The average of the iron-based waste surface areas calculated using the two surrogate bounding assumptions is 1,823,662 m^2. Adding this average waste iron-based metal surface area to the total steel packaging surface area (3,558,588 m^2, Table 6) yields an average repository total steel surface area of 5,382,250 m^2 (Table 7). Dividing the average repository total waste plus packaging steel surface area by the 12-panel repository volume of 5.31×10^5 m^3 yields D_s:

$$D_s = \frac{5{,}382{,}250\ m^2}{5.31 \times 10^5\ m^3} = 10.1\ m^2/m^3 \qquad \textbf{Equation 2}$$

The D_s value calculated for the 12-panel repository volume is 10 percent less than the D_s value used in the CRA19_12P PA (Table 8).

Table 7. Estimated total iron-based waste and packaging surface areas in the CRA19_12P PA waste inventory

Waste Surrogate Assumption	Waste Surface Area (m^2/kg)	Repository Total Waste Surface Area (m^2)	Repository Total Waste Plus Packaging Steel Surface Area (m^2)
Low estimate: 1-cm diameter iron spheres	0.0762	1,176,366	4,734,954
High estimate: 55-gallon drum	0.160	2,470,958	6,029,546
Average estimate	0.118	1,823,662	5,382,250

Table 8. Comparison of CRA-2019 PA and CRA19_12P PA steel surface areas per unit disposal volume

Performance Assessment	Waste Plus Packaging Steel Surface Area to Mass Ratio (m^2/kg)	Repository Total Waste Plus Packaging Steel Surface Area (m^2)	Steel Surface Area per Unit Disposal Volume (D_s. m^2/m^3)
CRA-2019 PA and CRA19_12P PA	0.0941	5,942,726	11.2
EPA Sensitivity Study	0.0853	5,382,250	10.1

In both the CRA-2019 and CRA19_12P PAs, the database parameters REFCON:ASDRUM (6 m^2/drum), REFCON:DRROOM (6,800 drums/room), and REFCON:VROOM (3,640 m^3/room) were used to calculate D_s:

$$D_S = \frac{A_d n_d}{V_R} \qquad \textbf{Equation 3}$$

Where:

A_d is the surface area of steel associated with a waste disposal drum (parameter REFCON:ASDRUM, m^2/drum),

V_R is the initial volume of a single room in the repository (parameter REFCON:VROOM, m^3), and

n_d is the ideal number of waste drums that can be closely packed into a single room (parameter REFCON:DRROOM).

Because the number of drums per room is an operational parameter, it is reasonable to adjust this value to achieve the required D_s value for EPA sensitivity study calculations. If D_s is 10.1 m^2/m^3 and VROOM and ASDRUM are held constant, n_d can be calculated:

$$n_d = \frac{V_r D_s}{A_d} = \frac{3{,}640\ {}^{m^3}/_{room} \times 10.1\ {}^{m^2}/_{m^3}}{6\ {}^{m^2}/_{drum}} = 6{,}127\ {}^{drums}/_{room} \qquad \textbf{Equation 4}$$

For EPA's sensitivity study, the REFCON:ASDRUM and REFCON:VROOM parameters remained unchanged at 6 m^2/drum and 3,640 m^3/room, respectively, and REFCON:DRROOM was set equal to 6,127 drums/room to achieve a D_s value of 10.1 m^2/m^3.

5.2 Minimum Brine Volume

Zeitler et al. (2025) used the CRA-2019 PA minimum total repository brine volume necessary for a DBR in the CRA19_12P PA calculations. The CRA-2019 PA minimum total brine volume is smaller than the 12-panel CRA19_12P PA minimum total brine volume because of the larger 12-panel repository volume. Use of the smaller minimum brine volume in the CRA19_12P PA calculations has a conservative effect on DBRs because a smaller minimum brine volume increases calculated baseline dissolved actinide solubilities used in WIPP PA.

DOE uses the minimum brine volume and WIPP inventory data to calculate organic ligand concentrations for the baseline Am(III), Th(IV), and Np(V) solubility calculations. The baseline actinide solubilities are calculated for WIPP brines assuming that the organic ligands inventory in the WIPP waste is dissolved in brine volumes equal to the minimum brine volume and in brine volumes up to five times the minimum brine volume. Larger multiples of the minimum brine volume result in lower baseline dissolved Am(III) and Np(V) concentrations because of increasing dilution of the organic ligands. Baseline dissolved Th(IV) concentrations are minimally affected by the increasing minimum brine volumes.

Use of the smaller CRA-2019 PA minimum brine volume for the CRA19_12P PA calculations resulted in less dilution of the organic ligands inventory, and in slightly higher predicted baseline dissolved Am(III) and Np(V) concentrations in the CRA19_12P PA than if the larger 12-panel repository minimum brine volume was used. As noted by Zeitler et al. (2025), these higher concentrations contribute to a conservative estimate of DBR releases in the CRA19_12P PA. Because of this conservatism, the CRA-2019 PA baseline actinide solubilities were retained for EPA's 12-panel sensitivity study.

5.3 Borehole Drilling Rate and Plugging Probabilities

The number of boreholes drilled and how they are plugged and abandoned is used to derive parameters that impact releases in PA. The drilling rate is the areal density of boreholes that would occur in the Delaware Basin after 10,000 years if the average annual rate of borehole drilling in the basin over the past 100 years continued unchanged for the next 10,000 years. Deep wells are defined as those greater than or equal to the depth of the repository. Shallow wells do not reach repository depth and do not affect repository performance. Increases in the deep drilling rate in PA increases the number of inadvertent drilling intrusions into the repository. Borehole plugging patterns describe the lengths and locations of the plugs, and the frequency of the types of plugs installed since 1988 is used to assign probabilities to plugging patterns that could be used in future boreholes.

These parameters are derived from data collected by the Delaware Basin Drilling Surveillance Program (DBDSP). EPA closely reviews the data collected by the DBDSP and reported annually in the Delaware Basin Monitoring Annual Reports (DBMARs). Data reported in the DBMARs are used to derive input parameters in PA and for FEPs and other purposes. For the CRA19_12P PA,

the Department used many of the assumptions and parameter values from the CRA-2019 PA, including the drilling rates and borehole plugging pattern probabilities (Zeitler et al. 2025).

In its previous review of the CRA-2019 PA, EPA noted several concerns with the deep drilling rate calculation and changes made to the method used to calculate borehole plugging pattern probabilities. These concerns are discussed at length with recommended resolutions in a Technical Support Document (EPA 2022e) prepared for EPA's CRA-2019 PA review. For that review, EPA also conducted sensitivity studies to evaluate the impacts of these parameters on PA. DOE made additional changes to the methodologies subsequent to the CRA-2019 PA, and these were incorporated in later DBMARs and in the RPPCR 19 Panel PA.

In reviewing the CRA19_12P PA, EPA chose to run its own sensitivity study using the most recent DOE (2024b) data for the deep drilling rate and borehole plugging pattern probabilities (Table 9). The principal concern in the drilling rate calculation was DOE's non-conservative assumption that all wells of unknown depth were shallow until complete information was made available from the various regulatory agencies and databases utilized by the DBDSP. DOE revised this assumption in the 2024 DBMAR and adopted EPA's recommendation of adding boreholes of unknown depth to the deep drilling rate calculation after applying a scaling factor based on the ratio of known deep to total known depth boreholes in the basin.

Table 9. Borehole parameters used in EPA sensitivity study, based on DBMAR 2024.

Parameter	Description	Units	Value
GLOBAL:LAMDAD	Deep drilling rate per unit area	km^{-2}	153.4
GLOBAL:ONEPLG	Probability of having Plug Pattern 1 (full plug)		0.3590
GLOBAL:TWOPLG	Probability of having Plug Pattern 2		0.4635
GLOBAL:THREEPLG	Probability of having Plug Pattern 3		0.1775

Another minor change to the calculations subsequent to the CRA-2019 PA adjusted the cutoff for categorizing between deep and shallow drilling from 2,150 feet to 2,104 feet. This was done to reflect the completion of mining of Panel 8 at 2,104 feet in 2022 due to the slight eastward stratigraphic dip of the repository layer. For DBMAR 2024, the deep drilling rate was calculated as 153.4 boreholes per km^2 per 10,000 years, which is more than triple the value calculated for the first WIPP compliance certification application. EPA used this number in its sensitivity study (Table 9).

Ongoing discussions with EPA following the CRA-2019 review led DOE to propose using the 9-township area surrounding WIPP and within the Delaware Basin as the region over which data on borehole plugging pattern frequencies would be gathered and used to calculate probabilities in PA. This is in contrast with the prior approach that used the entire New Mexico portion of the Delaware Basin. The 9-township area is already used by the DBDSP as a focus area over which information is gathered and other drilling-related parameters are derived. An expanded discussion of this change is documented in Day (2023). For PA purposes, the six plugging

configurations reported by the DBDSP are translated into three groups using the following scheme defined by Thompson et al. (1996) for the CCA and used to the present (Brunnell 2023):

Type VI = GLOBAL:ONEPLG

Types I, III, and V = GLOBAL:TWOPLG

Types II and IV = GLOBAL:THREEPLG

EPA used the plugging frequencies from DBMAR 2024 to calculate the probabilities as listed in Table 9 for its sensitivity study.

5.4 Dissolved Actinide Solubilities

Actinides mobilized in WIPP brine as dissolved species are modeled for each realization in WIPP PA using baseline actinide solubilities combined with sampled +III and +IV dissolved actinide uncertainty distributions. Zeitler et al. (2025) used the baseline actinide solubilities (Table 10) and dissolved actinide uncertainty distributions from the CRA-2019 PA in the CRA19_12P PA calculations.

Table 10. Actinide solubility calculations for the CRA-2019 PA, and Agency sensitivity calculations (minimum brine volume)

Property or Actinide Oxidation State	CRA-2019 PA		EPA Sensitivity Calculations	
Brine	Salado (GWB)	Castile (ERDA-6)	Salado (GWB)	Castile (ERDA-6)
III (M)	1.63×10^{-7}	1.78×10^{-7}	2.14×10^{-6}	1.43×10^{-6}
IV (M)	5.45×10^{-8}	5.44×10^{-8}	5.50×10^{-8}	5.84×10^{-8}
V (M)	4.02×10^{-7}	1.20×10^{-6}	4.38×10^{-7}	1.82×10^{-6}
VI (M)[a]	1×10^{-3}	1×10^{-3}	1×10^{-3}	1×10^{-3}

a – DOE did not develop a solubility model for the +VI actinides. Therefore, for all PAs, DOE assumed a fixed concentration for U(VI), which is the only +VI actinide predicted to be present in the WIPP repository in significant concentrations.

5.4.1 Baseline Actinide Solubilities

The Agency's review of the CRA-2019 PA (EPA 2022d, Section 7.4) identified significant issues with DOE's calculation of the baseline actinide solubilities that were reused in the CRA19_12P PA, including:

- Inconsistencies in the aqueous speciation data in the DATA0.FM4 EQ3/6 database that caused significantly underestimated baseline +III actinide solubilities,
- DOE's assumption that calcite precipitation would proceed to equilibrium, the assumed amounts of polyhalite in the Salado Formation, and the use of Phase 5 solubility data in DATA0.FM4 that caused excessive brine consumption, and

- DOE's inclusion of lead aqueous species and solid phases in the calculations without including Pitzer parameters in DATA0.FM4 and omitting lead solid phases that could precipitate under WIPP repository conditions.

EPA (2022d) did not accept the CRA-2019 PA baseline actinide solubility parameters because of these issues. EPA (2022d, Section 7.4.10) recalculated the baseline dissolved actinide solubilities in Salado Formation generic weep brine (GWB) and Castile Formation brines from borehole ERDA-6 using the PHREEQC geochemical modeling code and an EPA-revised WIPP database that addressed the DATA0.FM4 aqueous speciation data issues. The Agency also addressed likely calcite oversaturation in WIPP brines by assuming aragonite would form instead of calcite in these calculations. Because of database issues associated with iron and lead, the Agency did not include these constituents in its recalculation of the baseline actinide solubilities. The Agency's calculations resulted in baseline +III actinide solubilities that increased by approximately an order of magnitude over the CRA-2019 PA concentrations (Figure 16) and less consumption of water. The Th(IV) and Np(V) dissolved concentrations, calculated using the revised EPA database and modified assumptions, increased only slightly from the CRA-2019 PA concentrations.

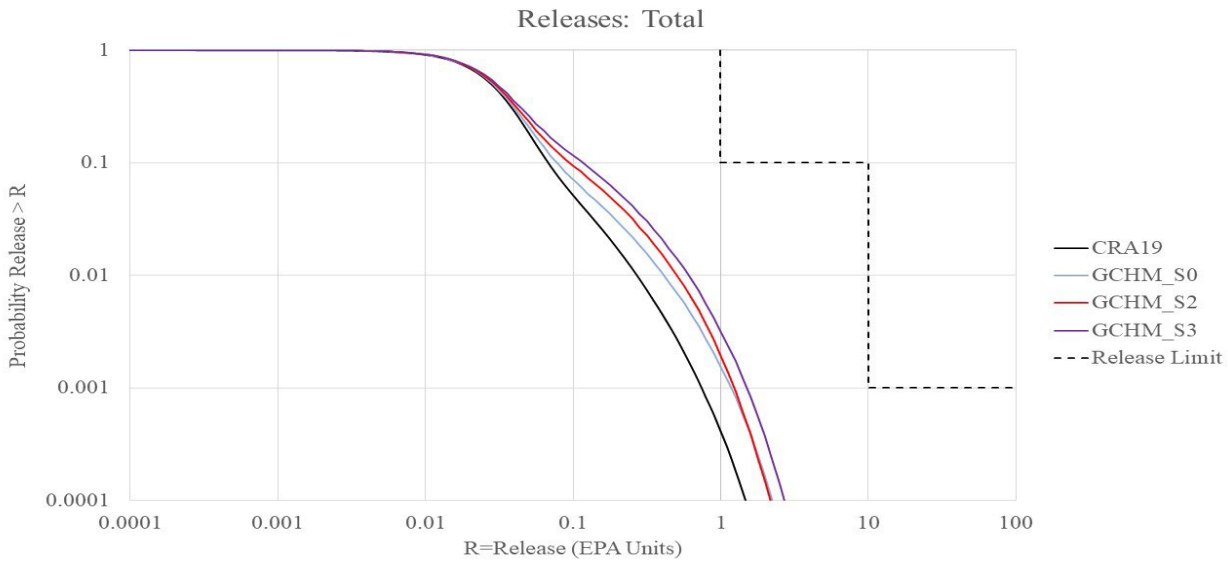

Source: EPA 2022d, Figure 13-4

Figure 16. Mean total repository releases calculated for the CRA-2019 PA (CRA19); the baseline actinide solubility sensitivity calculation (GCHM_S0); the baseline actinide solubility plus intrinsic and microbial colloid sensitivity calculation (GCHM_S2); and the sensitivity calculation combining revised baseline actinide solubility, revised intrinsic and microbial colloid, and revised actinide oxidation state parameters (GCHM_S3)

EPA (2022d, Section 13.2) performed sensitivity PA calculations during the CRA-2019 PA review to evaluate the effects of the increased dissolved +III actinide solubility parameters on predicted repository releases. The increased Am(III) and Pu(III) concentrations calculated by the Agency were included in four sensitivity PA calculations (Figure 16).The increased Am(III) and Pu(III) baseline solubilities alone increased mean total releases approximately 1.6-fold relative to the CRA-2019 PA but only at low probabilities because total releases are dominated by cuttings and cavings at higher probabilities (GCHM_S0, Figure 16). The issues associated with the CRA-2019 PA baseline actinide solubilities visibly increased releases and were therefore also addressed in the Agency's CRA19_12P sensitivity calculations by using EPA's (2022d) recalculated baseline actinide solubilities (Table 10).

5.4.2 Dissolved Actinide Solubility Uncertainty Distributions

The baseline actinide solubilities used in WIPP PA are constants. DOE accounts for uncertainties in these solubilities in each PA realization by sampling a CDF representing uncertainty and multiplying the solubilities by the antilog of the sampled value to determine the actinide concentrations. DOE develops the CDFs by comparing experimentally measured solubility data reported in the literature with concentrations predicted using EQ3/6 for the conditions of the experiments. DOE calculates difference values (D) between the predicted (S_p) and measured (S_m) solubilities using the equation:

$$D = log_{10}S_m - log_{10}S_p \qquad \textbf{Equation 5}$$

The difference value is negative if the calculated solubility is greater than the measured solubility, positive if the calculated solubility is less than the measured solubility, and zero if the calculated and measured solubilities are equal.

Zeitler et al. (2025) used the +III and +IV dissolved actinide solubility uncertainty distributions from the CRA-2019 PA for the CRA19_12P PA. EPA (2022d) accepted the CRA-2019 PA +IV actinide solubility uncertainty distribution because it included all experimental data that met the selection criteria, and it provided an adequate representation of the +IV actinide solubility uncertainty. Use of the CRA-2019 PA +IV actinide solubility distribution for the CRA19_12P PA therefore remains appropriate.

EPA (2022d) noted that the CRA-2019 PA +III actinide solubility uncertainty distribution was relatively equally distributed into two groups: lower difference values that are reasonably representative of crystalline $Am(OH)_3(s)$ solubility, and higher difference values that are more representative of less-crystalline, fine-grained $Am(OH)_3(s)$. EPA (2022d) found that this distribution of difference values adequately represented the uncertainty regarding the crystallinity of +III actinide solids in the long-term WIPP repository.

EPA (2022d) identified three literature publications with experimental $Nd(OH)_3(s)$ solubility data that should have been evaluated during the development of the CRA-2019 PA +III actinide solubility distribution. In response to a request from the Agency, DOE developed an updated

+III actinide solubility uncertainty distribution that combined difference values from the three recent investigations with difference values included in the CRA-2019 PA uncertainty distribution. However, EPA (2022d) did not recommend using this revised +III actinide solubility uncertainty distribution in future WIPP PAs, because it includes a relatively high proportion of difference values calculated with more-soluble, microcrystalline solids, and likely provides an overly conservative estimate of the uncertainty associated with the baseline +III actinide solubilities. Consequently, the Agency finds DOE's use of the CRA-2019 PA +III actinide solubility uncertainty distribution in the CRA19_12P PA to be acceptable. Future WIPP PAs will require re-evaluation of both the +III and +IV actinide solubility uncertainty distributions to account for changes in the EQ3/6 modeling database and in the available experimental data.

5.5 Colloids

WIPP PA calculations include the assumption that four types of colloids can form and be mobilized in WIPP repository brines:

- Mineral fragment colloids,
- Intrinsic colloids,
- Humic colloids, and
- Microbial colloids.

Zeitler et al. (2025) used the CRA-2019 PA colloid parameters for the CRA19_12P PA. EPA (2022d) reviewed the CRA-2019 PA colloid parameters and concluded that the mineral fragment colloid parameters were consistent with the available data. The Agency also found that intrinsic colloid parameters for uranium, neptunium, and plutonium and all humic colloid parameters provide reasonable upper bounds for these colloids under WIPP repository conditions. However, the Agency did not accept the CRA-2019 PA intrinsic colloid parameters for americium and thorium or any of the microbial colloid parameters.

5.5.1 Intrinsic Colloids

EPA (2022d) compared the CRA-2019 PA intrinsic colloid parameters (CONCINT) to available experimental sequential filtration data and found that the CRA-2019 PA parameters for U(IV), U(VI), Np(IV), Np(V), Pu(III), and Pu(IV) intrinsic colloids are consistent with the available data. EPA (2022d) determined that the CRA-2019 PA Am(III) intrinsic colloid parameter should be increased based on the results of sequential filtration data provided by Reed et al. (2013). EPA (2022d) also found that the Th(IV) intrinsic colloid parameter should be increased to adequately bound sequential filtration data reported by Borkowski (2012). The Th(IV) and Am(III) intrinsic colloid parameter values selected by EPA (2022d) for the Agency's CRA-2019 PA sensitivity calculations (GCHM_S2 and COMB) are summarized in Table 11. These parameter values are more defensible than the CRA-2019 PA parameter values because they bound the available data and were therefore also used in the Agency's CRA19_12P PA sensitivity calculations.

Table 11. Actinide concentrations associated with intrinsic colloids (parameter CONCINT) used in the CRA-2019 PA and in Agency sensitivity calculations for the CRA-2019 PA and the CRA19_12P PA

Actinide	DOE CRA-2019 PA	Agency Sensitivity Calculations
Th(IV) (M)	4.3×10^{-8}	4.8×10^{-7}
U(IV) (M)	1.4×10^{-6}	1.4×10^{-6}
U(VI) (M)	1.4×10^{-6}	1.4×10^{-6}
Np(IV) (M)	4.3×10^{-8}	4.3×10^{-8}
Np(V) (M)	4.3×10^{-8}	4.3×10^{-8}
Pu(III) (M)	4.3×10^{-8}	4.3×10^{-8}
Pu(IV) (M)	4.3×10^{-8}	4.3×10^{-8}
Am(III) (M)	9.5×10^{-9}	6.7×10^{-7}

5.5.2 Microbial Colloids

Microbial colloid concentrations are calculated in WIPP PA using a proportionality constant (PROPMIC) that is multiplied by the dissolved actinide solubility within a PA realization, with a maximum value (CAPMIC). As part of its review of CRA-2019, EPA (2022d, Section 8.3.4) undertook an independent study to understand how the CRA-2019 PA microbial colloid parameters compare to the broader literature. Literature included in this investigation specifically examined experiments and studies of microbial associations with actinides (such as uranium, thorium, plutonium, and americium), and analogs (such as rare earth elements like neodymium and europium) over a very wide range of salinities, pH values, and other geochemical parameters.

EPA (2022d) calculated PROPMIC values using data extracted from the literature following DOE's formula (Equation 6):

$$PROPMIC = \frac{[Actinide\ or\ Analog\ Sorbed]}{[Dissolved\ Actinide\ or\ Analog]} \qquad \textbf{Equation 6}$$

EPA (2022d) determined that most CRA-2019 PA PROPMIC values were significantly lower than the literature PROPMIC values.

For future WIPP PAs, EPA (2022d) recommended using the CCA americium, thorium, neptunium, and uranium PROPMIC values (Table 12) because these values bound the variability found in the literature. For Pu(III) and Pu(IV), EPA recommended a PROPMIC value of 2.18 as it bounds 75 percent of the data in the literature and omits outliers. The PROPMIC values recommended by EPA (2022d) are summarized in Table 12.

Cell counts in the literature surveyed by EPA (2022d, Section 8.3.4) did not exceed the 10^9 cells/ml biomass value measured by Reed et al. (2013) that was used to calculate CAPMIC for the CRA-2019 PA. EPA (2022d) recalculated significantly higher CAPMIC parameters using data

from Papenguth (1996) and 10^9 cells/ml biomass. EPA (2022d) noted that these recalculated values would be more defensible than the CRA-2019 PA CAPMIC parameter values in future WIPP PAs until more data can be collected in WIPP-specific experiments. The recalculated PROPMIC and CAPMIC values were used in the Agency's CRA-2019 PA sensitivity study (Table 12).

Table 12. Proportionality constants and maximum concentrations for microbial colloids

	Proportionality Constant Microbes[a] (Parameter PROPMIC)			Maximum Sorbed by Microbes (M, Parameter CAPMIC)		
Actinide	**CCA**	**CRA-2019 PA**	**Agency Sensitivity Calculations**	**CCA**	**CRA-2019 PA**	**Agency Sensitivity Calculations**
Th(IV)	3.1	0.21	3.1	0.0019	3.8×10^{-8}	2.12×10^{-2}
U(IV)	0.0021	0.21	0.0021	0.0021	3.8×10^{-8}	8.14
U(VI)	0.0021	0.21	0.0021	0.0023	3.8×10^{-8}	8.14
Np(IV)	12.0	0.21	12.0	0.0027	3.8×10^{-8}	1.27×10^{-4}
Np(V)	12.0	0.21	12.0	0.0027	3.8×10^{-8}	1.27×10^{-4}
Pu(III)	0.3	0.21	2.18	6.8×10^{-5}	3.8×10^{-8}	2.18×10^{-5}
Pu(IV)	0.3	0.21	2.18	6.8×10^{-5}	3.8×10^{-8}	2.18×10^{-5}
Am(III)	3.6	0.03	3.6	NA[b]	2.3×10^{-9}	6.28×10^{-6}

a – Units of moles colloidal actinide per mole dissolved actinide

b – Not applicable

Sources: DOE 1996, Appendix SOTERM, Table SOTERM-14; DOE 2014, Appendix SOTERM, Table SOTERM-21; DOE 2019, Appendix SOTERM, Table SOTERM-9

EPA (2022d) performed sensitivity calculations during the CRA-2019 PA review to evaluate the effects of the increased intrinsic and microbial colloid parameters on predicted repository releases. The Agency's sensitivity calculation GCHM_S2 combined the intrinsic and microbial colloid parameter changes with the increased baseline actinide solubilities used in the GCHM_S0 calculation (Figure 16). The combination of colloid parameter changes with higher baseline solubilities did not affect total releases at high probabilities, where releases are dominated by cuttings and cavings. The colloid parameter changes incorporated in the GCHM_S2 calculation slightly increased releases in the probability range from 0.001 to ~ 0.5 relative to the GCHM_S0 calculated releases, so the colloid parameter changes were also included in the Agency's CRA19_12P PA sensitivity calculations.

5.6 Actinide Oxidation States

For the CRA-2019 and CRA19_12P PAs, DOE assumed equal probabilities that aqueous and solid-phase plutonium, neptunium, and uranium will be present in either their more reduced oxidation states [Pu(III), Np(IV), and U(IV)] or in their more oxidized states [Pu(IV), Np(V), and U(VI)]. Neptunium and uranium do not contribute significantly to repository releases, so only the plutonium oxidation state affects PA results. EPA (2022d) evaluated the available data during the CRA-2019 PA review and concluded that it is highly likely that plutonium

concentrations in WIPP brines will be controlled by the solubility of Pu(III) solids in equilibrium with Pu(III) aqueous species. The assumption that Pu(III) solids dominate dissolved plutonium concentrations in repository brines therefore provides more defensible predictions of total mobilized plutonium concentrations in WIPP brines, so the Agency included this assumption in its CRA-2019 PA sensitivity study calculation GCHM_S3 (EPA 2022d, Section 13.2.4) and also included this assumption in its CRA19_12P PA sensitivity study.

The assumption that aqueous and solid-phase actinides will be present in their more reduced oxidation states for all PA realizations was included in the Agency's CRA-2019 PA sensitivity calculation GCHM_S3 to evaluate the effects of the reduced plutonium oxidation state assumption on predicted repository releases (EPA 2022d). Sensitivity calculation GCHM_S3 also included the increased baseline actinide solubilities, increased intrinsic colloid concentrations, and increased microbial colloid concentrations used in GCHM_S2, so comparison of the results of these calculations demonstrates the effects of the revised actinide oxidation states assumption (Figure 16). The assumption that Pu(III) aqueous and solid phases would be present in the repository resulted in increased mean total repository releases at low probabilities, so this assumption was also included in the Agency's CRA19_12P sensitivity calculations.

6.0 EPA 12-PANEL PA COMBINED SENSITIVITY ANALYSES

6.1 Analysis Methodology

DOE prepared the CRA19_12P PA Sensitivity Study to evaluate the effects of increasing the number of waste panels from ten to twelve on WIPP performance. The study was modeled after the Department's CRA-2019 PA and includes many of the assumptions and parameter values in that PA. For the RPPCR review, EPA performed its own calculation, called the RPPCR_12P Sensitivity Analysis, which is based on the CRA19_12P PA, to determine the sensitivity of releases to the issues EPA identified in Section 5. EPA's sensitivity analysis followed the Agency's Quality Assurance Project Plan (QAPP) developed during its CRA-2019 review, allowing the results to be used in supporting regulatory decisions (EPA 2022a). The QA checks are provided in Section 6.2 as screenshots to confirm that the parameter changes have been included in the calculation.

The parameter modifications for this RPPCR_12P PA Sensitivity Analysis are discussed in Section 5 of this report and summarized below in comparison to DOE's CRA19_12P PA.

Table 13. Borehole Drilling Rate and Plugging Probabilities

Material	Property	Description	Units	CRA19_12P	RPPCR_12P
GLOBAL	LAMBDAD	Drilling rate per unit area	$km^{-2}yr^{-1}$	9.90E-3	1.534E-2
GLOBAL	ONEPLG	Probability of having Plug Pattern 1		4.03E-1	3.590E-1
GLOBAL	TWOPLG	Probability of having Plug Pattern 2		3.31E-1	4.635E-1
GLOBAL	THREEPLG	Probability of having Plug Pattern 3		2.66E-1	1.775E-1

Table 14. Colloid Parameters

Parameter	Units	CRA19_12P	RPPCR_12P
AM:CONCINT	M	9.50E-09	6.70E-07
TH:CONCINT	M	4.30E-08	4.80E-07
AM:CAPMIC	M	2.30E-09	6.28E-06
NP:CAPMIC	M	3.80E-08	1.27E-04
PU:CAPMIC	M	3.80E-08	2.18E-05
TH:CAPMIC	M	3.80E-08	2.12E-02
U:CAPMIC	M	3.80E-08	8.14E+00
AM:PROPMIC	none	0.3	3.6
NP:PROPMIC	none	0.21	12
PU:PROPMIC	none	0.21	2.18
TH:PROPMIC	none	0.21	3.1
U:PROPMIC	none	0.21	0.0021

Table 15. Actinide Solubility

Actinide	Brine	Brine Volume	Units	Parameter	CRA19_12P	RPPCR_12P
Am(III)	Salado	1X	M	SOLMOD3:SOLSOH	1.63E-07	2.139E-06
Am(III)	Salado	2X	M	SOLMOD3:SOLSOH2	1.58E-07	1.091E-06
Am(III)	Salado	3X	M	SOLMOD3:SOLSOH3	1.56E-07	7.721E-07
Am(III)	Salado	4X	M	SOLMOD3:SOLSOH4	1.55E-07	6.180E-07
Am(III)	Salado	5X	M	SOLMOD3:SOLSOH5	1.54E-07	5.266E-07
Am(III)	Castile	1X	M	SOLMOD3:SOLCOH	1.78E-07	1.429E-06
Am(III)	Castile	2X	M	SOLMOD3:SOLCOH2	1.63E-07	7.256E-07
Am(III)	Castile	3X	M	SOLMOD3:SOLCOH3	1.58E-07	5.158E-07
Am(III)	Castile	4X	M	SOLMOD3:SOLCOH4	1.54E-07	4.153E-07
Am(III)	Castile	5X	M	SOLMOD3:SOLCOH5	1.52E-07	3.559E-07
Th(IV)	Salado	1X	M	SOLMOD4:SOLSOH	5.45E-08	5.497E-08
Th(IV)	Salado	2X	M	SOLMOD4:SOLSOH2	5.45E-08	5.509E-08
Th(IV)	Salado	3X	M	SOLMOD4:SOLSOH3	5.45E-08	5.514E-08
Th(IV)	Salado	4X	M	SOLMOD4:SOLSOH4	5.45E-08	5.516E-08
Th(IV)	Salado	5X	M	SOLMOD4:SOLSOH5	5.45E-08	5.517E-08
Th(IV)	Castile	1X	M	SOLMOD4:SOLCOH	5.44E-08	5.836E-08
Th(IV)	Castile	2X	M	SOLMOD4:SOLCOH2	5.44E-08	5.844E-08
Th(IV)	Castile	3X	M	SOLMOD4:SOLCOH3	5.44E-08	5.847E-08
Th(IV)	Castile	4X	M	SOLMOD4:SOLCOH4	5.44E-08	5.849E-08
Th(IV)	Castile	5X	M	SOLMOD4:SOLCOH5	5.44E-08	5.849E-08
Np(V)	Salado	1X	M	SOLMOD5:SOLSOH	4.02E-07	4.375E-07
Np(V)	Salado	2X	M	SOLMOD5:SOLSOH2	2.83E-07	3.218E-07
Np(V)	Salado	3X	M	SOLMOD5:SOLSOH3	2.42E-07	2.825E-07
Np(V)	Salado	4X	M	SOLMOD5:SOLSOH4	2.21E-07	2.629E-07
Np(V)	Salado	5X	M	SOLMOD5:SOLSOH5	2.09E-07	2.511E-07
Np(V)	Castile	1X	M	SOLMOD5:SOLCOH	1.20E-06	1.821E-06
Np(V)	Castile	2X	M	SOLMOD5:SOLCOH2	7.27E-07	1.417E-06
Np(V)	Castile	3X	M	SOLMOD5:SOLCOH3	5.52E-07	1.280E-06
Np(V)	Castile	4X	M	SOLMOD5:SOLCOH4	4.61E-07	1.211E-06
Np(V)	Castile	5X	M	SOLMOD5:SOLCOH5	4.05E-07	1.170E-06
U(VI)	Salado	All	M	SOLMOD6:SOLSOH	1.00E-03	1.000E-03
U(VI)	Castile	All	M	SOLMOD6:SOLCOH	1.00E-03	1.000E-03

Iron Surface Area

A value of 6,127 drums per room (DRROOM) is used to yield an Iron Surface Area Density, D_s, of 10.1 m^2/m^3 in RPPCR_12P. The value used in CRA19_12P is 6,804, which yielded a D_s of 11.2 m^2/m^3.

Actinide Oxidation State (GLOBAL:OXSTAT) is changed from 50 percent of realizations with lower oxidation states [Pu(III), Np(IV), and U(IV)] and 50 percent of realizations with higher oxidation states [Pu(IV), Np(V), and U(VI)] to 100 percent of realizations with lower oxidation states and 0 percent of realizations with higher oxidation states.

Table 16. Actinide Oxidation State

Attribute	Units	CRA19_12P	RPPCR_12P
Distribution	Uniform	0	0
Value		0.5	0.25
Maximum		1	0.25
Mean		0.5	0.25
Standard Deviation		0.289	0.289
Median		0.5	0.25
Minimum		0	0

6.2 Quality Assurance Screenshot Checks

The quality assurance screenshot checks are presented below:

Borehole Drilling Rate and Plugging Probabilities

Borehole Drilling Rate and Plugging Probabilities are used in CCDFGF to construct futures in a 10,000-year time frame. The following screenshots show their values (enclosed in red outline) used in each replicate:

```
[xintong@fwm RPPCR_12P]$ head -n 12 Analyses/RPPCR_12P/CCDFGF/RunCCDFGF/PRECCDFGF/Output/ccgf_RPPCR_12P_reltab_r1.dat
    0.135457E+06 ContactHandledWasteArea
    0.157600E+05 RemoteHandledWasteArea
    0.530600E+06 EXVOL
    0.100000E+03 ACTI
    0.318000E+00 VolumeFractionContactWaste
    0.100000E+01 VolumeFractionRemoteHandledWaste
    0.153400E-01 FinalDrillingRate
    0.359000E+00 PluggingPatternProb(1)
    0.463500E+00 PluggingPatternProb(2)
    0.177500E+00 PluggingPatternProb(3)
    0.100000E-03 FinalMiningRate
    0.600000E+03 MiningTransitionTime
[xintong@fwm RPPCR_12P]$ head -n 12 Analyses/RPPCR_12P/CCDFGF/RunCCDFGF/PRECCDFGF/Output/ccgf_RPPCR_12P_reltab_r2.dat
    0.135457E+06 ContactHandledWasteArea
    0.157600E+05 RemoteHandledWasteArea
    0.530600E+06 EXVOL
    0.100000E+03 ACTI
    0.318000E+00 VolumeFractionContactWaste
    0.100000E+01 VolumeFractionRemoteHandledWaste
    0.153400E-01 FinalDrillingRate
    0.359000E+00 PluggingPatternProb(1)
    0.463500E+00 PluggingPatternProb(2)
    0.177500E+00 PluggingPatternProb(3)
    0.100000E-03 FinalMiningRate
    0.600000E+03 MiningTransitionTime
[xintong@fwm RPPCR_12P]$ head -n 12 Analyses/RPPCR_12P/CCDFGF/RunCCDFGF/PRECCDFGF/Output/ccgf_RPPCR_12P_reltab_r3.dat
    0.135457E+06 ContactHandledWasteArea
    0.157600E+05 RemoteHandledWasteArea
    0.530600E+06 EXVOL
    0.100000E+03 ACTI
    0.318000E+00 VolumeFractionContactWaste
    0.100000E+01 VolumeFractionRemoteHandledWaste
    0.153400E-01 FinalDrillingRate
    0.359000E+00 PluggingPatternProb(1)
    0.463500E+00 PluggingPatternProb(2)
    0.177500E+00 PluggingPatternProb(3)
    0.100000E-03 FinalMiningRate
    0.600000E+03 MiningTransitionTime
[xintong@fwm RPPCR_12P]$
```

Colloid Parameters

All the modified Colloid Parameters are used in the PANEL calculation, and part of them are used in the BRAGFLO calculation. The following screenshots show the examination of a PANEL output file where the Colloid Parameters used in the mobile concentration limit calculations are selected and listed.

```
[xintong@fwm ~]$ gropecdb -input Analyses/RPPCR_12P/Analyses/RPPCR_12P/PANEL/RunPANEL/ALGEBRACDB/Output/alg1_panel_RPPCR_12P.cdb -user interac
tive

      GGGGG   RRRRRR    OOOOO   PPPPPP   EEEEEEE   CCCCC   DDDDDD   BBBBBB
     GG   GG  RR   RR  OO   OO  PP   PP  EE       CC   CC  DD   DD  BB   BB
     GG       RR   RR  OO   OO  PP   PP  EE       CC       DD   DD  BB   BB
     GG       RRRRRR   OO   OO  PPPPPP   EEEEE    CC       DD   DD  BBBBBB
     GG  GGG  RRRRR    OO   OO  PP       EE       CC       DD   DD  BB   BB
     GG   GG  RR  RR   OO   OO  PP       EE       CC   CC  DD   DD  BB   BB
      GGGGG   RR   RR   OOOOO   PP       EEEEEEE   CCCCC   DDDDDD   BBBBBB

                          GROPECDB Version 2.14
                       PRODUCTION Built 06/16/2020
                          Written by Amy Gilkey

                        Run on 03/25/2025 at 06:45:17
                      Run on x86_64 fwm Linux 3.10.0-116

 CAMDAT File:  Analyses/RPPCR_12P/Analyses/RPPCR_12P/PANEL/RunPANEL/ALGEBRACDB/Output/alg1_panel_RPPCR_12P.cdb
 Written on:  03/24/25 15:48:53

 Number of coordinates per node       =     3
 Number of nodes                      =     8
 Number of element blocks             =    66
 Number of elements                   =     1
                   in X direction     =     1
                   in Y direction     =     1
                   in Z direction     =     1
 Number of node sets                  =     0
 Number of side sets                  =     0

 Attributes (5):          THICK     ELEVAT    DEL_X     DEL_Y     DEL_Z
 Properties (39):         OXSTAT    DBRMINBV  YRSEC     VPANLEX   VREPOS
                          CITOBQ    AVOGADRO  INVCHD    INVRHD    ATWEIGHT
                          HALFLIFE  EPAREL    CONCMIN   CONCINT   CAPHUM
                          CAPMIC    PROPMIC   LOGSOLM   FRCDIS    FRCHUM
                          FRCMIC    FRCINT    FRCMIN    OXCUTOFF  SOLSOH
                          SOLCOH    SOLSOH2   SOLCOH2   SOLSOH3   SOLCOH3
                          SOLSOH4   SOLCOH4   SOLSOH5   SOLCOH5   SOLVAR
                          PHUMSIM   PHUMCIM   WUF       PROBDEG
```

```
 History Variables (118): BRNVOL00  SMFLOW00  SDETOTAL  SDMSR90   SDCSR90
                          SDESR90   SDMCS137  SDCCS137  SDECS137  SDMPB210
                          SDCPB210  SDEPB210  SDMRA226  SDCRA226  SDERA226
                          SDMRA228  SDCRA228  SDERA228  SDMTH229  SDCTH229
                          SDETH229  SDMTH230  SDCTH230  SDETH230  SDMTH232
                          SDCTH232  SDETH232  SDMPA231  SDCPA231  SDEPA231
                          SDMU233   SDCU233   SDEU233   SDMU234   SDCU234
                          SDEU234   SDMU235   SDCU235   SDEU235   SDMU236
                          SDCU236   SDEU236   SDMU238   SDCU238   SDEU238
                          SDMNP237  SDCNP237  SDENP237  SDMPU238  SDCPU238
                          SDEPU238  SDMPU239  SDCPU239  SDEPU239  SDMPU240
                          SDCPU240  SDEPU240  SDMPU241  SDCPU241  SDEPU241
                          SDMPU242  SDCPU242  SDEPU242  SDMPU244  SDCPU244
                          SDEPU244  SDMAM241  SDCAM241  SDEAM241  SDMCM244
                          SDCCM244  SDECM244  SDMCM248  SDCCM248  SDECM248
                          SDMCF252  SDCCF252  SDECF252  SDMPM147  SDCPM147
                          SDEPM147  SDMSM147  SDCSM147  SDESM147  SDMAM243
                          SDCAM243  SDEAM243  SDMCM243  SDCCM243  SDECM243
                          SDMCM245  SDCCM245  SDECM245  LDETOTAL  LDMAM241
                          LDCAM241  LDEAM241  LDMPU239  LDCPU239  LDEPU239
                          LDMPU238  LDCPU238  LDEPU238  LDMU234   LDCU234
                          LDEU234   LDMTH230  LDCTH230  LDETH230  U_MOLE
                          PU_MOLE   TH_MOLE   MF_U       MF_PU     MF_TH
                          LSD_U     LSD_PU    LSD_TH
 Global Variables (0):
 Nodal Variables (0):
 Element Variables (0):

 Number of time steps = 201 (including 201 history-only)
    First time = 0.00000E+00   0.00000E+00 years
    Last time  = 3.15569E+11   1.00000E+04 years
```

```
GROPE> select Property CONCINT, CAPMIC, PROPMIC
        3 Properties selected

GROPE> list Property

 Element Block 32)    "AM      "    32=ID     0 elements
    CONCINT      CAPMIC       PROPMIC
   6.70000E-07  6.28000E-06  3.60000E+00

 Element Block 36)    "NP      "    36=ID     0 elements
    CONCINT      CAPMIC       PROPMIC
   4.30000E-08  1.27000E-04  1.20000E+01

 Element Block 40)    "PU      "    40=ID     0 elements
    CONCINT      CAPMIC       PROPMIC
   4.30000E-08  2.18000E-05  2.18000E+00

 Element Block 43)    "TH      "    43=ID     0 elements
    CONCINT      CAPMIC       PROPMIC
   4.80000E-07  2.12000E-02  3.10000E+00

 Element Block 44)    "U       "    44=ID     0 elements
    CONCINT      CAPMIC       PROPMIC
   1.40000E-06  8.14000E+00  2.10000E-03

GROPE>
```

Actinide Solubility

All the modified Actinide Solubility parameters are also used in the PANEL calculation. The same PANEL output file used to confirm the Colloid Parameters modification is used for this check. The following screenshot shows that the solubility model's associated parameters are selected and listed.

```
GROPE> select Block 45, 46, 47, 48
        0 Elements selected
        4 Element Blocks selected

GROPE> list Property

 Element Block 45)    "SOLMOD3 "    45=ID     0 elements
    SOLSOH       SOLCOH       SOLSOH2      SOLCOH2      SOLSOH3      SOLCOH3
   2.13900E-06  1.42900E-06  1.09100E-06  7.25600E-07  7.72100E-07  5.15800E-07
    SOLSOH4      SOLCOH4      SOLSOH5      SOLCOH5      SOLVAR
   6.18000E-07  4.15300E-07  5.26600E-07  3.55900E-07  6.40137E-01

 Element Block 46)    "SOLMOD4 "    46=ID     0 elements
    SOLSOH       SOLCOH       SOLSOH2      SOLCOH2      SOLSOH3      SOLCOH3
   5.49700E-08  5.83600E-08  5.50900E-08  5.84400E-08  5.51400E-08  5.84700E-08
    SOLSOH4      SOLCOH4      SOLSOH5      SOLCOH5      SOLVAR
   5.51600E-08  5.84900E-08  5.51700E-08  5.84900E-08 -4.86204E-03

 Element Block 47)    "SOLMOD5 "    47=ID     0 elements
    SOLSOH       SOLCOH       SOLSOH2      SOLCOH2      SOLSOH3      SOLCOH3
   4.37500E-07  1.82100E-06  3.21800E-07  1.41700E-06  2.82500E-07  1.28000E-06
    SOLSOH4      SOLCOH4      SOLSOH5      SOLCOH5
   2.62900E-07  1.21100E-06  2.51100E-07  1.17000E-06

 Element Block 48)    "SOLMOD6 "    48=ID     0 elements
    SOLSOH       SOLCOH
   1.00000E-03  1.00000E-03

GROPE>
```

Iron Surface Area

The REFCON:DRROOM parameter is used in the BRAGFLO calculation, and it was selected and listed in the following screenshots from one of the BRAGFLO output files.

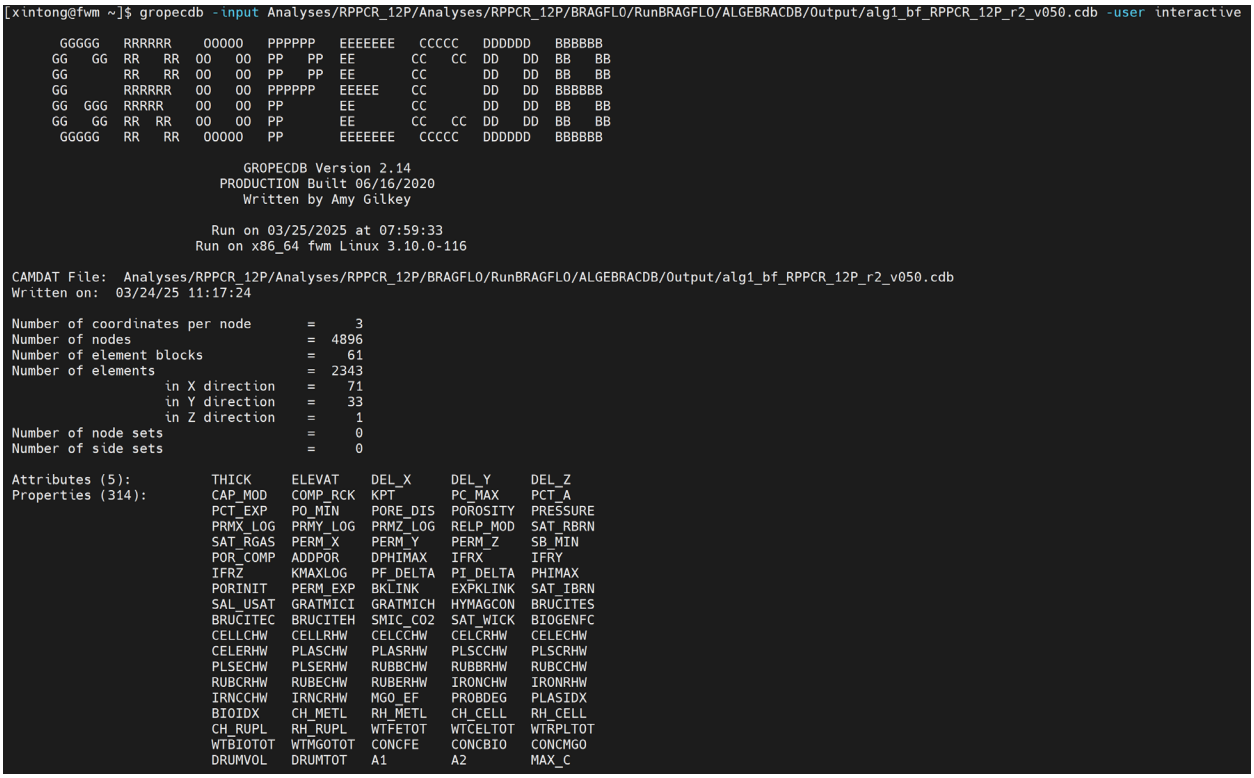

```
[xintong@fwm ~]$ gropecdb -input Analyses/RPPCR_12P/Analyses/RPPCR_12P/BRAGFLO/RunBRAGFLO/ALGEBRACDB/Output/alg1_bf_RPPCR_12P_r2_v050.cdb -user interactive

      GGGGG   RRRRRR    OOOOO   PPPPPP   EEEEEEE   CCCCC   DDDDDD   BBBBBB
     GG   GG  RR   RR  OO   OO  PP   PP  EE       CC   CC  DD   DD  BB   BB
     GG       RR   RR  OO   OO  PP   PP  EE       CC       DD   DD  BB   BB
     GG       RRRRRR   OO   OO  PPPPPP   EEEEE    CC       DD   DD  BBBBBB
     GG  GGG  RRRRR    OO   OO  PP       EE       CC       DD   DD  BB   BB
     GG   GG  RR  RR   OO   OO  PP       EE       CC   CC  DD   DD  BB   BB
      GGGGG   RR   RR   OOOOO   PP       EEEEEEE   CCCCC   DDDDDD   BBBBBB

                          GROPECDB Version 2.14
                       PRODUCTION Built 06/16/2020
                          Written by Amy Gilkey

                        Run on 03/25/2025 at 07:59:33
                      Run on x86_64 fwm Linux 3.10.0-116

 CAMDAT File:  Analyses/RPPCR_12P/Analyses/RPPCR_12P/BRAGFLO/RunBRAGFLO/ALGEBRACDB/Output/alg1_bf_RPPCR_12P_r2_v050.cdb
 Written on:  03/24/25 11:17:24

 Number of coordinates per node       =     3
 Number of nodes                      =  4896
 Number of element blocks             =    61
 Number of elements                   =  2343
                   in X direction     =    71
                   in Y direction     =    33
                   in Z direction     =     1
 Number of node sets                  =     0
 Number of side sets                  =     0

 Attributes (5):          THICK     ELEVAT    DEL_X     DEL_Y     DEL_Z
 Properties (314):        CAP_MOD   COMP_RCK  KPT       PC_MAX    PCT_A
                          PCT_EXP   PO_MIN    PORE_DIS  POROSITY  PRESSURE
                          PRMX_LOG  PRMY_LOG  PRMZ_LOG  RELP_MOD  SAT_RBRN
                          SAT_RGAS  PERM_X    PERM_Y    PERM_Z    SB_MIN
                          POR_COMP  ADDPOR    DPHIMAX   IFRX      IFRY
                          IFRZ      KMAXLOG   PF_DELTA  PI_DELTA  PHIMAX
                          PORINIT   PERM_EXP  BKLINK    EXPKLINK  SAT_IBRN
                          SAL_USAT  GRATMICI  GRATMICH  HYMAGCON  BRUCITES
                          BRUCITEC  BRUCITEH  SMIC_CO2  SAT_WICK  BIOGENFC
                          CELLCHW   CELLRHW   CELCCHW   CELCRHW   CELECHW
                          CELERHW   PLASCHW   PLASRHW   PLSCCHW   PLSCRHW
                          PLSECHW   PLSERHW   RUBBCHW   RUBBRHW   RUBCCHW
                          RUBCRHW   RUBECHW   RUBERHW   IRONCHW   IRONRHW
                          IRNCCHW   IRNCRHW   MGO_EF    PROBDEG   PLASIDX
                          BIOIDX    CH_METL   RH_METL   CH_CELL   RH_CELL
                          CH_RUPL   RH_RUPL   WTFETOT   WTCELTOT  WTRPLTOT
                          WTBIOTOT  WTMGOTOT  CONCFE    CONCBIO   CONCMGO
                          DRUMVOL   DRUMTOT   A1        A2        MAX_C
```

```
                        F_NO3     F_SO4     SMIC_H2   SMIC_H2O  GRATCORI
                        GRATCORH  INTRIN    COMPRES   DNSFLUID  REF_PRES
                        REF_TEMP  VISCO     WTF       COMP      QINIT
                        CORRMCO2  HUMCORR   STOIFX    FBETA     GRAVACC
                        PI        VPANLEX   VROOM     VREPOS    DRROOM
                        YRSEC     SECYR     ASDRUM    ATMPA     R
                        PLASFAC   DIP1      DIP2      TC_H2     TC_CO2
                        TC_CH4    TC_N2     TC_H2S    TC_O2     PC_H2
                        PC_CO2    PC_CH4    PC_N2     PC_H2S    PC_O2
                        ACF_H2    ACF_CO2   ACF_CH4   ACF_N2    ACF_H2S
                        ACF_O2    OMEGAA    OMEGAB    BIP_11    BIP_12
                        BIP_13    BIP_14    BIP_15    BIP_16    BIP_21
                        BIP_22    BIP_23    BIP_24    BIP_25    BIP_26
                        BIP_31    BIP_32    BIP_33    BIP_34    BIP_35
                        BIP_36    BIP_41    BIP_42    BIP_43    BIP_44
                        BIP_45    BIP_46    BIP_51    BIP_52    BIP_53
                        BIP_54    BIP_55    BIP_56    BIP_61    BIP_62
                        BIP_63    BIP_64    BIP_65    BIP_66    STCO_11
                        STCO_12   STCO_13   STCO_14   STCO_15   STCO_16
                        STCO_17   STCO_18   STCO_19   STCO_10   STCO_21
                        STCO_22   STCO_23   STCO_24   STCO_25   STCO_26
                        STCO_27   STCO_28   STCO_29   STCO_20   STCO_31
                        STCO_32   STCO_33   STCO_34   STCO_35   STCO_36
                        STCO_37   STCO_38   STCO_39   STCO_30   STCO_41
                        STCO_42   STCO_43   STCO_44   STCO_45   STCO_46
                        STCO_47   STCO_48   STCO_49   STCO_40   STCO_51
                        STCO_52   STCO_53   STCO_54   STCO_55   STCO_56
                        STCO_57   STCO_58   STCO_59   STCO_50   STCO_61
                        STCO_62   STCO_63   STCO_64   STCO_65   STCO_66
                        STCO_67   STCO_68   STCO_69   STCO_60   STCO_71
                        STCO_72   STCO_73   STCO_74   STCO_75   STCO_76
                        STCO_77   STCO_78   STCO_79   STCO_70   STCO_81
                        STCO_82   STCO_83   STCO_84   STCO_85   STCO_86
                        STCO_87   STCO_88   STCO_89   STCO_80   MW_FE
                        MW_CELL   MW_NACL   MW_CO2    MW_CH4    MW_N2
                        MW_H2S    MW_O2     MW_H2O    MW_H2     MW_FEOH2
                        MW_FES    MW_MGO    MW_MGOH2  MW_HYDRO  MW_MGCO3
                        DN_FE     DN_FEOH2  DN_FES    DN_CELL   DN_MGO
                        DN_MGOH2  DN_HYDRO  DN_MGCO3  DN_SALT   AVOGADRO
                        CITOBQ    COMP_POR  POR2PERM  LS_FIT    PERM_NEW
                        ATWEIGHT  HALFLIFE  INVCHD    INVRHD    DECAYNRG
                        SPECACT   INVCHDM   INVRHDM   SOLSAL    SOLCAS
                        SOLCOH    SOLSOH    SOLVAR    OXSTAT    GH2AVG
                        SRADO2    GDEPFAC   CONCMIN   CONCINT   CAPHUM
                        PROPMIC   CAPMIC    PHUMCIM   PHUMSIM

 History Variables (25):  BIGENFAC  DP1       DP2       THETA1    THETA2
                        MOL_NO3   MOL_SO4   DISP3SAL  DISP3CAS  HUMP3SAL
                        HUMP3CAS  MICP3SAL  MICP3CAS  TOTP3SAL  TOTP3CAS
```

```
                        HUMP3CAS  MICP3SAL  MICP3CAS  TOTP3SAL  TOTP3CAS
                        DISP4SAL  DISP4CAS  HUMP4SAL  HUMP4CAS  MICP4SAL
                        MICP4CAS  TOTP4SAL  TOTP4CAS  DEN0      PHIREF
 Global Variables (0):
 Nodal Variables (1):     DENND
 Element Variables (7):   SATBREL   FECONC    CH2OCONC  MGCONC    DENEL
                        PRESEL    ELEVE

 Number of time steps = 1 (including 0 history-only)
    Time =-1.57785E+08

GROPE> select Property DRROOM
       1 Properties selected

GROPE> list Property

 Element Block 35)    "REFCON  "    35=ID     0 elements
    DRROOM
   6.12700E+03

GROPE>
```

Actinide Oxidation State

GLOBAL:OXSTAT is one of the sampled parameters by LHS. The following screenshots list the value of OXSTAT for all 300 vectors in the RPPCR_12P calculation. The values are all smaller than 0.5, which indicates that 100 percent of realizations in the calculation have lower oxidation states Pu(III), Np(IV), and U(IV).

```
MariaDB [PA_Results_pcr]> select Material, Property, Analysis, Replicate, Vector, Value from LHS_SampledValues where Analysis='RPPCR_12P' and Property='OXST
AT';
+----------+----------+-----------+-----------+--------+----------------------+
| Material | Property | Analysis  | Replicate | Vector | Value                |
+----------+----------+-----------+-----------+--------+----------------------+
| GLOBAL   | OXSTAT   | RPPCR_12P |         1 |      1 |    0.1826054625213146 |
| GLOBAL   | OXSTAT   | RPPCR_12P |         1 |      2 |    0.1161681988835335 |
| GLOBAL   | OXSTAT   | RPPCR_12P |         1 |      3 |   0.05730447143316269 |
| GLOBAL   | OXSTAT   | RPPCR_12P |         1 |      4 |   0.04998843654990196 |
| GLOBAL   | OXSTAT   | RPPCR_12P |         1 |      5 |    0.2167041708528996 |
| GLOBAL   | OXSTAT   | RPPCR_12P |         1 |      6 |    0.1976956735551357 |
| GLOBAL   | OXSTAT   | RPPCR_12P |         1 |      7 |    0.1188310989737511 |
| GLOBAL   | OXSTAT   | RPPCR_12P |         1 |      8 |    0.1426720803976059 |
| GLOBAL   | OXSTAT   | RPPCR_12P |         1 |      9 |     0.178558292388916 |
| GLOBAL   | OXSTAT   | RPPCR_12P |         1 |     10 |    0.1002483415417373 |
| GLOBAL   | OXSTAT   | RPPCR_12P |         1 |     11 |    0.1078428518772125 |
| GLOBAL   | OXSTAT   | RPPCR_12P |         1 |     12 |    0.1695897926390171 |
| GLOBAL   | OXSTAT   | RPPCR_12P |         1 |     13 |    0.1618718568980694 |
| GLOBAL   | OXSTAT   | RPPCR_12P |         1 |     14 |    0.1882589048147202 |
| GLOBAL   | OXSTAT   | RPPCR_12P |         1 |     15 |   0.03088762164115906 |
| GLOBAL   | OXSTAT   | RPPCR_12P |         1 |     16 |     0.027539864173159 |
| GLOBAL   | OXSTAT   | RPPCR_12P |         1 |     17 |   0.08519062489271165 |
| GLOBAL   | OXSTAT   | RPPCR_12P |         1 |     18 |   0.06168883919715881 |
| GLOBAL   | OXSTAT   | RPPCR_12P |         1 |     19 |    0.0975397102488205 |
| GLOBAL   | OXSTAT   | RPPCR_12P |         1 |     20 |   0.08079201981425285 |
| GLOBAL   | OXSTAT   | RPPCR_12P |         1 |     21 |  0.004076507389545441 |
| GLOBAL   | OXSTAT   | RPPCR_12P |         1 |     22 |   0.07423664957284927 |
| GLOBAL   | OXSTAT   | RPPCR_12P |         1 |     23 |     0.204299488067627 |
| GLOBAL   | OXSTAT   | RPPCR_12P |         1 |     24 |    0.1547229172289371 |
| GLOBAL   | OXSTAT   | RPPCR_12P |         1 |     25 |   0.08401888236403465 |
| GLOBAL   | OXSTAT   | RPPCR_12P |         1 |     26 |    0.2283294868469238 |
| GLOBAL   | OXSTAT   | RPPCR_12P |         1 |     27 |    0.1918024773895741 |
| GLOBAL   | OXSTAT   | RPPCR_12P |         1 |     28 |   0.02103613793849945 |
| GLOBAL   | OXSTAT   | RPPCR_12P |         1 |     29 |   0.06879872679710389 |
| GLOBAL   | OXSTAT   | RPPCR_12P |         1 |     30 |    0.1497283536195755 |
| GLOBAL   | OXSTAT   | RPPCR_12P |         1 |     31 |    0.1052144281566143 |
| GLOBAL   | OXSTAT   | RPPCR_12P |         1 |     32 |    0.1201755405962467 |
| GLOBAL   | OXSTAT   | RPPCR_12P |         1 |     33 |    0.0949224217236042 |
| GLOBAL   | OXSTAT   | RPPCR_12P |         1 |     34 |   0.07615670427680016 |
| GLOBAL   | OXSTAT   | RPPCR_12P |         1 |     35 |   0.07991332277655601 |
| GLOBAL   | OXSTAT   | RPPCR_12P |         1 |     36 |    0.2385957649350166 |
| GLOBAL   | OXSTAT   | RPPCR_12P |         1 |     37 |    0.1027116754837334 |
| GLOBAL   | OXSTAT   | RPPCR_12P |         1 |     38 |   0.02251585737452842 |
| GLOBAL   | OXSTAT   | RPPCR_12P |         1 |     39 |   0.04366679534316063 |
| GLOBAL   | OXSTAT   | RPPCR_12P |         1 |     40 |    0.2091929458081722 |
| GLOBAL   | OXSTAT   | RPPCR_12P |         1 |     41 |   0.01762879922054708 |
| GLOBAL   | OXSTAT   | RPPCR_12P |         1 |     42 |   0.03631239533424378 |
| GLOBAL   | OXSTAT   | RPPCR_12P |         1 |     43 |   0.07176890835165978 |
| GLOBAL   | OXSTAT   | RPPCR_12P |         1 |     44 |    0.1454272137582302 |
```

GLOBAL	OXSTAT	RPPCR_12P	1	45	0.2211837412416935
GLOBAL	OXSTAT	RPPCR_12P	1	46	0.2024863077700138
GLOBAL	OXSTAT	RPPCR_12P	1	47	0.0674154655635357
GLOBAL	OXSTAT	RPPCR_12P	1	48	0.2262258151173592
GLOBAL	OXSTAT	RPPCR_12P	1	49	0.0911371587216854
GLOBAL	OXSTAT	RPPCR_12P	1	50	0.0089321865141391 76
GLOBAL	OXSTAT	RPPCR_12P	1	51	0.12778065668419
GLOBAL	OXSTAT	RPPCR_12P	1	52	0.2248277623951435
GLOBAL	OXSTAT	RPPCR_12P	1	53	0.1737922537326813
GLOBAL	OXSTAT	RPPCR_12P	1	54	0.2318322163820267
GLOBAL	OXSTAT	RPPCR_12P	1	55	0.04688767731189727
GLOBAL	OXSTAT	RPPCR_12P	1	56	0.2468737977743149
GLOBAL	OXSTAT	RPPCR_12P	1	57	0.1963648335635662
GLOBAL	OXSTAT	RPPCR_12P	1	58	0.03834218561649323
GLOBAL	OXSTAT	RPPCR_12P	1	59	0.01671748727560043
GLOBAL	OXSTAT	RPPCR_12P	1	60	0.1321768820285797
GLOBAL	OXSTAT	RPPCR_12P	1	61	0.02525561451911926
GLOBAL	OXSTAT	RPPCR_12P	1	62	0.1142972052097321
GLOBAL	OXSTAT	RPPCR_12P	1	63	0.05754465372301638
GLOBAL	OXSTAT	RPPCR_12P	1	64	0.09675563618540764
GLOBAL	OXSTAT	RPPCR_12P	1	65	0.2100743864523247
GLOBAL	OXSTAT	RPPCR_12P	1	66	0.1263789872825146
GLOBAL	OXSTAT	RPPCR_12P	1	67	0.150162623077631
GLOBAL	OXSTAT	RPPCR_12P	1	68	0.2127997249178588
GLOBAL	OXSTAT	RPPCR_12P	1	69	0.05456514209508895
GLOBAL	OXSTAT	RPPCR_12P	1	70	0.1866913267970085
GLOBAL	OXSTAT	RPPCR_12P	1	71	0.1928120266087353
GLOBAL	OXSTAT	RPPCR_12P	1	72	0.1104434230923653
GLOBAL	OXSTAT	RPPCR_12P	1	73	0.2178813023865223
GLOBAL	OXSTAT	RPPCR_12P	1	74	0.165131529122591
GLOBAL	OXSTAT	RPPCR_12P	1	75	0.2449377705156803
GLOBAL	OXSTAT	RPPCR_12P	1	76	0.1325734354509041
GLOBAL	OXSTAT	RPPCR_12P	1	77	0.180206859856844
GLOBAL	OXSTAT	RPPCR_12P	1	78	0.04142015472054482
GLOBAL	OXSTAT	RPPCR_12P	1	79	0.03464291229844094
GLOBAL	OXSTAT	RPPCR_12P	1	80	0.001094254553318024
GLOBAL	OXSTAT	RPPCR_12P	1	81	0.01458055302500725
GLOBAL	OXSTAT	RPPCR_12P	1	82	0.08877167955040932
GLOBAL	OXSTAT	RPPCR_12P	1	83	0.1771813845634461
GLOBAL	OXSTAT	RPPCR_12P	1	84	0.1599312913417816
GLOBAL	OXSTAT	RPPCR_12P	1	85	0.05132699996232987
GLOBAL	OXSTAT	RPPCR_12P	1	86	0.139755654335022
GLOBAL	OXSTAT	RPPCR_12P	1	87	0.2364922192692757
GLOBAL	OXSTAT	RPPCR_12P	1	88	0.2343564260005951
GLOBAL	OXSTAT	RPPCR_12P	1	89	0.005294798333197832
GLOBAL	OXSTAT	RPPCR_12P	1	90	0.1571761560440063
GLOBAL	OXSTAT	RPPCR_12P	1	91	0.01219392314553261
GLOBAL	OXSTAT	RPPCR_12P	1	92	0.2488471579551697
GLOBAL	OXSTAT	RPPCR_12P	1	93	0.16479028403759

GLOBAL	OXSTAT	RPPCR_12P	1	94	0.1371172994375229
GLOBAL	OXSTAT	RPPCR_12P	1	95	0.063941021412611
GLOBAL	OXSTAT	RPPCR_12P	1	96	0.2063491825759411
GLOBAL	OXSTAT	RPPCR_12P	1	97	0.1244177035987377
GLOBAL	OXSTAT	RPPCR_12P	1	98	0.1723887893557549
GLOBAL	OXSTAT	RPPCR_12P	1	99	0.1407894666492939
GLOBAL	OXSTAT	RPPCR_12P	1	100	0.240897181481123
GLOBAL	OXSTAT	RPPCR_12P	2	1	0.1698752953112125
GLOBAL	OXSTAT	RPPCR_12P	2	2	0.2123310862481594
GLOBAL	OXSTAT	RPPCR_12P	2	3	0.1948735611140728
GLOBAL	OXSTAT	RPPCR_12P	2	4	0.1553836596012116
GLOBAL	OXSTAT	RPPCR_12P	2	5	0.07076132893562317
GLOBAL	OXSTAT	RPPCR_12P	2	6	0.187369035333395
GLOBAL	OXSTAT	RPPCR_12P	2	7	0.02264150857925415
GLOBAL	OXSTAT	RPPCR_12P	2	8	0.08017209991812706
GLOBAL	OXSTAT	RPPCR_12P	2	9	0.06042316406965256
GLOBAL	OXSTAT	RPPCR_12P	2	10	0.2449256500601768
GLOBAL	OXSTAT	RPPCR_12P	2	11	0.1492967356741428
GLOBAL	OXSTAT	RPPCR_12P	2	12	0.2153320379555225
GLOBAL	OXSTAT	RPPCR_12P	2	13	0.2037655179202557
GLOBAL	OXSTAT	RPPCR_12P	2	14	0.1171947038173676
GLOBAL	OXSTAT	RPPCR_12P	2	15	0.1210310700535774
GLOBAL	OXSTAT	RPPCR_12P	2	16	0.1989070212841034
GLOBAL	OXSTAT	RPPCR_12P	2	17	0.2133002552390099
GLOBAL	OXSTAT	RPPCR_12P	2	18	0.2185342939198017
GLOBAL	OXSTAT	RPPCR_12P	2	19	0.06252893642522395
GLOBAL	OXSTAT	RPPCR_12P	2	20	0.09807387098670006
GLOBAL	OXSTAT	RPPCR_12P	2	21	0.05584527730941773
GLOBAL	OXSTAT	RPPCR_12P	2	22	0.1249825157225132
GLOBAL	OXSTAT	RPPCR_12P	2	23	0.04213671818375588
GLOBAL	OXSTAT	RPPCR_12P	2	24	0.1731086540222168
GLOBAL	OXSTAT	RPPCR_12P	2	25	0.1317780768871308
GLOBAL	OXSTAT	RPPCR_12P	2	26	0.207561276848428
GLOBAL	OXSTAT	RPPCR_12P	2	27	0.2479225096106529
GLOBAL	OXSTAT	RPPCR_12P	2	28	0.2278572419285774
GLOBAL	OXSTAT	RPPCR_12P	2	29	0.1451073823776096
GLOBAL	OXSTAT	RPPCR_12P	2	30	0.01731081947684288
GLOBAL	OXSTAT	RPPCR_12P	2	31	0.009689577668905259
GLOBAL	OXSTAT	RPPCR_12P	2	32	0.1829125565290451
GLOBAL	OXSTAT	RPPCR_12P	2	33	0.1717777599394321
GLOBAL	OXSTAT	RPPCR_12P	2	34	0.09525106146931649
GLOBAL	OXSTAT	RPPCR_12P	2	35	0.03951196819543838
GLOBAL	OXSTAT	RPPCR_12P	2	36	0.1643172973394394
GLOBAL	OXSTAT	RPPCR_12P	2	37	0.05996580109000206
GLOBAL	OXSTAT	RPPCR_12P	2	38	0.1376024142000824
GLOBAL	OXSTAT	RPPCR_12P	2	39	0.2015559260547161
GLOBAL	OXSTAT	RPPCR_12P	2	40	0.03452655851840973
GLOBAL	OXSTAT	RPPCR_12P	2	41	0.1090708540380001
GLOBAL	OXSTAT	RPPCR_12P	2	42	0.08427744656801224

GLOBAL	OXSTAT	RPPCR_12P	2	43	0.01194849640130997
GLOBAL	OXSTAT	RPPCR_12P	2	44	0.09101508885622024
GLOBAL	OXSTAT	RPPCR_12P	2	45	0.2472251722216606
GLOBAL	OXSTAT	RPPCR_12P	2	46	0.07762393637560308
GLOBAL	OXSTAT	RPPCR_12P	2	47	0.2201518525276333
GLOBAL	OXSTAT	RPPCR_12P	2	48	0.1822775472700596
GLOBAL	OXSTAT	RPPCR_12P	2	49	0.1349928387999535
GLOBAL	OXSTAT	RPPCR_12P	2	50	0.1970009903609753
GLOBAL	OXSTAT	RPPCR_12P	2	51	0.001972112357616425
GLOBAL	OXSTAT	RPPCR_12P	2	52	0.06611337095499038
GLOBAL	OXSTAT	RPPCR_12P	2	53	0.1589868453145027
GLOBAL	OXSTAT	RPPCR_12P	2	54	0.1016970698535442
GLOBAL	OXSTAT	RPPCR_12P	2	55	0.01849583327770233
GLOBAL	OXSTAT	RPPCR_12P	2	56	0.151245081871748
GLOBAL	OXSTAT	RPPCR_12P	2	57	0.1276670326292515
GLOBAL	OXSTAT	RPPCR_12P	2	58	0.2271974091231823
GLOBAL	OXSTAT	RPPCR_12P	2	59	0.005103696146979928
GLOBAL	OXSTAT	RPPCR_12P	2	60	0.1540636591613293
GLOBAL	OXSTAT	RPPCR_12P	2	61	0.07422825455665588
GLOBAL	OXSTAT	RPPCR_12P	2	62	0.08646074488759041
GLOBAL	OXSTAT	RPPCR_12P	2	63	0.1353872953355312
GLOBAL	OXSTAT	RPPCR_12P	2	64	0.1442837612330914
GLOBAL	OXSTAT	RPPCR_12P	2	65	0.2368850675225258
GLOBAL	OXSTAT	RPPCR_12P	2	66	0.1894060254096985
GLOBAL	OXSTAT	RPPCR_12P	2	67	0.1411521345376968
GLOBAL	OXSTAT	RPPCR_12P	2	68	0.004332770109176636
GLOBAL	OXSTAT	RPPCR_12P	2	69	0.02636076420545578
GLOBAL	OXSTAT	RPPCR_12P	2	70	0.03737099140882492
GLOBAL	OXSTAT	RPPCR_12P	2	71	0.05151901602745056
GLOBAL	OXSTAT	RPPCR_12P	2	72	0.2318502828478813
GLOBAL	OXSTAT	RPPCR_12P	2	73	0.1273815338313579
GLOBAL	OXSTAT	RPPCR_12P	2	74	0.1922720377147198
GLOBAL	OXSTAT	RPPCR_12P	2	75	0.1185081733763218
GLOBAL	OXSTAT	RPPCR_12P	2	76	0.2233088244497776
GLOBAL	OXSTAT	RPPCR_12P	2	77	0.06942757606506349
GLOBAL	OXSTAT	RPPCR_12P	2	78	0.01320791244506836
GLOBAL	OXSTAT	RPPCR_12P	2	79	0.05442475408315658
GLOBAL	OXSTAT	RPPCR_12P	2	80	0.1070163397490978
GLOBAL	OXSTAT	RPPCR_12P	2	81	0.1766282385587692
GLOBAL	OXSTAT	RPPCR_12P	2	82	0.0212118336558342
GLOBAL	OXSTAT	RPPCR_12P	2	83	0.0936757481098175
GLOBAL	OXSTAT	RPPCR_12P	2	84	0.04657349273562431
GLOBAL	OXSTAT	RPPCR_12P	2	85	0.08969354569911958
GLOBAL	OXSTAT	RPPCR_12P	2	86	0.03181028425693512
GLOBAL	OXSTAT	RPPCR_12P	2	87	0.1049243077635765
GLOBAL	OXSTAT	RPPCR_12P	2	88	0.2346937392652035
GLOBAL	OXSTAT	RPPCR_12P	2	89	0.07631401374936103
GLOBAL	OXSTAT	RPPCR_12P	2	90	0.1664123900234699
GLOBAL	OXSTAT	RPPCR_12P	2	91	0.1130233488976955

GLOBAL	OXSTAT	RPPCR_12P	2	92	0.04957273185253144
GLOBAL	OXSTAT	RPPCR_12P	2	93	0.1624276711046696
GLOBAL	OXSTAT	RPPCR_12P	2	94	0.02913006275892258
GLOBAL	OXSTAT	RPPCR_12P	2	95	0.2055590432882309
GLOBAL	OXSTAT	RPPCR_12P	2	96	0.1783118298649788
GLOBAL	OXSTAT	RPPCR_12P	2	97	0.04348935946822167
GLOBAL	OXSTAT	RPPCR_12P	2	98	0.1123218522965908
GLOBAL	OXSTAT	RPPCR_12P	2	99	0.2418085888028145
GLOBAL	OXSTAT	RPPCR_12P	2	100	0.2397344221174717
GLOBAL	OXSTAT	RPPCR_12P	3	1	0.1289825730025768
GLOBAL	OXSTAT	RPPCR_12P	3	2	0.050146909654140 47
GLOBAL	OXSTAT	RPPCR_12P	3	3	0.03169215515255928
GLOBAL	OXSTAT	RPPCR_12P	3	4	0.1470491835474968
GLOBAL	OXSTAT	RPPCR_12P	3	5	0.0002026131749153137
GLOBAL	OXSTAT	RPPCR_12P	3	6	0.241828595995903
GLOBAL	OXSTAT	RPPCR_12P	3	7	0.2033809226751328
GLOBAL	OXSTAT	RPPCR_12P	3	8	0.06495448648929596
GLOBAL	OXSTAT	RPPCR_12P	3	9	0.09031746506690978
GLOBAL	OXSTAT	RPPCR_12P	3	10	0.08149570792913437
GLOBAL	OXSTAT	RPPCR_12P	3	11	0.1980792371928692
GLOBAL	OXSTAT	RPPCR_12P	3	12	0.1734606550633908
GLOBAL	OXSTAT	RPPCR_12P	3	13	0.1246381163597107
GLOBAL	OXSTAT	RPPCR_12P	3	14	0.04074605077505112
GLOBAL	OXSTAT	RPPCR_12P	3	15	0.01965371429920197
GLOBAL	OXSTAT	RPPCR_12P	3	16	0.1379756250977516
GLOBAL	OXSTAT	RPPCR_12P	3	17	0.08586241647601128
GLOBAL	OXSTAT	RPPCR_12P	3	18	0.1536547684669494
GLOBAL	OXSTAT	RPPCR_12P	3	19	0.1611300076544285
GLOBAL	OXSTAT	RPPCR_12P	3	20	0.01320141479372978
GLOBAL	OXSTAT	RPPCR_12P	3	21	0.08874864712357522
GLOBAL	OXSTAT	RPPCR_12P	3	22	0.1908021950721741
GLOBAL	OXSTAT	RPPCR_12P	3	23	0.2069508619606495
GLOBAL	OXSTAT	RPPCR_12P	3	24	0.004297740459442138
GLOBAL	OXSTAT	RPPCR_12P	3	25	0.1898858864605427
GLOBAL	OXSTAT	RPPCR_12P	3	26	0.01602791622281075
GLOBAL	OXSTAT	RPPCR_12P	3	27	0.1943135304749012
GLOBAL	OXSTAT	RPPCR_12P	3	28	0.0492813366651535
GLOBAL	OXSTAT	RPPCR_12P	3	29	0.03615832164883614
GLOBAL	OXSTAT	RPPCR_12P	3	30	0.0971324834227562
GLOBAL	OXSTAT	RPPCR_12P	3	31	0.02787255048751831
GLOBAL	OXSTAT	RPPCR_12P	3	32	0.2315628069639206
GLOBAL	OXSTAT	RPPCR_12P	3	33	0.1594443762302399
GLOBAL	OXSTAT	RPPCR_12P	3	34	0.1654468877613545
GLOBAL	OXSTAT	RPPCR_12P	3	35	0.1101702728681266
GLOBAL	OXSTAT	RPPCR_12P	3	36	0.2276558811962605
GLOBAL	OXSTAT	RPPCR_12P	3	37	0.1635044729709625
GLOBAL	OXSTAT	RPPCR_12P	3	38	0.06643733978271485
GLOBAL	OXSTAT	RPPCR_12P	3	39	0.2152619445323944
GLOBAL	OXSTAT	RPPCR_12P	3	40	0.2023360462486744

GLOBAL	OXSTAT	RPPCR_12P	3	41	0.08455288708209992
GLOBAL	OXSTAT	RPPCR_12P	3	42	0.1783841606974602
GLOBAL	OXSTAT	RPPCR_12P	3	43	0.1049782088398934
GLOBAL	OXSTAT	RPPCR_12P	3	44	0.2234581476449966
GLOBAL	OXSTAT	RPPCR_12P	3	45	0.1475664022518322
GLOBAL	OXSTAT	RPPCR_12P	3	46	0.2258071298897266
GLOBAL	OXSTAT	RPPCR_12P	3	47	0.2090853229165077
GLOBAL	OXSTAT	RPPCR_12P	3	48	0.1166124941408634
GLOBAL	OXSTAT	RPPCR_12P	3	49	0.1359696531295777
GLOBAL	OXSTAT	RPPCR_12P	3	50	0.1685997140407562
GLOBAL	OXSTAT	RPPCR_12P	3	51	0.1806004793941975
GLOBAL	OXSTAT	RPPCR_12P	3	52	0.2389372123777866
GLOBAL	OXSTAT	RPPCR_12P	3	53	0.0550641332520172
GLOBAL	OXSTAT	RPPCR_12P	3	54	0.05962995603680611
GLOBAL	OXSTAT	RPPCR_12P	3	55	0.1330115675926209
GLOBAL	OXSTAT	RPPCR_12P	3	56	0.01010859712958336
GLOBAL	OXSTAT	RPPCR_12P	3	57	0.02551709696650505
GLOBAL	OXSTAT	RPPCR_12P	3	58	0.1845206049084663
GLOBAL	OXSTAT	RPPCR_12P	3	59	0.1513432024419308
GLOBAL	OXSTAT	RPPCR_12P	3	60	0.05440595716238022
GLOBAL	OXSTAT	RPPCR_12P	3	61	0.1130865381658077
GLOBAL	OXSTAT	RPPCR_12P	3	62	0.0945048375427723
GLOBAL	OXSTAT	RPPCR_12P	3	63	0.2483870540559292
GLOBAL	OXSTAT	RPPCR_12P	3	64	0.008738943785429
GLOBAL	OXSTAT	RPPCR_12P	3	65	0.1250627485010773
GLOBAL	OXSTAT	RPPCR_12P	3	66	0.06812555298209191
GLOBAL	OXSTAT	RPPCR_12P	3	67	0.03912190333008766
GLOBAL	OXSTAT	RPPCR_12P	3	68	0.1409506404399872
GLOBAL	OXSTAT	RPPCR_12P	3	69	0.1323382125794887
GLOBAL	OXSTAT	RPPCR_12P	3	70	0.04398612797260285
GLOBAL	OXSTAT	RPPCR_12P	3	71	0.07493492752313613
GLOBAL	OXSTAT	RPPCR_12P	3	72	0.0713259556889534
GLOBAL	OXSTAT	RPPCR_12P	3	73	0.1447868007421494
GLOBAL	OXSTAT	RPPCR_12P	3	74	0.005641622692346573
GLOBAL	OXSTAT	RPPCR_12P	3	75	0.09849921479821205
GLOBAL	OXSTAT	RPPCR_12P	3	76	0.0791774021089077
GLOBAL	OXSTAT	RPPCR_12P	3	77	0.02386972472071647
GLOBAL	OXSTAT	RPPCR_12P	3	78	0.0453781259059906
GLOBAL	OXSTAT	RPPCR_12P	3	79	0.1074157299101353
GLOBAL	OXSTAT	RPPCR_12P	3	80	0.03296889558434486
GLOBAL	OXSTAT	RPPCR_12P	3	81	0.07551765874028206
GLOBAL	OXSTAT	RPPCR_12P	3	82	0.06143555641174316
GLOBAL	OXSTAT	RPPCR_12P	3	83	0.2340233573317528
GLOBAL	OXSTAT	RPPCR_12P	3	84	0.1562105204164982
GLOBAL	OXSTAT	RPPCR_12P	3	85	0.2116707314550877
GLOBAL	OXSTAT	RPPCR_12P	3	86	0.02240077123045921
GLOBAL	OXSTAT	RPPCR_12P	3	87	0.1221462179720402
GLOBAL	OXSTAT	RPPCR_12P	3	88	0.2443064898252487
GLOBAL	OXSTAT	RPPCR_12P	3	89	0.1764915284514427

GLOBAL	OXSTAT	RPPCR_12P	3	90	0.1095551936328411
GLOBAL	OXSTAT	RPPCR_12P	3	91	0.2367735370993614
GLOBAL	OXSTAT	RPPCR_12P	3	92	0.1962430045008659
GLOBAL	OXSTAT	RPPCR_12P	3	93	0.1183656147122383
GLOBAL	OXSTAT	RPPCR_12P	3	94	0.1861685036122799
GLOBAL	OXSTAT	RPPCR_12P	3	95	0.2474477100372314
GLOBAL	OXSTAT	RPPCR_12P	3	96	0.2206722401082516
GLOBAL	OXSTAT	RPPCR_12P	3	97	0.2132513538002968
GLOBAL	OXSTAT	RPPCR_12P	3	98	0.2197543856501579
GLOBAL	OXSTAT	RPPCR_12P	3	99	0.1022734507918358
GLOBAL	OXSTAT	RPPCR_12P	3	100	0.17115708142519

300 rows in set (0.24 sec)

MariaDB [PA_Results_pcr]>

6.3 Analysis Results

The overall mean CCDF is computed as the arithmetic mean of the mean CCDFs from each replicate. Figure 17 compares the overall mean CCDFs for total releases between the four analyses, CRA-2019, CRA19_12P, CRA19_COMB,[1] and RPPCR_12P. Table 17 summarizes the comparison of releases for those analyses at EPA compliance points. As seen in Figure 17 and Table 17, total mean normalized releases for RPPCR_12P and its upper 95 percent confidence limit (RPPCR_12P UCL) remained below the regulatory limits of 1.0 EPA units at the upper compliance point and 10.0 EPA units at the lower compliance point.

[1] CRA19_COMB is the sensitivity study that combines all parameter values and distribution changes that EPA conducted in its review of CRA-2019.

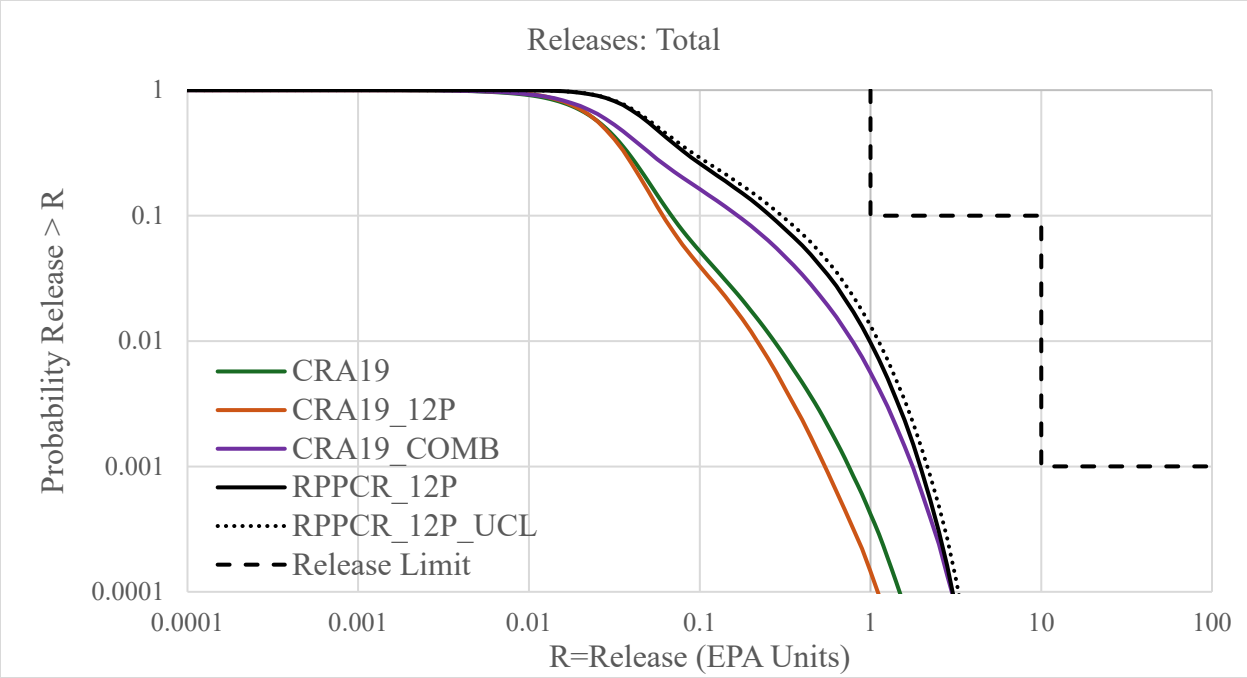

Figure 17. Normalized total releases for analyses CRA-2019 (CRA19), CRA19_12P, CRA19_COMB, and RPPCR_12P. The upper 95 percent confidence limit for RPPCR_12P analysis is also plotted. They are all under EPA regulatory release limits.

The difference in total releases between CRA-2019 and CRA19_12P analyses has been discussed in Zeitler et al. (2025) and summarized in Section 4 of this report. The release difference between CRA-2019 and CRA19_COMB analyses has been discussed in EPA (2022c). The increase in calculated total mean repository releases in CRA19_COMB, compared to CRA-2019, is due to the cumulative effect of parameter changes of borehole plugging pattern probability, actinide baseline solubility, colloid, and actinide oxidation state parameters. The parameter changes in the RPPCR_12P analysis, compared to CRA19_12P, are summarized in Section 6.1.

Table 17. Statistics on the overall mean for total normalized releases

Analysis	Probability	Mean Total Release	Release Limit	Probability	Mean Total Release	Release Limit
DOE CRA-2019	0.1	0.0685	1	0.001	0.7505	10
DOE CRA19_12P	0.1	0.0610	1	0.001	0.5436	10
EPA CRA19_COMB	0.1	0.1669	1	0.001	1.766	10
EPA RPPCR_12P	0.1	0.2588	1	0.001	1.967	10

EPA's RPPCR_12P analysis uses the same actinide baseline solubility, colloid, and actinide oxidation state parameters as in its CRA19_COMB analysis. However, the RPPCR_12P uses updated parameters for borehole drilling rate, borehole plugging probability, and iron surface density. The increase in total releases in RPPCR_12P, compared to CRA19_COMB, is primarily

due to the parameter changes in the borehole drilling rate and iron surface density. The updated borehole drilling rate parameter has a direct impact on releases of the Cuttings and Cavings release pathway. As shown in Figure 18, RPPCR_12P has significantly higher Cuttings and Cavings releases at both low probabilities and high probabilities.

The larger repository volume in a 12-panel performance assessment decreases the iron surface density by 10 percent. It, in turn, decreases gas generation and brine consumption. The increase in releases for the Spallings pathway in the RPPCR_12P, as shown in Figure 19, is a combined consequence of higher drilling rates and overall higher-pressure conditions in the repository. The higher-pressure conditions and the availability of brine in the repository increase the direct brine releases for the RPPCR_12P, especially for the high probability, low consequence releases (Figure 20). The releases from the Culebra are not discussed here, as the contribution to the total releases from this release mechanism is minimal.

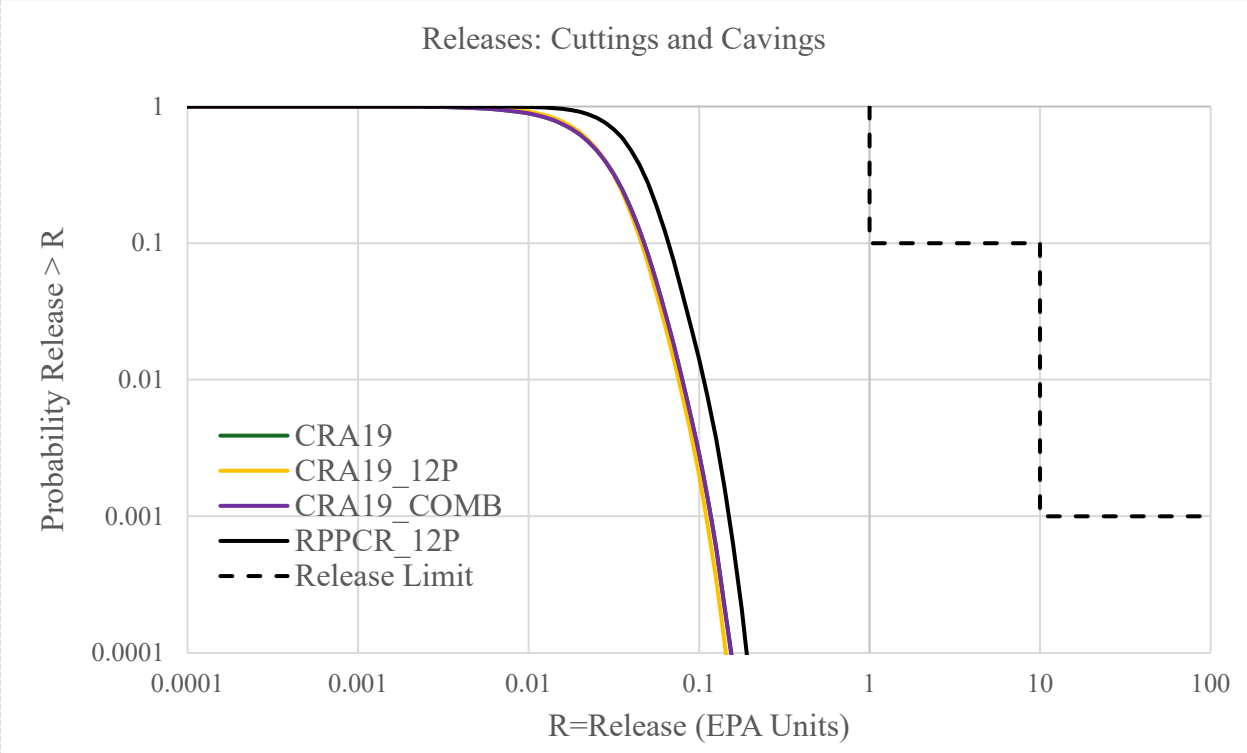

Figure 18. Cuttings and cavings releases for analyses CRA-2019 (CRA19), CRA19_12P, CRA19_COMB, and RPPCR_12P. The change in the drilling rate parameter in RPPCR_12P has a direct impact on the releases of this release pathway.

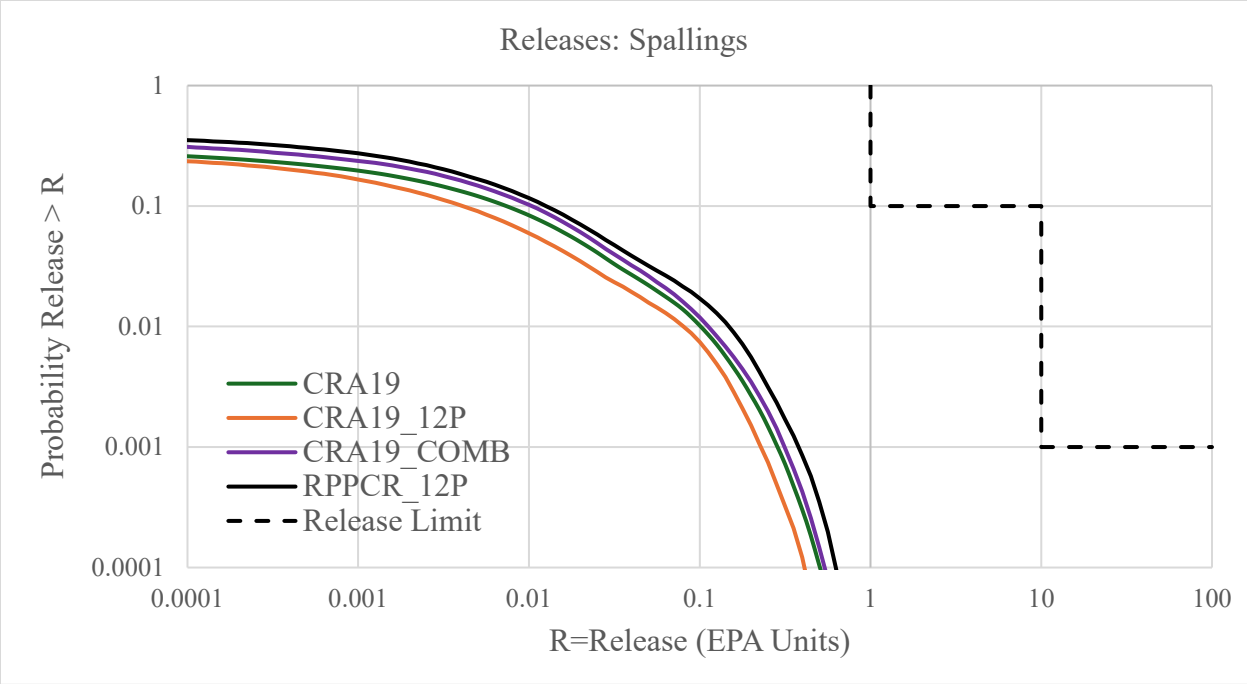

Figure 19. Spallings releases for analyses CRA-2019 (CRA19), CRA19_12P, CRA19_COMB, and RPPCR_12P. The high drilling rate and high repository pressure conditions contribute to the higher spalling releases in RPPCR_12P.

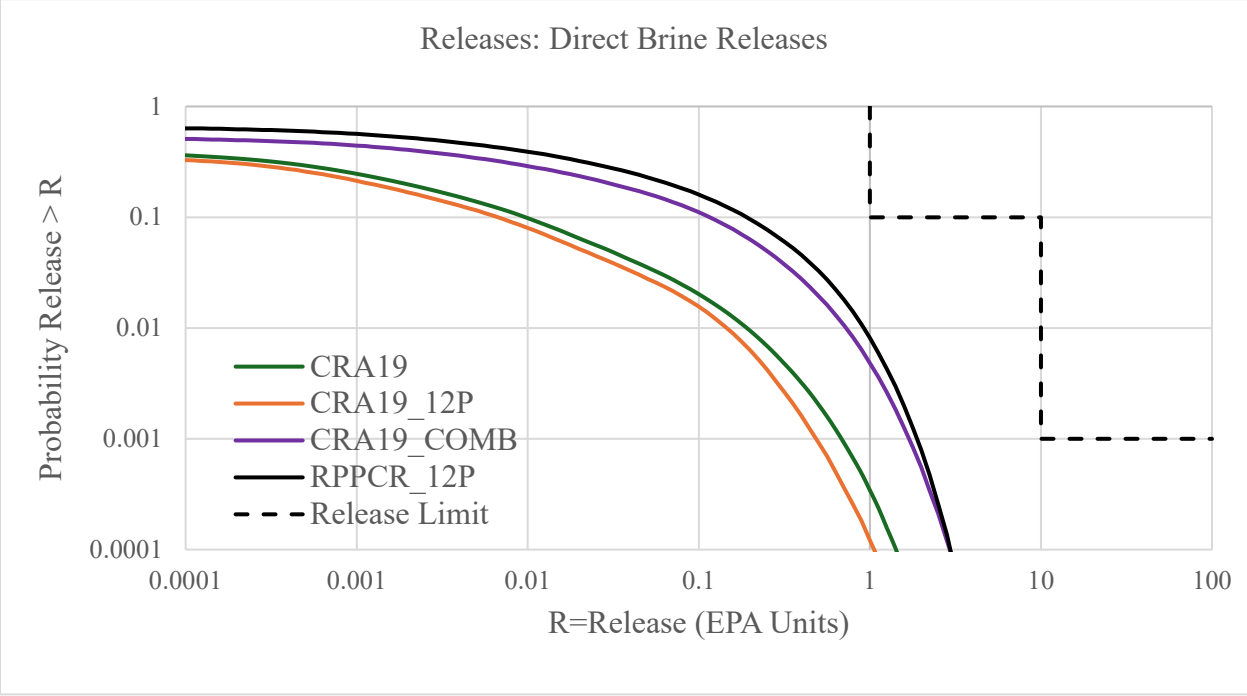

Figure 20. Direct brine releases for analyses CRA-2019 (CRA19), CRA19_12P, CRA19_COMB, and RPPCR_12P. The high repository pressure conditions and more brine in the repository contribute to the higher direct brine releases in RPPCR_12P.

7.0 CONCLUSIONS

EPA's evaluation of DOE's RPPCR involved reviewing DOE's 19-panel RPPCR PA in addition to DOE's 12-panel sensitivity study. The RPPCR PA evaluates the repository performance of the original waste panels 1 through 10, replacement panels 11 and 12, and seven additional conceptual panels, numbered 13 through 19. These additional panels were identified by DOE as conceptual and were used to demonstrate that the WIPP site has the potential capacity to hold the 6.2 million cubic feet of TRU waste authorized by the LWA. Although the Agency concluded that DOE's RPPCR PA adequately supported this potential, EPA is not making a determination on the overall adequacy of a 19-panel repository and is not approving DOE's RPPCR PA or DOE's comparison with the disposal standards at this time. EPA's review of the 19-panel RPPCR PA is being documented separately, and its primary purpose will be to provide feedback to DOE on changes to be made in future PAs to accommodate potential future increases in the size of the WIPP repository.

DOE's 12-panel sensitivity study, CRA19_12P, focused on evaluating the effects of only the two replacement panels on WIPP performance by increasing the number of waste panels from ten to twelve. The Agency's detailed review of DOE's 12-panel sensitivity study, CRA19_12P, provides the basis for EPA's decision on DOE's RPPCR. To support an independent technical review of DOE's 12-panel sensitivity study, EPA performed the following activities:

- Evaluated DOE's APPA Peer Review and found that the peer panel's conclusion pertaining to the geometric simulations used to address the proposed off-axis repository extension was reasonable and appropriate. The Agency considers the methodology acceptable for use in the 12-panel PA.
- Reviewed DOE's FEPs analysis and found that the analysis was reasonable and adequately documented for the purpose of the CRA19_12P PA. Although EPA identified a few residual concerns that need to be addressed for the next CRA, EPA anticipates that only minor changes (if any) will be made to future screening decisions.
- Assessed DOE's modifications of three conceptual submodels: Disposal System Geometry; Repository Fluid Flow; and Direct Brine Release, and the subsequent peer review of those modifications. The Agency accepts DOE's conceptual model modifications.
- Considered DOE's revisions to the repository volume and area, and related model input parameters. EPA finds that these numerical model changes are consistent with the revised conceptual models.
- Evaluated DOE's update of the Salado flow and DBR computational grids implemented in BRAGFLO. The conceptual modifications of the BRAGFLO Salado flow and DBR models proposed by DOE to accommodate off-axis, western waste panels were considered adequate for a 19-panel repository by the APPA Peer Panel (Falta et al. 2021, p. 28) and are also considered adequate for accommodating off-axis waste panels by EPA. EPA,

therefore, concludes that similar conceptual approaches are appropriate for developing Salado flow and DBR grids for a 12-panel analysis where two of those panels are located in an off-axis, West RoR.

The BRAGFLO Salado flow grid used in the 12-panel analysis also has an expanded representation of a Castile brine reservoir. The Agency concurs with this approach and agrees with DOE that the increase in the volume of grid cells representing the reservoir in the CRA19_12P BRAGFLO Salado flow grid is expected to have an inconsequential effect.

- Reviewed revisions to the panel neighboring assignment approach to simulate the effects of multiple intrusions into multiple, randomly selected waste panels. As noted by both the APPA Peer Review Panel and EPA, the adequacy of the neighboring approach depends on the degree to which conditions in the surrogate Waste Panel (Panel 5) conservatively approximate conditions in the first intruded panel. Since the design of Panel 5 differs from most other panels because it has no closures, it provides a conservative approximation of the potential conditions. EPA, therefore, considers the neighboring approach adopted by DOE to be reasonable for a 12-panel analysis.
- Assessed the additional Culebra Release Point included in the 12-panel analysis. This release point was located above the centroid of the two replacement panels and was added to better simulate flow from borehole intrusions in the western area of the repository. Because of the increased travel time due to the greater distance of the additional release point from the LWA boundary, only a small fraction of releases from this point reaches the boundary within the 10,000-year regulatory time frame. EPA considers the addition of a second release point to be appropriate.
- Evaluated revisions to the computer codes and migration to the WIPP PA HPC/Linux Cluster to ensure that the codes still meet the requirements of 40 CFR 194.23 (Models and Computer Codes). The Agency finds that the versions of the computer codes used to support the 12-panel analysis are approved.
- Reviewed DOE's assumptions pertaining to the determination of waste concentration, as a fraction of the volume occupied by waste, calculated as the total waste volume divided by the total waste panel volume. The Agency considers DOE's calculated waste fraction used in the 12-Panel Analysis to be appropriately conservative.
- Provided a summary of DOE's CRA19_12P Analysis Results, which were based on the 10-panel CRA-2019 PA calculations as modified to consider the effects of a larger repository waste disposal volume and footprint.
- Critiqued DOE's 12-panel sensitivity study results. EPA concurs with DOE's conclusion that the differences between the results for the CRA-2019 PA and the CRA19_12P sensitivity study are minor. This lack of significant differences could be expected because of the similar input parameters and increases in drilling penetrations due to a larger repository footprint are offset by decreases in waste concentration due to a larger

repository volume. However, EPA identified several concerns that were resolved in the Agency's sensitivity analysis described below.

- Conducted a sensitivity analysis to evaluate the cumulative effects of several parameter changes: borehole drilling rates and plugging pattern probabilities, iron surface area, actinide baseline solubility, colloids, and actinide oxidation state. These changes resulted in greater total mean normalized releases than for the CRA19_12P. However, both the mean and the upper 95 percent confidence limit remained below the regulatory limits of 1.0 EPA units at the upper compliance point and 10.0 EPA units at the lower compliance point.

In summary, EPA performed a detailed review of DOE's supporting documentation pertaining to its 12-panel sensitivity study. EPA is in general agreement with DOE's approach and DOE's interpretation of the PA results. Although EPA had concerns pertaining to several of DOE's input parameters, these concerns were alleviated based on the results of EPA's independent sensitivity analysis demonstrating that the total mean normalized releases still fall below EPA's regulatory limits. As a result, the Agency has determined that there is a reasonable expectation that the 12-panel configuration of the repository will comply with the standards and requirements in 40 CFR parts 191 and 194. EPA therefore approves DOE's Planned Change Request to use replacement Panels 11 and 12 at the WIPP repository for disposal of TRU radioactive waste.

8.0 REFERENCES

Borkowski, M. 2012. *Numerical Values for Graphs Presented in Report LCO-ACP-08, Rev. 0, Entitled Solubility of An(IV) in WIPP Brine: Thorium Analog Studies in WIPP Simulated Brine, and for Graphs Published in Borkowski, M., et al. Radiochimica Acta 98 (9-11), 577-582 (2010).* LA-UR- 12-26640; LANL-CO ACRSP ACP-01/2012, Rev. 0. Los Alamos National Laboratory, Los Alamos, New Mexico.

Brunell, S. 2019. Analysis Package for Normalized Releases in the 2019 Compliance Recertification Application Performance Assessment (CRA-2019 PA). ERMS 571373. Carlsbad, NM: Sandia National Laboratories.

Brunell, S. 2023. Memo to WIPP Records Center. Subject: "Update to Parameters Defining Drilling Rate and Plugging Pattern Probabilities in PA Calculations". ERMS 579154. Carlsbad, NM: Sandia National Laboratories.

Brunell, S., C. Hansen, D. Kicker, S. Kim, S. King, and J. Long. 2021. Summary Report for the 2020 Additional Panels Performance Assessment (APPA). ERMS 574494. Carlsbad, NM: Sandia National Laboratories.

Day, B. 2015. *Review of the Technical Basis for REFCON:ASDRUM, DRROOM, and VROOM Performance Assessment Analysis Parameters with Comparison to the Currently Emplaced Steel Surface Area per Unit Volume in the WIPP Repository.* ERMS 564670. Sandia National Laboratories, Carlsbad, New Mexico.

Day, K. 2023. Memo to Steve Wagner. Subject: Borehole Plugging Practices White Paper. ERMS 578970. Carlsbad, NM: Los Alamos Technical Associates.

Docherty, P. 2023. Analysis Report for Modeling the Castile Pressurized Brine Reservoir. ERMS 578976. Carlsbad, NM: Sandia National Laboratories.

DOE (U.S. Department of Energy). 1996. *Title 40 CFR 191 Parts B and C Compliance Certification Application*. U.S. Department of Energy Carlsbad Field Office.

DOE (U.S. Department of Energy). 2014. *Title 40 CFR 191 Parts B and C Compliance Recertification Application*. U.S. Department of Energy Carlsbad Field Office.

DOE (U.S. Department of Energy). 2019. *Title 40 CFR 191 Parts B and C Compliance Recertification Application*. U.S. Department of Energy Carlsbad Field Office.

DOE (U.S. Department of Energy). 2024a. *Planned Change Request for the use of Replacement Panels 11 and 12.* Letter from Mark Bollinger (DOE) to Lee Veal (EPA). CBFO:ERCD:MG:SV:24-0168. U.S. Department of Energy, Carlsbad Operations Office, Carlsbad New Mexico. March.

DOE (U.S. Department of Energy). 2024b. *Delaware Basin Monitoring Annual Report*. DOE/WIPP-24-2308 Rev. 0. Carlsbad, NM; DOE Carlsbad Field Office.

EPA (U.S. Environmental Protection Agency). 2017. *Technical Support Document for Section 194.24: Evaluation of the Compliance Recertification Actinide Source Term, Gas Generation, Backfill Efficacy, Water Balance and Culebra Dolomite Distribution Coefficient Values*. Docket ID No. EPA-HQ-OAR-2014-0609. U.S. Environmental Protection Agency, Office of Radiation and Indoor Air. Washington, DC. June 2017.

EPA (U.S. Environmental Protection Agency). 2022a. Quality Assurance Project Plan for: Modeling Analyses and Verification of PHREEQC Databases and Input Files Performed to Support EPA's Review of DOE's Compliance Recertification Application 2019 (CRA-2019) at the Waste Isolation Pilot Plant. Docket ID No. EPA-HQ-OAR-2019-0534-0047. U.S. Environmental Protection Agency, Office of Radiation and Indoor Air. Washington, DC. April 2022.

EPA (U.S. Environmental Protection Agency). 2022b. *Technical Support Document: for Sections 194.23, 194.32, 193.33, and 194.54 Review of Changes to WIPP Performance Assessment Features, Events, and Processes in the 2019 CRA*. Docket ID No. EPA-HQ-OAR-2019-0534-0054. U.S. Environmental Protection Agency, Office of Radiation and Indoor Air. Washington, DC. April 2022.

EPA (U.S. Environmental Protection Agency). 2022c. *Technical Support Document: Overview of EPA Review of U.S. Department of Energy 2019 WIPP Compliance Recertification Application Performance Assessment.* Docket ID No. EPA-HQ-OAR-2019-0534-0049. U.S. Environmental Protection Agency, Office of Radiation and Indoor Air. Washington, DC. April 2022.

EPA (U.S. Environmental Protection Agency). 2022d. *Technical Support Document for Section 194.24: Evaluation of the Compliance Recertification Application (CRA-2019) Actinide Source Term, Gas Generation, Backfill Efficacy, Water Balance and Culebra Dolomite Distribution Coefficient Values*. Docket ID No. EPA-HQ-OAR-2019-0534-0052. U.S. Environmental Protection Agency, Office of Radiation and Indoor Air. Washington, DC. April 2022.

EPA (U.S. Environmental Protection Agency). 2022e. *Technical Support Document for Section 194.33: Review of Borehole Drilling Rate and Plugging Pattern Frequency Calculations in the CRA-2019 Performance Assessment*. Docket ID No. EPA-HQ-OAR-2019-0534-0051. U.S. Environmental Protection Agency, Office of Radiation and Indoor Air. Washington, DC. April 2022.

EPA (U.S. Environmental Protection Agency). 2023. EPA Review of DOE Peer Review of Conceptual Changes Incorporated in the APPA Model. Docket ID No. EPA-HQ-OAR-2001-0012-0774. Office of Radiation and Indoor Air, Center for Waste Management and Regulations. Washington, DC. April.

EPA (U.S. Environmental Protection Agency). 2024. *Twelve-panel PA sensitivity study for EPA's review of the Waste Isolation Pilot Plant Replacement Panel Planned Change Request.* Letter from Tom Peake (EPA) to Michael Gerle (DOE). U.S. Environmental Protection Agency, Office of Radiation and Indoor Air. Washington, DC. November 26, 2024.

Falta, Ronald W., Mengsu Hu, Edward M. Kwicklis, Carl I. Steefel, Sherilyn C. Williams-Stroud, and John A. Thies. 2021. *Waste Isolation Pilot Plant, Additional Panels Performance Assessment (APPA) Changed Conceptual Models Peer Review Report.* CBFO (U.S. Department of Energy, Carlsbad Field Office), Carlsbad, NM 2021. December.

Hansen, C., S. King, J. Bethune, and S. Brunell. 2023. Analysis Plan for the Performance Assessment for Replacement Panels Planned Change Request. AP-204, Rev. 1. ERMS 579449. Carlsbad, NM: Sandia National Laboratories.

Kirchner, T., A. Gilkey, and J. Long. 2014. Summary Report on the Migration of the WIPP PA Codes from VMS to Solaris. AP-162, Rev. 1. ERMS 561757. Carlsbad, NM: Sandia National Laboratories.

Kirchner, T., A. Gilkey, and J. Long. 2015. Addendum to the Summary Report on the Migration of the WIPP PA Codes from VMS to Solaris. AP-162. ERMS 564675. Carlsbad, NM: Sandia National Laboratories.

Kirkes, G.R. 2021a. Baseline Features, Events, and Processes List for the Waste Isolation Pilot Plant, Revision 4. February 16, 2021. ERMS 574784. Sandia National Laboratories, Carlsbad, NM.

Kirkes, G.R. 2021b. Performing FEPs Baseline Impact Assessments for Planned or Unplanned Changes, Revision 5. March 21, 2021. ERMS 574990. Sandia National Laboratories, Carlsbad, NM.

Kirkes, G. R. 2021c. *Features, Events, and Processes Assessment for the Additional Panels Performance Assessment*. ERMS 574493. Carlsbad, NM: Sandia National Laboratories.

LANL (Los Alamos National Laboratory). 2018. *Estimation of Cellulose, Plastic, and Rubber Emplacement and Operational Materials in the Waste Isolation Pilot Plant (WIPP).* LANL-CO. INV-SAR-51, Revision 0, December 13, 2018. LANL-CO Record ID# INV-1812-05-01-01.

Long, J. 2023. Computational Code Execution and File Management for the Replacement Panels Planned Change Request (RPPCR). ERMS 579728. Carlsbad, NM: Sandia National Laboratories.

Papenguth, H.W. 1996. *Parameter Record Package for Colloidal Actinide Source Term Parameters. Mobile-Colloidal-Actinide Source Term. 4. Microbes.* Memorandum to C.T. Stockman, May 7, 1996. ERMS 235856. Sandia National Laboratories, Albuquerque, New Mexico.

Reed, D.T., J.S. Swanson, J.F. Lucchini, and M.K. Richmann. 2013. *Intrinsic, Mineral and Microbial Colloid Enhancement Parameters for the WIPP Actinide Source Term.* LCO-ACP-18, Revision 0. Los Alamos National Laboratory, Carlsbad, New Mexico.

Thompson, T.W., W.E. Coons, J.L Krumhansl, and F.D. Hansen. 1996. Inadvertent Intrusion Borehole Permeability. Title 40 CFR Part 191 Compliance Certification Application for the Waste isolation Pilot Plant, MASS Attachment 16-3. Carlsbad, NM: US Department of Energy, Carlsbad Area Office.

Van Soest, G.D. 2018. *Performance Assessment Inventory Report – 2018*. Los Alamos National Laboratory Carlsbad Operations INV-PA-18, Revision 0, December 12, 2018.

Vignes, C., J.E. Bean, and B. Reedlunn. 2023. Improved Modeling of Waste Isolation Pilot Plant Disposal Room Porosity. SAND2023-04826. Carlsbad, NM: Sandia National Laboratories

Zeitler, Todd, James Bethune, Sarah Brunell, Paul Docherty, Sungtae Kim, Seth King, and Justin Wilgus. 2025. Analysis Report for a 12-panel PA Sensitivity Study, Revision 0. Sandia National Laboratories, Carlsbad, New Mexico. January 14.